Synthesis and characterization of 8 arm-Poly(ethylene glycol) Based hydrogels via Michael addition or click chemistry for Biomedical Applications

Vorgelegt von

M.Sc. Zhenfang Zhang

aus Henan

Von der Fakultät II - Mathematik und Naturwissenschaften

der Technischen Universität Berlin

zur Erlangung des akademischen Grades

Doktor der Ingenieurwissenschaften

Dr.-Ing.

Genehmigte Dissertation

Promotionsausschuss:

Vorsitzender: Prof. Dr. Nediljko Budisa

Berichter/Gutachter: Prof. Dr. Ir. Marga C. Lensen

Berichter/Gutachter: Prof. Dr. Rainer Haag

Tag der wissenschaftlichen Aussprache: 24. March 2015

Berlin 2015

D83

Table of contents

List of abbreviations:

8PEG	8arm star-shaped Poly(ethylene glycol) with acrylate-end groups
8PEG-8PEG	Hydrogel based on pure 8PEG
hPG-8PEG	Hybrid hydrogel consisting of hPG and 8PEG building blocks
8PEG-OH	8arm, star-shaped Poly(ethylene glycol) with OH-end groups
8PEG Hap	Nanocomposite hydrogels of 8PEG and hydroxyapatite
8PEG-NH_3	hydrogels synthesized by mixing of 8PEG and NH_3
8PEG-NH_3-UV	Hydrogel with further UV stabilizing of 8PEG-NH_3
8PEG-UV	The UV-curing 8PEG hydrogels via photopolymerization
ACP	Amorphous Calcium Phosphate
AFM	Atomic Force Microscopy
Az	Azide
Alk	Alkyne
β-TCP	β-tricalcium phosphate
CP	Calcium phosphate
CL	Crosslinker
CLSM	Confocal Laser Scanning Microscopy
CuAAC	Cu-catalyzed azide-alkyne click cycloaddition
C=C	Double-bond
Dex-AE	Dextran-allyl isocyanateethylamine
DSC	Differential scanning calorimetry
E	Young's Modulus
ECM	Extracellular matrix
EDX	Energy Dispersive X-Ray diffraction
FBS	Fetal Bovine Serum
F/d curve	Force-distance curve
G''	Storage Modulus
G'	Loss Modulus

GAG	Glycosaminoglycan
HA	Hyaluronic acid
HAp	Hydroxyapatite
hPG	Hyperbranched polyglycerol
LC-MS	Liquid Chromatography Mass Spectroscopy
LMWH	Low-molecular-weight heparin
Mw	Molecular weight
Ms	Gel mass after swelling
Md	Dry gel mass
NPs	Nanoparticles
OSMs	Carboxylic acid terminated sulfamethazine oligomers
PCL	Poly(ε-caprolatone)
PCLA	Poly(ε-caprolatone-co-lactic acid)
PEG	Poly(ethylene glycol)
PEG DMA	Poly(ethylene glycol) dimethacrylate
PEGDA	Poly(ethylene glycol) diacrylate
PHEMA	Poly(hydroxyethyl methacrylate)
PLGA	Poly(lactic-co-glycolic acid)
PNIPAAm	Poly(N-isopropylacrylamide)
POM	Cross-polarizing optical microscopy
PVA	Poly(vinyl alcohol)
PI	Photoinitiator
Qm	Swelling degree
Ra	Arithmetic Average (common measure for surface roughness)
RM	Replica Molding
RMS	Root Mean Square (common measure for surface roughness)
SAED	Selected area electron diffraction
SEM	Scanning Electron Microscopy
sECMs	Semi-synthetic ECMs

TEM	Transmission Electron Microscopy
Tg	Glass Transition Temperature
T_m:	Melting temperatures
TGA	Thermogravimetric Analysis
UV	Ultraviolet
WAXD	Wide-angle X-ray diffraction
XRD	X-ray diffraction
ξ	Related measure of distance between crosslinks
υ_1	Symmetric stretching of phosphate
υ_3	Asymmetric stretching of phosphate

Scope and Organization of the Thesis

Hydrogels are three-dimensional networks of hydrophilic polymers, which have been extensively researched, especially for applications in cell culture, tissue engineering, and also in drug delivery system. Among various kinds of hydrogels, poly(ethylene glycol)(PEG)-based hydrogel is one of the most widely used and studied gels, due to its excellent biocompatible and unique bio-anti adhesive characteristics, as well as the versatility of the PEG macromer chemistry. But the most common used PEG-based hydrogels, formed through photopolymerization methods, lack the functionality and degradable properties, which is essential for the biomedical application. Thus, the aim of this thesis is to develop novel gel fabrication methods, which are utilized to form hydrogels with the near-ideal network connectivity, improved physical properties as well as the versatility with respect to bioconjugation, and further to investigate the functionality and degradable properties of the new gel systems.

The experimental studies in this thesis are mainly organized in three parts. The first part of the work (Chapter2-3) describes the new PEG-based hydrogels system, formed through amine-type Michael addition chemistry, and the mechanical characterization, the functionality, as well as crystallization behavior of the hydrogels. In the second part (Chapter 4), we report on the synthesis of the composite PEG-based hydrogels incorporated with Calcium Phosphate phase, and the characterization, as well as the specific cell adhesion test. Moreover, the third part (Chapter 5) focuses on the controlled degradation properties of gels, which have been prepared by click chemistry. The outline of the thesis is as follows:

Chapter 1 gives a literature overview of currently developed hydrogel matrices for biomedical application. The usage and types of common hydrogels will be introduced. Various methods including physical or chemical crosslinking to fabricate hydrogels are reviewed and discussed. Particular emphasis is laid on the relationship between crosslinking methods and the hydrogel network structure.

Chapter 2 explores a novel type of chemical cross-linking, other than photopolymerization. Amine- Michael type addition reaction, occurring between amine groups and acrylate groups on PEG polymers is used for in-situ formation of hydrogel system bringing advantageous properties with post-functionality. Characterization of the gel formation kinetics, as well as rheological analysis, degradation and chemical composition of the formed hydrogels are reported.

Chapter 3 reports on the crystallization properties of PEG-based hydrogels formed by amine- Michael type addition reaction from Chapter 2. Several characterization methods (POM, SEM, AFM) are used to confirm the crystalline type and morphology. The mechanism of large crystalline domain formation is also postulated.

Chapter 4 describes the synthesis of composite PEG-based hydrogels by in situ mixing with Calcium and Phosphate salt solutions, and demonstrates how the inorganic phase affects the mechanical properties, degradation and swelling behavior of the composite gels. The morphology of the hydrogels is studied by SEM, as well as AFM in swollen state. Two different type of cells (fibroblasts and osteoblasts) are utilized to investigate the specific affinity between composite gels and cells.

Finally, in **Chapter 5** the use of click chemistry to form hydrogels with controlled degradable properties has been developed. The impact of degradation on hydrogel swelling and mechanical properties is studied and characterization of the rheological properties in swollen state is provided. In an effort to evaluate whether the hydrogels are potentially suitable for biomedical application, their cytocompatibility in vitro is assessed as well.

Note: I worked in close collaboration with Axel Loebus in the Lensen Lab to complete this research project. Other persons also contributed significantly to the herein displayed results, for example were the cell tests performed by Gonzalo de Vicente and Christine Strehmel, and the mercapto-functionalized fluorescent dye provided by Manar Arafeh.

Chapter 1.

General Introduction

1.1 Biomaterials

A definition [1]of biomaterial is " a substance that has been engineered to take a form which, alone or as part of a complex system, is used to direct, by control of interactions with components of living systems, the course of any therapeutic or diagnostic procedure, in human or veterinary medicine." The use of biomaterials includes the progress in diagnostic methods, and the regeneration of diseased tissues and organs as well as the delivery of active ingredients. Historically, the medical materials were mainly chosen from natural sources, but most of them were deemed to fail, because important notions relating to infection and the biological reaction to materials were not yet established. In the beginning of the twentieth century, synthetic polymers, ceramics and metal alloys were developed for biomedical applications, which can provide better performance, increased functionality and more reproducibility than their naturally derived counterparts. Currently, synthetic biomaterials play central roles in modern strategies in regenerative medicine and tissue engineering as designable biophysical and biochemical milieus that direct cellular behavior and function [2, 3].

It is estimated that over 40.000 pharmaceutical formulations, 8.000 medical devices and 2.500 diagnostic products employing biomaterials are in current clinical practice. Moreover in 2007, in the United States only, biomaterials generate a market of about $200 billion per year, with a robust annual growth rate of ~9% [4,5]. Although considerable progress has been made already, much work remains to be done for the development of more functional medical materials and the expanded use of biomaterials into new fields of application. Due to the growing interest and need for new biomaterials, a great deal of research has been devoted to synthesizing new materials from a range of natural and synthetic chemistries and 3-D macrostructures to offer materials with a wide range of properties and/or controlled responses for application in tissue engineering, repair and regeneration [2]. We have chosen to focus on synthetic biomaterials: hydrogels, which are attractive owing to their high water content, ease of fabrication and functionalization, and biological

tissue-like properties, and have demonstrated great potential for biomedical applications.

1.2 Hydrogels

Hydrogels which are prepared from macromolecules containing hydrophilic groups, such as -OH, -COOH, $-SO_3H$, -CONH-, and $-CONH_2-$, either embedded in or grafted to their polymeric back bones, are appealing for biological applications because of their high water content and biocompatibility. Hydrogels can absorb up to thousands of times their dry weight in aqueous solutions owing to the hydrophilic network chains [6]. The most frequently referred definition is the one given by Peppas[7] that hydrogels are water-swollen, cross-linked polymeric structures. During the crosslinking process, the constituent building blocks bond, associate or entangle with each other, ultimately forming a network of macroscopic dimensions. Several distinct levels of crosslinking can be observed during the gelation process. At the beginning, the building blocks grow and branch out, but remain soluble. As the crosslinking continues, clusters form, and then the size of the clusters increases. Eventually, a gel point is reached where all the building blocks are linked to each other at multiple points. The presence of crosslinks ensures the structural and mechanical integrity of the hydrogels and prevents them from dissolution when exposed to an aqueous environment [8].

The suitability of hydrogels as biomedical materials and their performance in a particular application depend to a large extent on their bulk structure. In general, the crosslinked structure of hydrogels is characterized by, i) junctions or tie points, which may be formed from strong chemical linkages (such as covalent and ionic bonds), ii) permanent or temporary physical entanglements, iii) junctions, and iv) weak interactions (such as hydrogen bonds), shown in Figure 1. The most important parameters used to characterize the network structure of hydrogels include: 1) M_C, the average molecular weight between crosslinks; 2) ξ, the related measure of distance between crosslinks (i.e., mesh size; Figure 1) [9]. The molecular weight between two consecutive crosslinks, which can be either chemical or physical in

nature, is a measure of the degree of crosslinking of the polymer. It is important to note that due to the random nature of the polymerization process only average values of Mc can be calculated. The two prominent theoretical treatments used to describe the network structure of hydrogels and to determine these parameters are derived from equilibrium swelling theory and rubber elasticity theory [9-12].

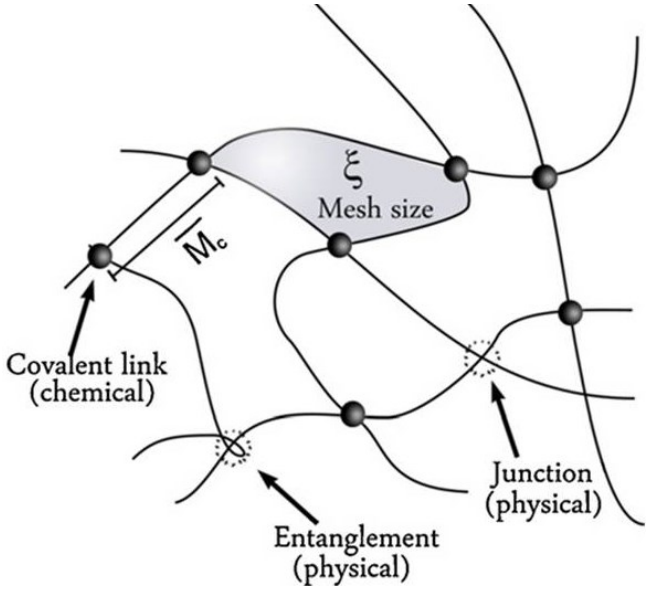

Figure 1. Network structure of a hydrogel showing junctions, entanglements, and covalent linkages [9].

1.2.1 Applications of hydrogels

Due to their good biocompatibility, flexibility in fabrication, variable composition, and desirable physical characteristics (similar to physiological conditions), as well as the hydrophilic nature of hydrogels with the similarity to the void-filling component of the extracellular matrix, hydrogels are thus used for a wide range of biomedical applications. They can serve as scaffolds that provide a 3D structure for tissue engineering [13, 14], as carriers for drug delivery[15, 16], as suitable matrices for biosensors [17, 18], as adhesives or barriers between tissue and material surfaces [19,20] or act as cell sheets for reversible control of cell attachment [9, 21].

For example, hydrogels have been widely utilized as scaffolds for tissue engineering (Figure 2) [22]. As scaffolds, hydrogels are used to provide bulk and mechanical

constitution to a tissue construct for cell adhesion or suspension within the 3D gel framework. In addition, incorporation of various peptide domains into the hydrogel structure can dramatically increase the tendency for cellular attachment. In this context, it is desired that gel scaffolds need to be completely biodegradable so that after tissue is grown, the resulting structures are made entirely from biological components. Alginate-based polymers have been demonstrated that they could be crosslinked using calcium ions for the treatment of diabetic animals [23]. Moreover, poly(ethylene glycol) dimethacrylate (PEG DMA) and PEG have been photo-polymerized to form hydrogel networks with encapsulated bovine and ovine chondrocytes for cartilage regeneration [24,25]. Additionally, polymeric microcapsules containing cells can be immobilized in hydrogels such as agarose gels to enhance the functionality of transplanted constructs [26].

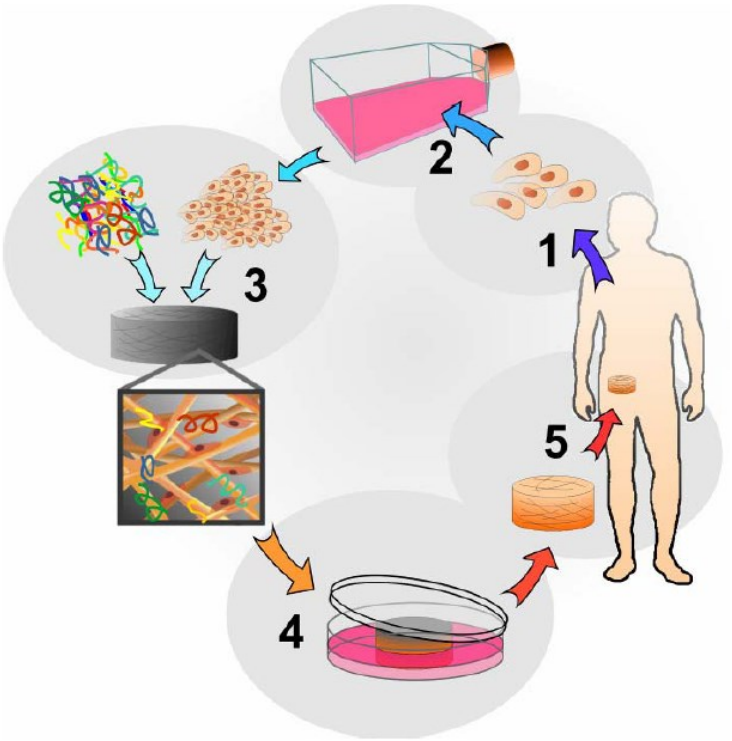

Figure 2. Schematic illustration of typical tissue engineering approaches. 1: A small amount of cells are removed from the body. 2: Cells are screened for phenotype and proliferate. 3: Seeding cells into 3D scaffolds together to enhance proliferation. 4: The seeded scaffolds are further cultured. 5: Implanting the regenerated tissue into body to replace the damaged tissue [22].

Another hydrogels' major application for biomedical field is drug delivery system,

and by now there are several commercial products already available on the market. In particular, macromolecular drugs, such as proteins or oligonucleotides, tend to rely on hydrogels as delivery systems, because hydrogel preparation procedures are beneficial in preserving protein stability, and the release of protein drugs from the hydrogel matrix in a controlled fashion maintains a therapeutic effective concentration of the protein drug in the surrounding tissues or in the circulation over an extended period of time [27]. Researchers have engineered their physical and chemical properties to optimize them by controlling the degree of swelling, crosslinking density, and degradation rate. Delivery kinetics can be engineered according to the desired drug release schedule [28–30] and triggered intelligently by interaction with biomolecular [31, 32].

As an example Anseth et al. developed a peptide functionalized PEG hydrogel where the affinity peptides were immobilized via thiol-acrylate photopolymerization. And in order to control the release of encapsulated recombinant MCP-1 from PEG hydrogels, the spacer distance between the affinity peptide and the crosslinking site was tailored [33]. More recently, Sun and coworkers mixed Dextran-allyl isocyanateethylamine (Dex-AE) with PEG diacrylate at different ratios and subsequently utilized photopolymerization to fabricate a hydrogel matrix, which loaded with multiple growth factors affecting the neovascularization of ischemic and wounded tissues. It was found that reducing the degree of substitution of cross-linking groups resulted in reduced rigidity, increased swelling, increased VEGF release rate, and rapid hydrogel disintegration, which was beneficial for tissue ingrowth [34].

1.3 Types of hydrogels

Hydrogels can be characterized based on their derivation and composition as natural, synthetic, hybrid, or composite hydrogels. In the following section, the various types of hydrogels are introduced.

1.3.1 Natural hydrogels

Many hydrogels based on natural polymers, such as alginate, chitosan, hyaluronic acid (HA), fibrin and agarose [22, 27], which are derived from various components of the mammalian extracellular matrix, as building blocks have been developed. The macromonomer repeat units utilized in these gels are shown in Figure 3 [27]. Collagen is the main protein of the mammalian extracellular matrix, while HA is a polysaccharide that is found in nearly all animal tissues. Moreover, alginate and agarose are polysaccharides that are derived from marine algae sources. These natural polymer networks display multiple advantages for biomedical applications with respect to their often inherent biocompatibility, biodegradability, and good cell adhesion properties. Many of the components used in their synthesis comprise much of in vivo structure and, hence, can also offer environmental advantages as ECM-mimics for cell-based devices. The natural extracellular matrix has more in common with these biopolymer gels as compared to synthetic polymer hydrogels, generally resulting in better cell survival and differentiation [35].

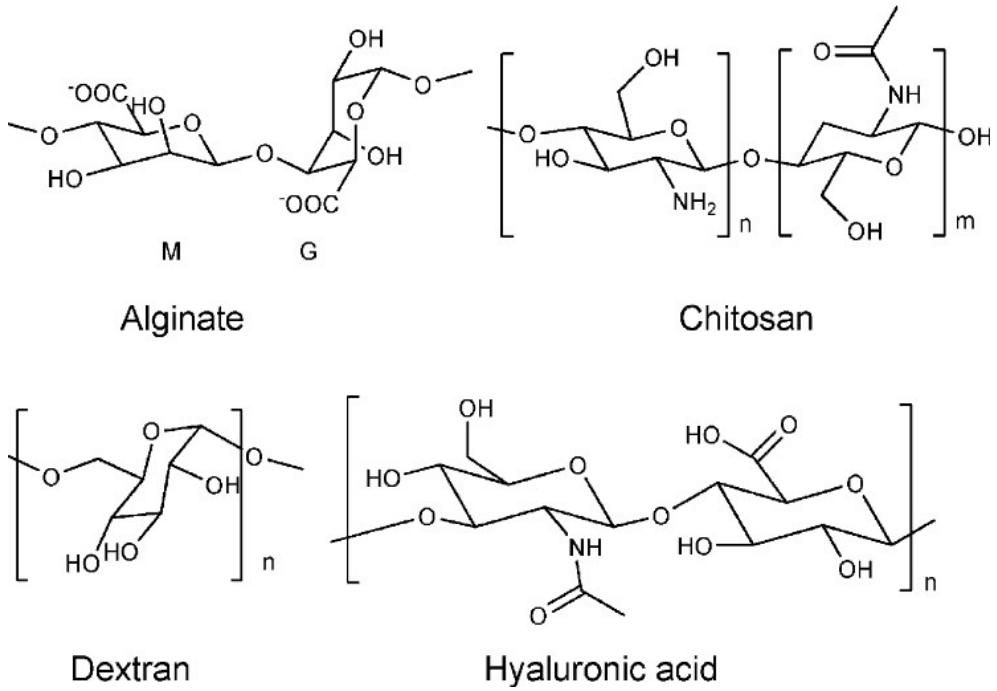

Figure 3. Most commonly used polysaccharides for hydrogel preparation for biomedical applications (M = mannuronic acid, G = guluronic acid) [27].

For example, Wang et al. have developed a pH-sensitive superabsorbent alginate-based hydrogel composed of sodium alginate-g-poly(sodium acrylate) and polyvinylpyrrolidone by free-radical solution polymerization using ammonium persulfate as initiator and N,N-methylene-bisacrylamide as cross-linker [36]. In addition, chitosan-based hydrogels have also gained increasing interest because of their potential applications in the field of tissue engineering. Yu et al. have reported the synthetic hydrogels mimicking the extracellular matrix (ECM) are prepared by cross-linking a thiol-modified chitosan. The results demonstrated that the hydrogels were biocompatible and the cells could migrate into the hydrogels. Moreover, cells were viable and preserved their 3D cell morphology inside the hydrogels [37]. Moreover, hyaluronic acid is a glycosaminoglycan (GAG) that is composed of repeating disaccharide units and is in particular prevalent during wound healing and in joints. Horn et al. combined thiol-modified HA with acrylate-functionalized PEG to create hydrogels suitable for spinal cord repair using Michael addition reaction [38].

1.3.2 Synthetic hydrogels

The hydrogels based on natural polymers lack adequate mechanical properties, and tunable structure and degradability, also leading to potential immunogenic responses which compromise their utilization as biomaterials [39]. However, synthetic polymers, like polypeptides, polyesters and polyphosphazenes, etc., usually can be designed and synthesized into crosslinked networks with molecular-scale control over structure such as crosslinking density and with tailored properties, such as biodegradation, mechanical strength, and chemical and biological response to stimuli. Control of these material properties has helped to advance the understanding of cellular interactions with synthetic substrates and the body's response to foreign materials [40,41]. Nevertheless, the incorporation of biofunctional molecules into the synthetic hydrogels can provide additional, biological cues for differentiation and proliferation of cells and tissue regeneration [42]. In addition, many synthetic gels are made using harsh synthetic chemistry,

which requires care to ensure that contaminants and unreacted reagents present during synthesis are subsequently removed.

For example, synthetic polymers, such as poly (ethylene glycol) (PEG), poly(vinyl alcohol) (PVA), poly(N-isopropylacrylamide) (PNIPAAm) and poly(hydroxyethyl methacrylate) (PHEMA) (Figure 4), have been widely used to fabricate hydrogels for biomedical applications. PEG hydrogels are one of the most widely studied and extensively used polymers as matrices for controlling drug delivery, as well as cell delivery vehicles for promoting tissue regeneration [43-46], because they have advanced properties, such as good biocompatibility, nonimmunogenity, and resistance to protein adsorption [47, 48]. PEG macromers with linear or branched (multiarm or star) structures can have a variety of functional groups, such as methyloxyl, carboxyl, amine, thiol, azide, vinyl sulfone, azide, acetylene, and acrylate, which are versatile for hydrogel formation [46, 49].

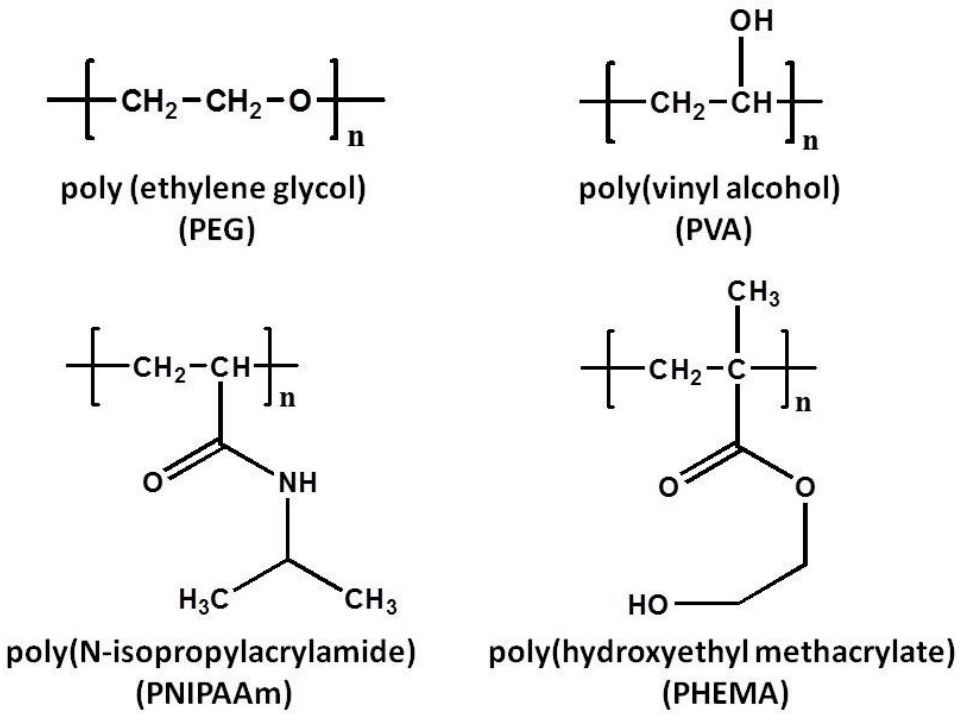

Figure 4. Representative chemical structures of synthetic polymers.

In particular, functional PEG star polymers are regarded as a particularly interesting class of materials since they represent versatile building blocks for

structured polymer hydrogels [50, 51]. The network properties, the swelling and the elasticity of the resulting gels can be controlled by tuning the length of arms and functionalities [52]. In the present study, star-shaped PEG molecules (having 8 arms with acrylate end groups; **8PEG**) were utilized for hydrogel synthesis.

In addition, PVA hydrogels for cartilage replacements were developed by Oka and collaborators and the physical aspects of hydrogels including lubrication, load bearing and biocompatibility were examined. In order to mimic that of normal human cartilage, the tensile strength of PVA hydrogels was up to 17 MPa with a novel annealing process. They showed that PVA artificial knee menisci in rabbits lasted beyond two years with no loss in integrity or mechanical properties [53]. Monodisperse PNIPAAm submicrometric microgels were reported by Lapeyre et al., which were modified with a phenylboronic acid derivative. It was demonstrate that those microgels were sensitive to the glucose at pH conditions close to the pKa of the PBA derivative (pKa = 8.2), with a swelling degree proportional to the concentration of glucose. Therefore those microgels could be designed to colorimetric sensors based on the light diffraction of colloidal crystals [54]. In addition, a biodegradable PHEMA scaffold was developed by Bryant et al. with controlled porosity. Myoblast growth and proliferation could be enhanced by covalent binding of Collagen. Those biodegradable PHEMA scaffolds are an important development given that the primary obstacle to the success of PHEMA gels is the lack of biodegradation [55].

1.3.3 Hybrid hydrogels

Traditional hydrogels are bulk gels consisting of inert synthetic polymers that are randomly interconnected, and do not exhibit biological activities, hierarchical organization, and structural integrity. By mimicking the native ECM, which is considered as a hybrid material, containing multiple structural and functional components interdigitated at all length scales, hydrogels can also be prepared from the combination of a synthetic polymer and a biopolymer, two different biopolymers, or two different synthetic polymers [56-58]. The new entities of hybrid hydrogels can

be expected to: 1) mimic the structure and functionality of biological tissue; 2) improve their mechanical properties as well as their biological functions for enhanced performance, 3) provide physical anchorage and structural reinforcement 4）change the biodegradability profile [59]. Many researchers have created novel hybrid hydrogel systems that synergistically combine well-evolved biological mechanisms, such as high affinity and specificity of binding, with controlled hydrogel properties (e.g., mechanical stability and environmental-responsive properties), by integrating biological entities with synthetic hydrogels.

For example, a modular and hybrid hydrogel for 3D cell culture was developed by Prestwich and coworkers, in order to replicate the complexity of the native ECM environment, which was necessary to allow cells to rebuild and replicate a given tissue. These semi-synthetic ECMs (sECMs) employ thiol-modified derivatives of HA that can form covalently crosslinked, biodegradable hydrogel matrices for cell attachment, and PEGDA for stability and enhanced crosslinking kinetics. These covalently crosslinked, biodegradable hydrogels are suitable for 3D culture of primary and stem cells in vitro, and for tissue formation in vivo. Moreover, these hybrid hydrogels allow inclusion of the appropriate biological cues needed to recapitulate the complexity of a given ECM environment [60].

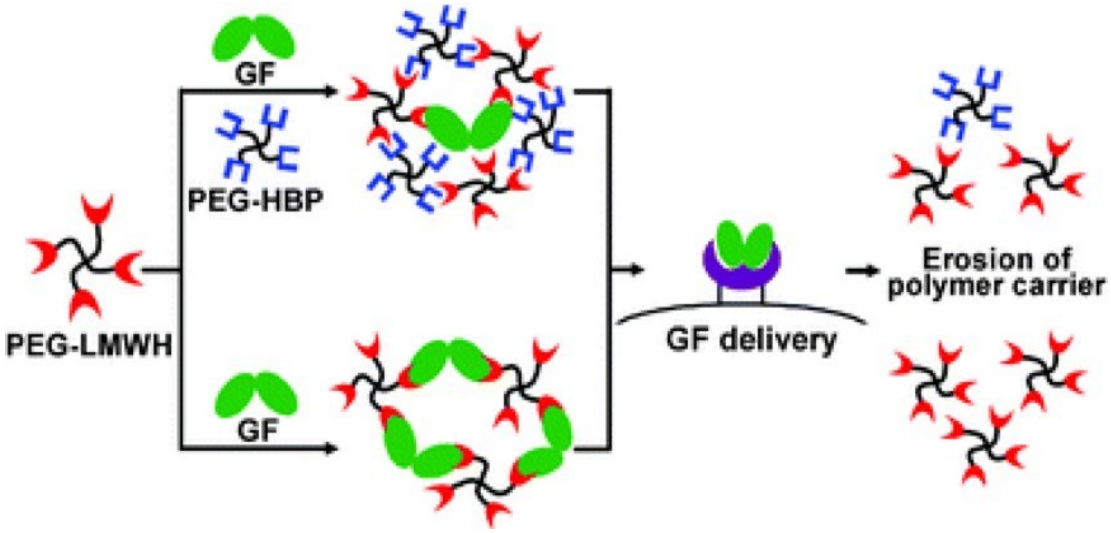

Figure 5. Schematic of noncovalent hydrogel assembly and erosion strategies employing PEG-LMWH [62].

In addition, Kiick and coworkers have developed hybrid hydrogels, combining star PEGs and low-molecular-weight heparin (LMWH), for non-covalent assembly of responsive hydrogels. In this approach, firstly PEG-LMWH was synthesized through a four-arm star, thiol functionalized PEG reacting with maleimide-functionalized LMWH, and then it was employed for hydrogel formation with various heparin-binding macromolecules (Figure 5). Four-arm star PEGs modified with HBPs (PEG-HBP) were employed for non-covalent hydrogel assembly with PEG-LMWH. Self-supporting hybrid hydrogels immediately formed upon mixing of solutions of the PEG-LMWH and PEG-HBP which still remained available for binding multiple growth factors. Furthermore, by controlling the rate of degradation of the hydrogel network the rate of release could be directly controlled, which is potentially useful for the treatment of ischemic conditions [61, 62].

1.3.4 Composite hydrogels

In general, composite polymer hydrogels may be defined as cross-linked three-dimensional polymer networks containing large amounts of water in the presence of inorganic phase. The inorganic phase can be used to either crosslink the hydrogel via attaching to polymer chains, or to be entrapped within the hydrogel network adding unique physical properties to the hydrogels, such as responsiveness to mechanical, optical, thermal, acoustic , magnetic or electric stimulation [63].

In 2002, a new concept of 'nanocomposite hydrogel' with a unique organic/inorganic network structure by extending nanomaterials to the field of hydrogels system was created [64]. The organic /inorganic network structures of nanocomposite hydrogels are proposed in Figure 6 [63]. Unlike organic polymeric hydrogels, which generally exhibit mechanically weak and brittle properties due to the restriction by a large number of crosslinks [65], highly stable, structurally homogeneous nanocomposite hydrogels, with extraordinary mechanical properties were achieved [64]. The extraordinary mechanical properties and new functions of nanocomposite hydrogels gels are attributed to their unique network structure. For

example, Hou et al found that the composite hydrogels from PNIPAM and polysiloxane nanoparticles (approximately 100-500 nm) could modulate cell adhesion by controlling temperature, as well as increase the mechanical strength and cell adhesion number by increasing the nanoparticle concentration [66]. Therefore, the nanocomposite hydrogels with advantageous chemical, physical, and biological properties can be obtained through the combination and formulation of polymers with nanoparticles.

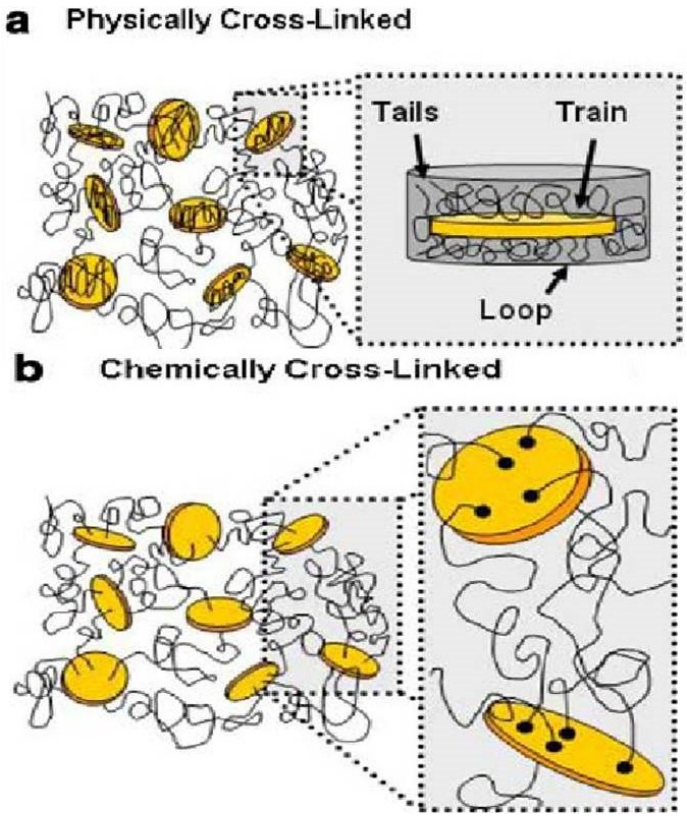

Figure 6. Network structure models of nanocomposite hydrogels formed via physical or chemical crosslinking methods [63].

In addition, composite hydrogels including synthetic bone substitutes based on Calcium Phosphate (CP) for bone tissue engineering have been developed. Bone tissue itself is a brilliant example of composite material consisting of nanocrystals of carbonated apatite spatially arranged within a hydrated collagen matrix, with considerable mechanical properties and intrinsic remodeling capability [67]. However, CP alone is difficult to shape into the complex forms required for bone treatment

that limit its applicability, because of its hardness and brittleness，as well as the poor compressive strength [68,69]. Therefore, by mimicking organic/inorganic biocomposites existing in nature, which have excellent mechanical and biological properties, the use of composites including CP granulates embedded in an organic matrix is a valid alternative to tissue transplants. For example, the specific tissue reaction after subcutaneous implantation of β-tricalcium phosphate (β-TCP) embedded into hydrogels composed of methylcellulose and hyaluronic acid was studied. A well vascularized connective tissue soon after implantation and the continuous degradation of composite materials over a period of 60 days from the periphery towards the core were observed [70].

1.4. Hydrogel synthesis methods

Hydrogels are water-swollen, cross-linked polymeric structures, and as the term 'cross-linked' implies, crosslinks have to be present to prevent dissolution of the hydrophilic polymer chains in an aqueous phase. There are a great variety of methods to establish crosslinking to prepare hydrogel networks, e.g. both physical and chemical methods have been utilized for crosslinking to create hydrogels. Physically crosslinked hydrogels are formed by physical interactions between different polymer chains. Chemically crosslinked hydrogels are formed by covalent bonds which are present between different polymer chains [71, 72]. Nevertheless, in this section we focus on the synthesis methods of PEG-based hydrogels, because on the one hand, in the herein presented PhD project, PEG is main macromonomer for hydrogel synthesis and on the other hand, similar crosslinking methods can be utilized for the synthesis of other kinds of polymer-based hydrogels.

1.4.1 Methods for physical crosslinking

Physical cross-linking is appealing for biomedical applications as it allows minimally invasive administration of the hydrogel, which can be formed in situ upon injection. In particular, compared with chemical crosslinking, crosslinking agents are avoided

with the use of physically crosslinked gels. This is of advantage because crosslinking agents are often toxic compounds that affect the integrity of the substances to be entrapped (e.g. proteins, cells), and need to be extracted from the gels before they can be applied [72]. Physically crosslinked hydrogels are formed by non-permanent reversible bonds based on hydrophobic/hydrophilic interactions [73, 74], hydrogen bonding [75, 76], crystallization [77, 78], ionic interactions [79, 80], or peptide Interactions [81, 82]. Among these methods to prepare physically cross-linked hydrogels, hydrophobic interactions are the most frequently exploited tools because of the strong interactions in aqueous solutions and relatively simple preparation by using amphiphilic block copolymers.

PEG alone cannot be utilized to form physically crosslinked hydrogels due to the fully soluble properties. The most common strategies to prepare physically crosslinked PEG-based hydrogels are based on block or graft copolymers containing a PEG segment, because these copolymers are able to self-assemble in water to form hydrogels, in which the hydrophobic segments of the polymers are aggregated. These copolymers can be composed of a water-soluble PEG backbone, for example PCL-PEG-PCL, to which hydrophobic units are attached, or hydrophobic chains containing water-soluble PEG grafts, for example PLGA-g-PEG [83]. In contrast to permanent networks formed by chemical cross-linking, these hydrogel networks are usually stimuli-sensitive, which means that they can be reversibly transformed into solutions by varying the environmental conditions. External physical or chemical triggers, such as pH, temperature, ionic strength or light can be used to control the sol-gel transitions [84]. For example, a pentablock copolymer (OSMs–PCLA–PEG–PCLA–OSMs) was synthesized by coupling sulfamethazine oligomers (OSMs) to the triblock copolymer(PCLA–PEG–PCLA). Both the temperature and PH play a vital role in the sol-gel transition after the copolymer mixes with water. In addition, the sol–gel transition of these block copolymer solutions was fine-tuned by controlling the PEG length, the hydrophobic to hydrophilic block ratio (PCLA/PEG), and the molecular weight of the sulfamethazine oligomer [85, 86].

1.4.2 Methods for Chemical crosslinking

Chemical cross-linking will yield covalent bonds between different polymer chains, and the resulting hydrogel network is in general more stable and more resistant to mechanical forces than physically cross-linked networks. In addition, the physicochemical properties of chemically crosslinked hydrogels, such as permeability, molecular diffusivity, equilibrium water content, elasticity, modulus, and degradation rate, can be controlled, while on the other hand, the versatility of chemical crosslinking methods facilitates the incorporation of chemical and physical cues into the gel matrix [7, 87]. Many coupling reactions, such as photopolymerization [88, 89], Michael addition reaction [90, 92], click chemistry [93-95], native chemical ligation [96, 97], and enzyme-catalyzed reaction [98, 99], have been used to obtain cross-linked polymers. This section focuses on a variety of chemically crosslinking methods, such as photopolymerization, Michael addition and click chemistry in Figure 7 [100], which are relevant to the present PhD project.

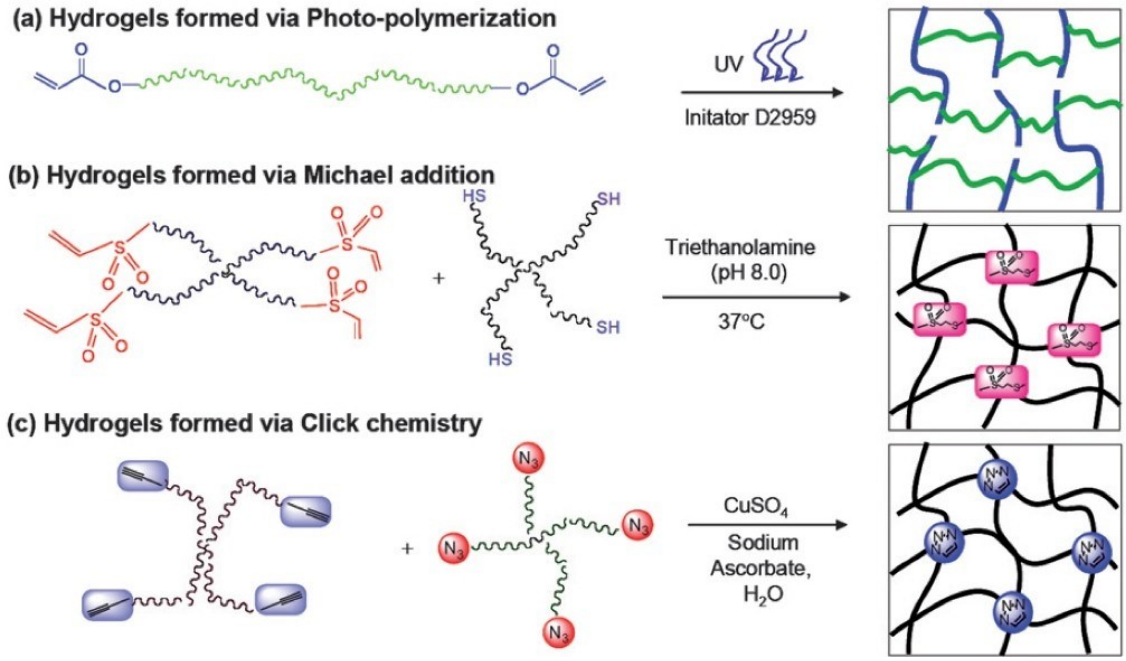

Figure 7. Reaction scheme for preparing PEG-based hydrogels via a) photopolymerization, b) Michael addition chemistry c) click chemistry [100].

1.4.2.1 Crosslinking by photopolymerization

Photopolymerization, a form of radical polymerization, is the most widely used method to prepare hydrogel networks because of the chemical versatility and ease of fabrication. The polymerization reaction of macromonomers containing two or more vinyl groups can be initiated by exposure to UV or visible light, in the presence of a photosensitive compound, called a photoinitiator, and can be carried out under physiological conditions (Figure 7a). The photopolymerizaion process is fast, taking usually only seconds to minutes to complete, can be conducted at room or body temperature without the use of organic solvents, and offers spatial and temporal control over the polymerization process allowing for fabrication of complex 3-D shapes [101, 102]. The main disadvantages of photopolymerization, however, are lower conversion of the functional groups, leading to unreacted groups, which remain in the body and may cause local inflammatory reaction or systematic immune response [103]. Besides, harmful free radicals and potentially damaging polymerization conditions can affect cell viability [104]. Furthermore, photopolymerization methods usually lead to the hydrogel network non-idealities, containing irregular polymer chains that may adversely affect drug release performance and material properties [105].

Since the first hydrogels were synthesized by photopolymerization in the 1960s, it remains a widely used approach of preparing PEG-based hydrogels for biomedical applications [106, 107]. PEG prepolymers are usually modified with meth(acrylates) to form crosslinkable macromonomers that form hydrogels with a range of different chemistries through photopolymerization.

Biodegradation properties can be introduced into the photochemically crosslinked PEG-based hydrogels, by designing a polymer composed of a central PEG chain and telechelic oligomeric blocks or other degradable moieties, and gel degradation is easily tailored by varying the length and/or chemistry of the hydrolytically labile group [108, 109]. Moreover, to make bioactive PEG hydrogels,

researchers usually incorporate bioactive molecules into PEG hydrogel networks, by photo-copolymerization of acrylated biomolecules [110, 111]. Recently, an alternative approach, called thiol-acrylate photopolymerization has been developed by Anseth and coworkers to fabricate and bioactively modify PEG hydrogels [39, 112]. In addition, patterned structures, as well as photoreversible systems - meaning that upon exposure to light the previously formed gels photodegrade - of PEG-based hydrogels can be obtained by photopolymerization, which are potentially quite useful for biomedical application [113].

1.4.2.2 Crosslinking by Michael type addition reactions

Unlike photopolymerization, resulting in some damage of the cells, Michael addition reactions for hydrogel preparation can overcome this problem with some other benefits, such as controlled reaction time, ability to form different types of bonds, and relatively mild reactivity with biomolecules [114, 115]. This reaction involves the efficient coupling of electron poor olefins (e.g. acrylates) with a vast array of nucleophiles (e.g. amines, thiols) [92], for example in Figure 7b. Michael addition reactions, which have been first introduced by Hubbell and co-workers, are suitable for the preparation of injectable hydrogels, because this chemical reaction occurs in aqueous medium at physiological pH and room temperature [116]. The main disadvantages of this reaction are the presence of thiol groups, which may reduce the native disulfide bonds of the encapsulated proteins and cause protein denaturation, leading to decreased bioactivity and increased immunogenicity and lacking of spatial and temporal control over the network structure during network gelation [117].

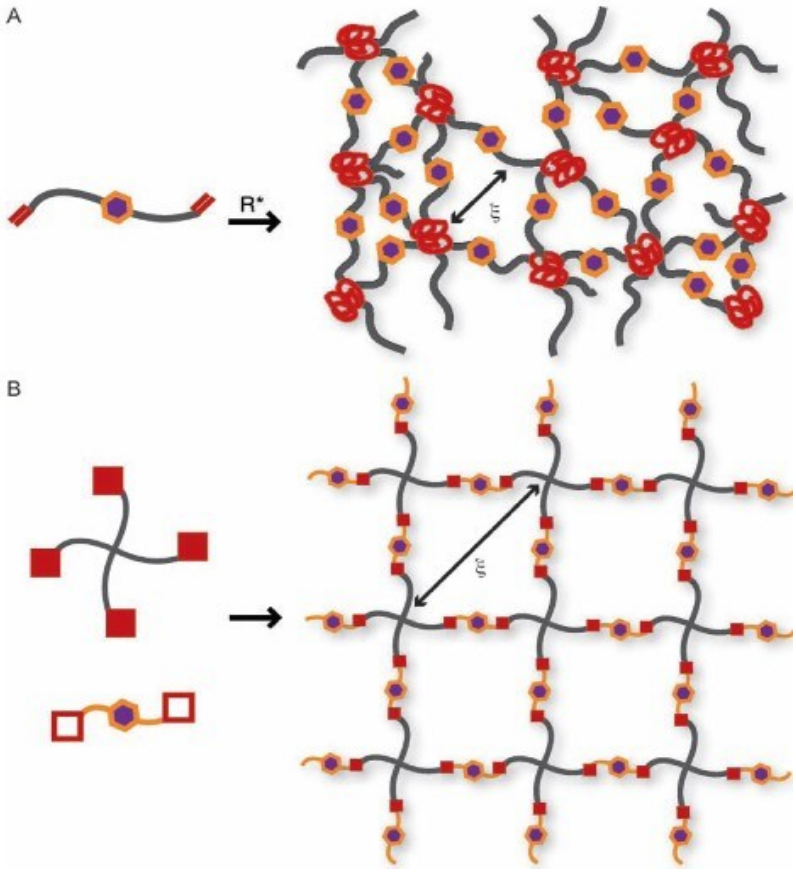

Figure 8. Schematic structures of PEG hydrogels formed via: A, chain-growth, for example photopolymerization B, step-growth, for example Michael addition reaction [118].

In contrast to the chain growth mechanism of photopolymerization, Michael addition reaction to prepare PEG-based hydrogels proceeds via a step growth mechanism, and the resulting network structures are shown in Figure 8 [118]. The randomly coiled poly(methacrylate) chains are formed by free radical chain polymerization in Figure 8A. However, nearly perfect networks by step growth polymerization can be formed through multifunctional PEG monomers polymerized by Michael addition reaction (Figure 8B). Nearly perfect network structure formation permits more precise control over the gel crosslinking density and subsequent material properties, which often lead to superior mechanics when compared to chain growth networks of similar crosslink density [90]. Meanwhile this ideal network is highly beneficial for the delivery of therapeutics, due to the precisely controlled release kinetics and accurate mathematical predictions of drug dosing prior to the delivery [117].

1.4.2.3 Crosslinking by click chemistry

Recently, click reaction utilized for hydrogel fabrication,(Figure 7c) another type of step-growth mechanism, has gained great interest due to its rapid and specific reaction, as well as its versatility with respect to bioconjugation [119]. The near-ideal network connectivity and improved physical properties can be obtained by the utilization of copper-catalyzed azide-alkyne click cycloaddition (CuAAC) [120]. Additionally, efficient post-functionalization of these reactive hydrogels encouraged the incorporation of a variety of biomolecules into the hydrogel matrix in a controlled manner, which is very attractive since it allows easier fabrication of various functional and responsive materials [120, 121]. The advantages of this copper(I)-catalyzed reaction to fabricate hydrogels networks include fast reaction rate and quantitative conversion.

However, the major drawback for conventional click hydrogels is that these cycloaddition reactions are usually catalyzed by copper ion, which is a rather toxic ion and needs to be removed after hydrogel formation [122-124]. To address this issue, metal-free click reactions provide an attractive alternative. The utilization of metal-free click-reactions, such as the strain-promoted [3+2] cycloaddition reactions, thiolene reactions, and Diels-Alder cycloadditions, to fabricate hydrogels have been actively developed [125, 126]. The specificity and fidelity of metal-free click chemistry offers great potential for a variety of biomedical applications, including live cell imaging, cell surface engineering, and cell encapsulation. In addition, more recently, Bowman et al. reported the discovery of CuAAC reaction via photochemical reduction of Cu(II) to Cu(I), and it is demonstrated that this technique affords comprehensive spatial and temporal control and can be applied for small molecule synthesis, patterned material fabrication and patterned chemical modification [127], which also have been utilized in the herein present PhD project for hydrogels formation.

1.4.2.4 Crosslinking by mixed-mode polymerization

PEG-based hydrogels can also be fabricated via mixed-mode polymerizations which exhibit characteristics between chain and step-growth polymerizations [100]. This gelation of mixed-mode polymerization overcomes the disadvantages of chain-growth polymerizations (toxic initiator, no control over network structure) and step-growth polymerizations (low crosslinking density, long polymerization time, no spatial and temporal control over gelation) mentioned in the above sections [104, 112, 117, 128]. The network structure that results from this mechanism can be tuned from being chain-like to more step-like. Furthermore, the mixed-mode polymerizations facilitate the incorporation of biomolecules, such as peptides, into the gel matrix at lower concentrations [112, 129].

One such method is mixed-mode polymerizations of alkynes monomers and multifunctional thiols developed by Anseth and coworkers for hydrogel synthesis, in which vinyl groups can react with consecutively with two thiols [130, 131]. In mixed-mode photopolymerization, the commonly used initiator in chain-growth photo polymerization is not required [130]. And highly crosslinked polymer networks, as well as spatial and temporal control, can be achieved via thiol-yne photopolymerizations, without the network non-idealities commonly found in photopolymerized hydrogels [131].

References

[1] Williams, D. F. On the nuture of biomaterials*.Biomaterials* **2009**, 30, 5897-5909.

[2] Ratner, B. D.; Bryant, S. J. Biomaterials: where we have been and where we are going. *Annu. Rev. Biomed. Eng.* **2004**, 6, 41-75..

[3] Langer, R.; Tirrell, D.A. Designing materials for biology and medicine. *Nature* **2004**, 428, 487–492.

[4] Langer, R.; Peppas, N. A. Advances in Biomaterials, Drug Delivery, and Bionanotechnology. *AIChE Journal* **2003**, 49, 2990-3006.

[5] King, R. G.; Donohue, G. F. Estimates of medical device spending in the United States. **2007**.

[6]. Hoffman, A. S. Hydrogels for biomedical applications. *Adv. Drug Deliv. Rev.* **2002**, 43, 3–12.

[7] Peppas, N. A.; Bures, P.; Leobandung, W.; Ichikawa, H. Hydrogels in pharmaceutical formulations. *Eur. J. Pharm. Biopharm.* **2000**, 50, 27–46.

[8] Bohidar, H. B.; Dubin, P.; Osade, Y. Polymer Gels: Fundamentals and Applications (ACS Symposium Series). Washington, *DC: American Chemical Society;* **2003**.
[9] Slaughter, B. V.; Khurshid, S. S.; Fisher, O. Z.; Khademhosseini, A.; Peppas. N. A. Hydrogels in Regenerative Medicine *Adv. Mater.* **2009**, 21, 3307–3329
[10] Kloczkowski, A. Application of statistical mechanics to the analysis of various physical properties of elastomeric networks – a review. *Polymer* **2002**, 43, 1503–1525.
[11] Boyce, M. C.; Arruda, E. M. Constitutive models of rubber elasticity: a review. Rubber *Chem. Technol.* **2000**, 73, 504–523.
[12] Gent, A. N. Rubber and rubber elasticity - review. *J. Polym. Sci., Part C: Polym. Symp.* **1974**, 1–17.
[13] Elisseeff, J.; Mcintosh, W.; Fu, K.; Blunk, B. T.; Langer, R. Controlled-release of IGF-I and TGF-beta1 in a photopolymerizing hydrogel for cartilage tissue engineering. *J. Orthop.Res.* **2001,** 19, 1098-1104.
[14] Anseth, K. S.; Burdick, J. A. New Directions in Photopolymerizable Biomaterials. *MRS Bull.* **2002,** 27, 130-136.
[15] Pescosolido, L.; Piro, T.; Vermonden, T.; Coviello, T.; Alhaique, F.; Hennink, W. E.; Matricardi, P. Biodegradable IPNs based on oxidized alginate and dextran-HEMA for controlled release of proteins, *Carbohydr. Polym.* **2011**, 86, 208-213.
[16] Chan, A.W.; Neufeld, R.J. Tuneable semi-synthetic network alginate for absorptive encapsulation and controlled release of protein therapeutics. *Biomaterials* 2010, 31, 9040-9047.
[17] Deligkaris, K.; Tadele T. S.; Olthuis, W.; van den Berg, A. Hydrogelbased devices for biomedical applications. *Sensors and ActuatorsB: Chemical* **2010,** 147, 765-774.
[18] Topuz, F.; Buenger, D.; Tanaka, D.; Groll, J. Hydrogels in biosensing applications. *Comprehensive biomaterials* **2011**, 491-517.
[19] Strehin, I.; Nahas, Z.; Arora, K.; Nguyen, T.; Elisseeff, J. A versatile pH sensitive chondroitin sulfate-PEG tissue adhesive and hydrogel. *Biomaterials,* **2010,** 31, 2788-2797.
[20] Hubbell, J. A. Hydrogel systems for barriers and local drug delivery in the control of wound healing. *J. Controlled Release*, **1996**, 39, 305-313.
[21] Hou, Y.; Matthews, A. R.; Smitherman, A. M.; Bulick, A. S.; Hahn, M. S.; Hou, H.; Han, A.; Grunlan, M. A. Thermoresponsive nanocomposite hydrogels with cell-releasing behavior. *Biomaterials*, **2008**, 29, 3175-3184.
[22] Stock, U. A.; Vacanti, J. P. Tissue engineering: current state and prospects. *Annu Rev Med* **2001**, 52, 443-451..
[23] Lim, F.; Sun, A. M. Microencapsulated islets as bioartificial endocrine pancreas. *Science* **1980**, 210, 908-910.
[24] Elisseeff, J.; Anseth, K.; Sims, D.; McIntosh, W.; Randolph, M.; Langer, R. Transdermal photopolymerization for minimally invasive implantation. *Proc. Natl. Acad. Sci.* **1999**, 96, 3104-3107.
[25] Elisseeff, J.; McIntosh, W.; Anseth, K.; Riley, S.; Ragan, P.; Langer, R. Photoencapsulation of chondrocytes in poly(ethylene oxide)-based semi-interpenetrating networks. *J. Biomed. Mater. Res.* **2000**, 51, 164-171.
[26] S. Lahooti, M. V. Sefton, Agarose enhances the viability of intraperitoneally implanted microencapsulated L929 fibroblasts. *Cell Transplant.* **2000**, 9, 785-796.

[27] Vermonden, T.; Censi, R.; Hennink, W. E. Hydrogels for Protein Delivery *Chem. Rev.* **2012**, 112, 2853−2888

[28] Peppas, N.A. Hydrogels and drug delivery. *Curr. Opin. Colloid Interface Sci.* **1997**, 2, 531-537.

[29] Peppas, N. A.; Wood, K. M.; Blanchette, J. O. Hydrogels for oral delivery of therapeutic proteins. *Expert Opin. Biol. Ther.* **2004**, 4, 881-887.

[30] An, Y. J.; Hubbell, J. A. Intraarterial protein delivery via intimally-adherent bilayer hydrogels. *J. Controlled Release* **2000**, 64, 205-215.

[31] Bergmann, N. M.; Peppas, N. A. Molecularly imprinted polymers with specific recognition for macromolecules and proteins. *Prog. Polym. Sci.* **2008**, 33, 271-288.

[32] Peppas, N. A. Intelligent Biomaterials as Pharmaceutical Carriers in Microfabricated and Nanoscale Devices. *MRS Bull.* **2006**, 31, 888-893.

[33] Lin, C. C.; Boyer, P. D.; Aimetti, A. A.; Anseth, K. S. Regulating MCP-1 diffusion in affinity hydrogels for enhancing immuno-isolation, *J. Control. Release* **2010,** 142, 384-391.

[34] Sun, G.; Shen, Y. I.; Kusuma, S.; Fox-Talbot, K.; Steenbergen, C. J.; Gerecht, S. Functional neovascularization of biodegradable dextran hydrogels with multiple angiogenic growth factors. *Biomaterials* **2011**, 32, 95-106.

[35] Balakrishnan, B.; Banerjee, R. Biopolymer-based hydrogels for cartilage tissue engineering. *Chem. Rev.* **2011**, 111, 4453.

[36] Wang, W. B.; Wang, A. Q. Synthesis and swelling properties of pH-sensitive semi-IPN superabsorbent hydrogels based on sodium alginate-g-poly(sodium acrylate) and polyvinylpyrrolidone. *Carbohydr. Polym.* **2010**, 80, 1028–1036.

[37]Wu, Z. M.; Zhang, X. G.; Zheng, C.; Li, C. X.; Zhang, S. M.; Dong, R. N.; Yu, D. M. Disulfide-crosslinked chitosan hydrogel for cell viability and controlled protein release. *Eur. J. Pharm. Sci.* **2009**, 37, 198–206.

[38] Horn, E. M.; Beaumont, M.; Shu, X. Z.; Harvey, A.; Prestwich, G. D.; Horn, K. M.; Gibson, A. R.; Preul, M. C.; Panitch, A. Influence of cross-linked hyaluronic acid hydrogels on neurite outgrowth and recovery from spinal cord injury. *J. Neurosurg.* **2007**, 6, 133–140.

[39] Zhu, J. M. Bioactive modification of poly(ethylene glycol) hydrogels for tissue engineering. *Biomaterials* **2010**, 31, 4639-4656.

[40] Drury, J. L.; Mooney, D. J. Hydrogels for tissue engineering: scaffold design variables and applications. *Biomaterials* **2003**, 24, 4337-4351.

[41] Place, E. S.; George, J. H.; Williams C. K.; Stevens, M. M. Synthetic polymer scaffolds for tissue engineering. *Chem. Soc. Rev.* **2009,** 38, 1139-1151.

[42] Mart, R. J.; Osborne, R. D.; Stevens, M. M.; Ulijn, R. V. Peptide-based stimuli-responsive biomaterials. *Soft Matter* **2006**, 2, 822-835.

[43] Peppas, N. A.; Hilt, J. Z.; Khademhosseini A.; Langer, R. Hydrogels in biology and medicine: From molecular principles to bionanotechnology. *Adv. Mater.* **2006**, 18, 1345–1360.

[44] Drury, J. L.; Mooney. D. J. Hydrogels for tissue engineering: scaffold design variables and applications. *Biomaterials* **2003**, 24, 4337–4351.

[45] Mellott, M. B.; Searcy, K.; Pishko, M. V.; Release of protein from highly cross-linked hydrogels of poly(ethylene glycol) diacrylate fabricated by UV polymerization. *Biomaterials* **2001**, 22, 929–941.

[46] Peppas, N. A.; Keys, K. B.; Torres-Lugo, M.; Lowman, A. M. Poly(ethylene glycol)-containing hydrogels in drug delivery. *J. Control. Release.* **1999**, 62, 81–87.

[47] Lee, J. H.; Lee, H. B.; Andrade, J. D. Blood compatibility of polyethylene oxide surfaces. *Prog Polym Sci* **1995**, 20, 1043-1479.
[48] Alcantar, N. A.; Aydil, E. S.; Israelachvili, J. N. Polyethylene glycol-coated biocompatible surfaces. *J Biomed Mater Res* **2000**, 51, 343-351.
[49] Nuttelman, C. R.; Rice, M. A.; Rydholm, A. E.; Salinas, C. N.; Shah, D. N.; Anseth, K. S. Macromolecular monomers for the synthesis of hydrogel niches and their application in cell encapsulation and tissue engineering. *Prog. Polym. Sci.* **2008**, 33, 167– 179.
[50] Keys, K. B.; Andreopoulos, F. M.; Peppas, N. A. Poly(ethylene glycol) star polymer hydrogels. *Macromolecules* **1998**, 31, 8149-8156.
[51] Dalton, P.D.; Hostert, C.; Albrecht, K.; Moeller, M.; Groll, J. Structure and properties of urea-crosslinked star poly[(ethylene oxide)-ran- (propylene oxide)] hydrogels. *Macromol Biosci* **2008**, 8, 923-931.
[52] Sukumar, V. S.; Lopina, S. T. Network model for the swelling properties of end-linked linear and star poly(ethylene oxide) hydrogels. *Macromolecules* **2002**, 35,, 10189-10192.
[53] Kobayashi, M.; Chang, Y. S.; Oka, M. A two year in vivo study of polyvinyl alcohol-hydrogel (PVA-H) artificial meniscus. *Biomaterials* **2005,** 26, 3243-3248.
[54] Lapeyre, V.; Gosse, I.; Chevreux, S.; Ravaine, V. Monodispersed glucose- responsive microgels operating at physiological salinity. *Biomacromolecules* **2006**, 7, 3356-3363.
[55] Bryant, S. J.; Cuy, J. L.; Hauch, K. D.; Ratner, B. D. Photo-patterning of porous hydrogels for tissue engineering. *Biomaterials* **2007**, 28, 2978-2986.
[56] Zagris, N. Extracellular matrix in development of the early embryo. *Micron* **2001**, 32, 427-438.
[57] Aumailley, M.; Gayraud, B. Structure and biological activity of the extracellular matrix. *J. Mol. Med.* **1998**, 76, 253-265.
[58] Daley, W. P.; Peters, S. B.; Larsen, M. Extracellular matrix dynamics in development and regenerative medicine. *J. Cell Sci.* **2008,** 121, 255-264.
[59] Liu, L. S.; Kost, J.; Yan, F.; Spiro, R. C. Hydrogels from Biopolymer Hybrid for Biomedical, Food, and Functional Food Applications. *Polymers* **2012**, 4, 997-1011.
[60] Serban, M. A.; Prestwich, G. D. Modular extracellular matrices: solutions for the puzzle. *Methods* **2008**, 45, 93-98.
[61] Yamaguchi, N.; Chae, B. S.; Zhang, L.; Kiick, K. L.; Furst, E. M. Rheological characterization of polysaccharide-poly(ethylene glycol) star copolymer hydrogels. *Biomacromolecules* **2005**, 6, 1931-1940.
[62] Kiick, K. L. Peptide - and protein -mediated assembly of heparinized hydrogels. *Soft Matter* **2008**, 4, 29-37.
[63] Schexnailder, P.; Schmidt, G. Nanocomposite polymer hydrogels *Colloid Polym Sci* **2009**, 287, 1-11.
[64] Haraguchi, K.; Takehisa, T. Nanocomposite hydrogels: a unique organic/inorganic network structure with extraordinary mechanical, optical, and swelling/de-swelling properties. *Adv Mater* **2002**, 14, 1120-1124.
[65] Yoshida, R.; Uchida, K.; Kaneko, Y.; Sakai, K.; Kikuchi, A.; Sakurai, Y.; Okano, T. Comb-type grafted hydrogels with rapid deswelling response to temperature changes. nature 1995, 374, 240-242.
[66] Hou, Y.; Matthews, A. R.; Smitherman, A. M.; Bulick, A. S.; Hahn, M. S.; Hou, H.; Han, A.;

Grunlan, M. A. Thermoresponsive nanocomposite hydrogels with cell-releasing behavior. *Biomaterials* **2008**, 29, 3175-3184.
[67] Weiner, S.; Wagner, H. D. The material bone: structure-mechanical function relations. *Annu Rev Mater Sci* **1998**, 28, 271-98.
[68] Snyders, R. V.; Eppley, B. L.; Krukoueski, M.; Delfino, J. J. Enhancement of repair in experimental calvarial bone defects using calcium sulfate and dextran beads. *J. Oral. Maxillofac. Surg.* **1993**, 51, 517-524.
[69] Yamaguschi, I.; Tokuchi, K.; Fukuzaki, H.; Koyama, Y.; Takakuda, K.; Monma, H.; Tanaka, J. Preparation and microstructure analysis of chitosan/hydroxyapatite nanocomposites. *J.Biomed. Mater. Res.* **2001**, 55, 20-27.
[70] Ghanaati, S. et al. An injectable bone substitute composed of beta-tricalcium phosphate granules, methylcellulose and hyaluronic acid inhibits connective tissue influx into its implantation bed in vivo. *Acta Biomater* **2011**, 7, 4018-4028.
[71] Van Tomme, S. R.; Storm, G.; Hennink, W. E. In situ gelling hydrogels for pharmaceutical and biomedical applications. *International Journal of Pharmaceutics.* **2008**, 355, 1-18.
[72] Hennink, W. E.; van Nostrum, C. F. Novel crosslinking methods to design hydrogels. *Advanced Drug Delivery Reviews* **2012**, 64, 223-236
[73] Bae, S. J.; Suh, J. M.; Sohn, Y. S.; Bae, Y. H.; Kim, S. W.; Jeong, B. Thermogelling poly(caprolactone-6-ethylene glycol-b-caprolactone) aqueous solutions. Macromolecules 2005, 38, 5260-5265.
[74] Nagahama, K.; Ouchi, T.; Ohya, Y. Temperature-induced hydrogels through self-assembly of cholesterol-substituted star PEG-b-PLLA copolymers: An injectable scaffold for tissue engineering. *Advanced Functional Materials* **2008**, 18, 1220-1231.
[75] Mathur, A. M.; Hammonds, K. F.; Klier, J.; Scanton, A. B. Equilibrium swelling of poly(methacrylic acid-g-ethylene glycol) hydrogels. *J. Controlled Release* 1998, 54, 177-184.
[76] Boeckl, M. S.; Perry, J.; Leber, E. R.; Nair, P.; Ratner, B. D. Development and characterization of poly(vinyl alcohol)-amino acid hydrogels for the use as biomaterials. *Polym. Preprints* **2003**, 44, 677-478.
[77] De Jong, S. J.; Van Nostrum, C. F.; Kroon-Batenburg, L. M. J.; Kettenes-van Den Bosch, J. J.; Hennink, W. E. Oligolactate-grafted dextran hydrogels: Detection of stereocomplex crosslinks by X-ray diffraction. *Journal of Applied Polymer Science* **2002**, 86, 289-293.
[78] Bos, G. W.; Hennink, W. E.; Brouwer, L. A.; Den Otter, W.; Veldhuis, T. F. J.; Van Nostrum, C. F.; Van Luyn, M. J. A. Tissue reactions of in situ formed dextran hydrogels crosslinked by stereocomplex formation after subcutaneous implantation in rats. *Biomaterials* **2005**, 26, 3901-3909.
[79] LeRoux, M. A.; Guilak, F.; Setton, L. A. Compressive and shear properties of alginate gel: Effects of sodium ions and alginate concentration. *J. Biomed.Mater. Res.* **1999**, 47, 46-53.
[80] Zhao, L.; Weir, M. D.; Xu, H. H. An injectable calcium phosphate-alginate hydrogel-umbilical cord mesenchymal stem cell paste for bone tissue engineering. *Biomaterials* **2010**, 31, 6502-6510.
[81] Wu, K.; Yang, J.; Koňák, Č.; Kopečková, P.; Kopeček, Novel Synthesis of HPMA Copolymers Containing Peptide Grafts and Their Self-Assembly Into Hybrid Hydrogels. *J. Macromol. Chem. Phys.* 2008, 209, 467-475.
[82] Micklitsch, C. M.; Knerr, P. J.; Branco, M. C.; Nagarkar, R.; Pochan, D. J.; Schneider, J. P. Zinc-

Triggered Hydrogelation of a Self-Assembling β-Hairpin Peptide. *Angew. Chem.* **2011**, 123, 1615-1617.
[83] Jeong, B. et al. Thermosensitive sol-gel reversible hydrogels. *Advanced Drug Delivery Reviews* **2012**, 64, 154-162.
[84] Censi, R.; Vermonden, T.; Deschout, H.; Braeckmans, K.; Di Martino, P.; De Smedt, S.; Van Nostrum, C.; Hennink, W. E. Photopolymerized thermosensitive poly(HPMAlactate)-PEG-based hydrogels: effect of network design on mechanical properties, degradation, and release behavior. *Biomacromolecules* **2010**, 11, 2143-2151.
[85] Shim, W. S.; Yoo, J. S.; Bae, Y. H.; Lee, D. S. Novel injectable pH and temperature sensitive block copolymer hydrogel. *Biomacromolecules* **2005**, 6, 2930-2934.
[86] Shim, W. S.; Kim, S. W.; Lee, D. S. Sulfonamide-based pH- and temperature-sensitive biodegradable block copolymer hydrogels. *Biomacromolecules* **2006**, 7, 1935-1941.
[87] Lin, C. C.; Metters, A. T. Hydrogels in controlled release formulations: Network design and mathematical modeling. *Adv. Drug Deliv. Rev.* **2006**, 58, 1379-1408.
[88] Lee, H. J.; Lee, J. S.; Chansakul, T.; Yu, C.; Elisseef, J. H.; Yu, S. M. Collagen mimetic peptide-conjugated photopolymerizable PEG hydrogel. *Biomaterials* **2006**, 27, 5268-5276.
[89] Censi, R.; Vermonden, T.; van Steenbergen, M. J.; Deschout, H.; Braeckmans, K.; De Smedt, S. C.; van Nostrum, C. F.; di Martino, P.; Hennink, W. E. Photopolymerized thermosensitive hydrogels for tailorable diffusion-controlled protein delivery. *Journal of Controlled Release* **2009**, 140, 230-236.
[90] Lutolf, M. P.; Hubbell, J. A. Synthesis and Physicochemical Characterization of End-Linked Poly(ethylene glycol)-co-peptide Hydrogels Formed by Michael-Type Addition. *Biomacromolecules* **2003**, 4, 713-722.
[91] Hiemstra, C.; Van der Aa, L. J.; Zhong, Z.; Dijkstra, P. J.; Feijen, J. Rapid in situ-forming degradable hydrogels from dextran thiols through Michael addition. *Biomacromolecules* **2007**, 8, 1548-1556.
[92] Mather, B. D.; Viswanathan, K.; Miller, K. M.; Long, T. E. Michael addition reactions in macromolecular design for emerging technologies. *Prog Polym Sci* **2006**, 31, 487-531.
[93] Altin, H.; Kosif, I.; Sanyal, R. Fabrication of "Clickable" Hydrogels via Dendron−Polymer Conjugates. *Macromolecules* **2010**, 43, 3801-3808.
[94] Zhang, J.; Xu, X. D.; Wu, D. Q.; Zhang, X. Z.; Zhuo, R. X. Synthesis of thermosensitive P(NIPAAm-*co*-HEMA)/cellulose hydrogels via "click" chemistry. *Carbohydr. Polym*. **2009**, 77, 583-589.
[95] Aimetti, A. A.; Machen, A. J.; Anseth, K. S. Poly(ethylene glycol) hydrogels formed by thiol-ene photopolymerization for enzyme-responsive protein delivery. *Biomaterials* **2009**, 30, 6048-6054.
[96] Dirksen, A.; Meijer, E. W.; Adriaens, W.; Hackeng, T. M. Strategy for the synthesis of multivalent peptide-based nonsymmetric dendrimers by native chemical ligation *Chem. Commun.* **2006**, 1667-1669.
[97] Su, J.; Hu, B. H.; Lowe, W. L. Jr; Kaufman, D. B.; Messersmith, P. B. Anti- inflammatory peptide-functionalized hydrogels for insulin-secreting cell encapsulation. *Biomaterials* **2010**, 31, 308-314.
[98] Freddi, G.; Anghileri, A.; Sampaio, S.; Buchert, J.; Monti, P.; Taddei, P. Tyrosinasecatalyzed modification of Bombyx mori silk fibroin: grafting of chitosan under heterogeneous reaction

conditions. *J Biotechnol* **2006**, 125, 281-294.
[99] Park, K. M.; Shin, Y. M.; Joung, Y. K.; Shin, H.; Park, K. D. In situ forming hydrogels based on tyramine conjugated 4-Arm-PPO-PEO via enzymatic oxidative reaction. *Biomacromolecules* **2010**, 11, 706-712.
[100] Liu, S. Q.; Tay, R.; Khan, M.; Rachel Ee, P. L.; Hedrickc, J. L.; Yang, Y. Y. Synthetic hydrogels for controlled stem cell differentiation. *Soft Matter* **2010**, 6, 67-81.
[101] Nicodemus, G. D.; Bryant, S. J. Cell encapsulation in biodegradable hydrogels for tissue engineering applications. *Tissue Eng., Part B: Rev*. **2008**, 14, 149-165.
[102] Ifkovits, J. L.; Burdick, J. A. Review: photopolymerizable and degradable biomaterials for tissue engineering applications. *Tissue Eng.* **2007**, 13, 2369-2385.
[103] Fournier, E.; Passirani, C.; Montero-Menei, C. N.; Benoit, J. P. Biocompatibility of implantable synthetic polymeric drug carriers: focus on brain biocompatibility. *Biomaterials* **2003,** 24, ,3311-3331.
[104] Fedorovich, N. E.; Oudshoorn, M.H.; van Geemen, D.; Hennink, W.E;. Alblas, J.; Dhert, W. J. A. The effect of photopolymerization on stem cells embedded in hydrogels. *Biomaterials* **2009**, 30, 344-353.
[105] Metters, A. T.; Anseth, K. S.; Bowman, C. N. A statistical kinetic model for the bulk degradation of PLA-b-PEG-b-PLA hydrogel networks: Incorporating network non-idealities. *J. Phys. Chem. B.* **2001**, 105, 8069-8076.
[106] Wichterle, O.; Lı´m, D. Hydrophilic Gels for Biological Use. *Nature* **1960**, 185, 117–118.
[107] Kloxin, A. M.; Kasko, A. M.; Salinas, C. N.; Anseth, K. S. Photodegradable hydrogels for dynamic tuning of physical and chemical properties. *Science* **2009**, 324, 59–63.
[108] Metters, A. T.; Anseth, K. S.; Bowman, C. N. Fundamental studies of a novel, biodegradable PEG-b-PLA hydrogel. *Polymer* **2000**, 41, 3993-4004.
[109] Lu, S.; Anseth, K. S. Release behaviour of high molecular weight solutes from poly(ethylene glycol)-based degradable networks. *Macromolecules* **2000**, 33, 2509-2515.
[110]Zhu, J,; Beamish, J. A.; Tang, C.; Kottke-Marchant, K.; Marchant, R. E. Extracellular matrix-like cell-adhesive hydrogels form RGD-containing poly(ethylene glycol) diacrylate. *Macromolecules* **2006,** 39, 1305-1307.
[111] Zhu, J.; Tang, C.; Kottke-Marchant, K.; Marchant, R. E. Design and synthesis of biomimetic hydrogel scaffolds with controlled organization of cyclic RGD peptides. *Bioconjug. Chem.* **2009**, 20, 333-339.
[112]Salinas, C. N.; Anseth, K. S. Mixed mode thiol-acrylate photopolymerizations for the synthesis of PEG-peptide hydrogels. *Macromolecules* **2008**, 41, 6019-6026.
[113] Andreopoulos, F. M.; Beckman, E. J.; Russell, A. J. Light-induced tailoring of PEG-hydrogel properties. *Biomaterials* **1998**, 19, 1343-1352.
[114] Elbert, D. L.; Luthof, M. P.; Pratt, A. B.; Halstenberg, S.; Hubbell, J. A. Protein release from PEG hydrogels that are similar to ideal Flory-Rehner Networks, *Proc. Int. Symp. Controlled Release Bioact. Mater.* **2001**, 28, 987-988.
[115] Metters, A.; Hubbell, J. Network formation and degradation behavior of hydrogels formed by Michael-type addition reactions. *Biomacromolecules* **2005**, 6, 290-301.
[116] Lutolf, M.; Raeber, G.; Zisch, A.; Tirelli, N.; Hubbell, J. Cell-Responsive Synthetic Hydrogels. *Adv. Mater.* **2003**, 15, 888-892.
[117] Lin, C. C.; Anseth, K. S. PEG hydrogels for the controlled release of biomolecules in

regenerative medicine. *Pharm. Res.* **2009**, 26, 631–643.
[118] Kloxin, A. M.; Kloxin, C. J.; Bowman, C. N.; Anseth, K. S. Mechanical Properties of Cellularly Responsive Hydrogels and Their Experimental Determination. *Adv. Mater.* **2010**, 22, 3484-3494.
[119] Liu, S. Q.; Ee, P. L. R.; Ke, C. Y.; Hedrick J. L.; Yang, Y. Y. Biodegradable poly(ethylene glycol)-peptide hydrogels with well-defined structure and properties for cell delivery. *Biomaterials* **2009**, 30, 1453–1461.
[120] Malkoch, M.; Vestberg, R.; Gupta, N.; Mespouille, L.; Dubois, P.; Mason, A. F.; Hedrick, J. L.; Liao, Q.; Frank, C. W.; Kingsbury, K.; Hawker, C. J. Synthesis of well-defined hydrogel networks using Click chemistry. *Chem. Commun.* **2006**, 2774-2776.
[121] Altin, H.; Kosif, I.; Sanyal, R. Fabrication of Clickable Hydrogels viaDendron-Polymer Conjugates. *Macromolecules* **2010**, 43, 3801-3808.
[122] Kolb, H. C.; Finn, M. G.; Sharpless, K. B. Click Chemistry: Diverse Chemical Function from a Few Good Reactions. *Angew. Chem., Int. Ed.,* **2001**, 40, 2004–2021.
[123] Lodge, T. P. A Virtual Issue of Macromolecules: "Click Chemistry in Macromolecular Science". *Macromolecules* **2009,** 42, 3827–3829.
[124] Letelier, M. E.; Sánchez-Jofré, S.; Peredo-Silva, L.; Cortés-Troncoso, J.; Aracena-Parks, P. Mechanisms underlying iron and copper ions toxicity in biological systems: Pro-oxidant activity and protein-binding effects. *Chem. Biol. Interact.* **2010**, 188, 220-227.
[125] Becer, C. R.; Hoogenboom, R.; Schubert, U. S. Click Chemistry beyond Metal-Catalyzed Cycloaddition. *Angew. Chem. Int. ed.* **2009**, 48, 4900- 4908.
[126] Debets, M. F.; van der Doelen, C. W.; Rutjes, F. P.; van Delft, F. L. Azide: a unique dipole for metal-free bioorthogonal ligations. *ChemBioChem* **2010,** 11, 1168-1184.
[127] Adzima, B. J.; Tao, Y.; Kloxin, C. J.; DeForest, C. A.; Anseth, K. S.; Bowman. C. N.; Spatial and temporal control of the alkyne-azide cycloaddition by photoinitiated Cu(II) reduction, *nature chemistry* **2011**, 3, 256-259.
[128] Rydholm, A. E.; Reddy, S. K.; Anseth, K. S.; Bowman, C. N. Controlling network structure in degradable thiol-acrylate biomaterials to tune mass loss behavior. *Biomacromolecules* **2006,** 7, 2827-2836.
[129] Salinas, C. N.; Anseth, K. S. The enhancement of chondrogenic differentiation of human mesenchymal stem cells by enzymatically regulated RGD functionalities. *Biomaterials* **2008,** 29, 2370-2377.
[130] Cramer, N. B.; Scott, J. P.; Bowman, C. N. Photopolymerizations of thiol-ene polymers without photoinitiators. *Macromolecules* **2002,** 35, 5361-5365.
[131] Fairbanks, B. D.; Scott, T. F.; Kloxin, C. J. ; Anseth, K. S.; Bowman, C. N. Thiol-Yne Photopolymerizations: Novel Mechanism, Kinetics, and Step-Growth Formation of Highly Cross-Linked Networks. *Macromolecules* **2009,** 42, 211-217.

Chapter 2.

In situ formation of novel poly(ethylene glycol)-based hydrogels via amine-Michael type addition with tunable mechanics and chemical functionality

---

Abstract

In this chapter, the synthesis of a novel PEG-based hydrogel formed by amine-Michael type addition is reported. Star-shaped PEG molecules (having 8 arms with acrylate end groups; **8PEG**) are utilized as macromonomers, and NH_3 in ammonia solution (30%) is used as crosslinker, a small and volatile molecule, which unreacted remains can be easily removed from the gel matrix. A distinct relationship between hydrogel structure and properties has been obtained, i.e. higher amounts of NH_3 in the reaction lead to higher crosslinking density, higher bulk and surface elasticity and smoother surface morphologies. Thus, the network architecture can be tailored by changing the addition of NH_3 amount to produce gels with tunable gelation time, besides controlled mechanical and physicochemical characteristics. Moreover, it is demonstrated that the incomplete amine-Michael type addition chemistry leads to gel formation with plenty of residual acrylate groups that were verified by LC-MS analysis and Raman spectroscopy. Those residual acrylate groups enable us on the one hand to (bio)functionalize the gels, e.g. via a second Michael-type addition reaction, employing thiol-reactive (bio)functional molecules and/or to perform additional UV-curing (photo-initiated crosslinking) to further stabilize the pre-formed gels with higher mechanical integrity, much denser network structure and less water uptake capacity. The proof of principle of the post-gelation reactivity is demonstrated by fabricating nano-scale precise 3D patterns and by using a thiolated fluorescent dye, which reacts at the surface of the crosslinked gel and shows a small but clear penetration profile of around 50 µm from the surface into the bulk of the reactive gel.

2.1 Introduction

Hydrogels, i.e. three-dimensional hydrophilic cross-linked polymer networks, have been widely used in a diverse range of applications [1], such as drug delivery, biosensors, tissue engineering and wound healing, owing to their excellent biocompatibility, tunable chemical and physical properties and capability of incorporating bioactive molecules [2-4]. Moreover, when compared with natural hydrogels, e.g. alginate, hyaluronic acid and collagen gels, synthetic hydrogels are superior to offer great control over not only the gel's chemical composition but also its mechanical properties and overall architecture, as well as the ease to incorporate chemical and physical cues into the gel matrix and to customize their transport properties [5].

One of the conventional and robust gel formation methods is step-growth polymerization, especially for Michael-type conjugate addition [6, 7]. Much effort has been focused on hydrogels formed via step-growth polymerization because of the many favorable characteristics: the possibility of fine-tuning the gel network structure, highly selective and physiological conditions, and providing a promising method to prepare biomimetic scaffolds via the incorporation of bioactive molecules [8, 9]. As a popular strategy, Michael addition chemistry between thiols and either acrylates or vinyl sulfones has been employed for in situ formation of hydrogels [10-12]. Hubbell and co-workers have used this approach to cross-link polyethylene glycol (PEG)-based hydrogels, which were obtained within 10 minutes with complete conversion of thiols and acrylates, when the two species were combined in a 1:1 ratio [13]. The main disadvantages of this reaction, however, are during synthesis the very badly smelling precursors with thiol groups, the fact that several synthetic and time-consuming scaffold functionalization steps are required, the risk of denaturing disulfide bearing biomolecules, and the lack of spatial and temporal control over the network structure [14].

Thus, other, efficient methodologies for the synthesis of reactive or

functionalizable hydrogels are required, driven by the desire to control bioactive functionality of the gels for eventual application in cell biology, tissue engineering and medical science [15, 16]. Most synthetic hydrogels that lack inherent bioadhesive properties need the engineered introduction of biofunctional features into the gel matrix, for example by covalent attachment of certain biomolecules [2, 4]. Anseth and co-workers developed a versatile hydrogel, which was formed via a Huisgen-type cyclo-addition reaction and subsequently functionalized by photochemical thiol-ene conjugation with biological entities [17, 18]. Now, one increasingly important area of research is finding easy ways to fabricate multifunctional and tunable hydrogels with defined structure and mechanical properties, but without compromising synthetic simplicity or efficiency. The common aim is to establish a platform for the creation of well-defined niches for (3D-)cell culture and understanding the role of biomechanical versus biochemical signals within the scaffolds on cell function, with the final goal of promoting the regeneration of tissue structures.

In this chapter, the novel gel formation method of incomplete amine-Michael type addition chemistry is described. It is demonstrated that the hydrogels are formed by amine-Michael type addition with well controlled molecular structure, gelation time, mechanical properties and swelling behavior via tuning the addition of NH_3 amount, and possessing residual acrylate groups for chemical functionalization. The flexibility of the novel method indeed offers the opportunity to create a variety of tailored mechanical properties, degradation and functionality hydrogels with well-defined physicochemical properties and versatile functionalization.

2.2 Materials and Methods

2.2.1 Materials

All chemicals were purchased from Aldrich and used as received unless stated otherwise. Solvents were at least analytical grade quality. The silicon masters were purchased from Amo GmbH (Aachen). 8arm PEG-OH with a molecular weight of 15

KDa was purchased from Jenkem technology USA.

2.2.2 Synthesis of 8PEG-acrylate (8PEG)

First, 8-arm, star-shaped PEG with OH-end groups (**8PEG-OH**; 15 kDa**)** and K_2CO_3 was dried in a vacuum oven at 100 °C for 4 h. Then, **8PEG-OH** (5g) and K_2CO_3(3g) were added in 50 ml CH_2Cl_2(DCM) under N_2-atomsphere. Acryloyl Chloride (1 mL) was added dropwise in a water-ice bath. The mixture was stirred at 60 °C for 4 days. The solution was filtered, and then poured into the cold petroleum ether (cooled by water-ice). The solution was stirred for 10 min, and then separated to get the crude product. The crude product was dissolved in 50 mL of DCM and then extracted with saturated NaCl-solution for 3 times. The organic layer was collected. The solution was dried by magnesium-sulfate overnight, then filtered to remove MgSO4 and subsequently the solvent was removed under reduced pressure to get the final product as a white solid. Isolated yield (72%).NMR analysis revealed complete conversion of hydroxyl-groups into acrylate functions. ^{1}HNMR (400 MHz, $CDCl_3$): (O**CH_2CH_2**O 3.64ppm (1496H), (C=O)O**CH_2** 4.31ppm (16H), =C-**H** trans 5.83ppm (8H), C**H**=C 6.15ppm (8H), =C-**H** cis 6.42ppm (8H).

2.2.3 Preparation of mercapto-functionalized fluorescent dye

11-mercaptoundecanoylchloride

Thionylchloride (0.07 g, 5.88×10^{-4} mol) was added to a solution of 11-mercaptoundecanoic acid (0.126 g, 5.76×10^{-4} mol) in 10 ml of dichloromethane and the reaction was kept under reflux overnight. At the end the excess solvent and thionylchloride were evaporated under vacuum to yield 0.14 g (100%) of the chloride product as a brown oil. ^{1}H-NMR (400 MHz, $CDCl_3$): δH 2.88-2.84 (t, 2H), 2.66-2.63 (t, 1H), 1.69-1.61 (m, 4H), 1.36-1.27 ppm rest of the protons; ESI-MS (m/z) calcd 236.10, obsd 279.13 [M++ Na++H2O+2H+].

N-fluoresceinyl-11-mercaptoundecanyramide

A solution of 11-mercaptoundecanoyl-chloride as prepared in the previous step

was dissolved in 10 ml of acetone and then added dropwise to a solution of aminofluorescein (0.54 g, 1.55 × 10^{-3} mol). After keeping the reaction mixture to stir in an ice bath for two hours the reaction mixture was filtered and the residue was evaporated under vacuum and then purified by recrystallization from ethanol to yield 0.68 g (80%) as an orange solid. ^{1}H-NMR (400 MHz, DMSO-d_6): δH/ppm: 7.90-7.88 (d, 1H), 7.74-7.72 (d, 1H), 7.56-7.55 (s, 1H), 6.66-6.65 (d, 2H), 6.61 (s, 1H), 6.59 (s,1H), 6.53-6.52 (d, 1H), 6.51-6.50 (d, 1H) 2.84-2.80 (t, 1H), 2.63-2.2.60 (t, 1H), 2.28-2.25 (t, 2H), 1.63-1.45 (m, 4H), 1.26-1.17 rest of the protons ; ESI-MS (m/z) calcd 547.20, obsd 547.20 [M+].

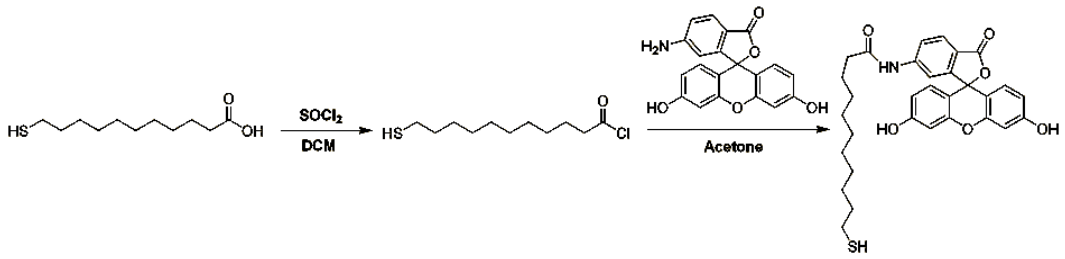

Scheme 1. Reaction scheme to produce mercapto-functionalized fluorescent dye

2.2.4 8PEG-NH_3 hydrogel Synthesis

The preparation of **8PEG-NH_3** hydrogels was performed by adding the ammonium solution (30% NH_3 in H2O) into the precursor solution of 8-arm poly(ethylene glycol) acrylate (**8PEG**) with 40% water content at room-temperature under vigorous magnetic stirring until the solution turned into a viscous liquid. Compositions were set in order to receive 12 wt%, 6 wt%, 3 wt%, 1.5 wt% and 0.75 wt% NH_3-**8PEG** by weight. Then, the resulting liquids were deposited on a glass slide and covered with a glass cover slip. The required time for gelation of 12 wt%, 6 wt%, 3 wt%, 1.5 wt% and 0.75 wt% **8PEG-NH_3** gels are 0.4h, 0.5h, 1h, 2h and 4h, respectively.

2.2.5 UV stabilizing of 8PEG-NH_3 hydrogel

For the eventual UV stabilizing, 1% photoinitiator (PI) (Irgacure 2959) was added to the **8PEG** solutions before NH_3 addition. After the same process as described above for the in situ prepared **8PEG-NH_3** gel, the gels were exposed to UV light (340 nm) for 15 minutes to obtain **8PEG-NH_3** UV gels.

2.2.6 Surface-modification of 8PEG-NH_3 hydrogel

First, the mercapto-functionalized fluorescent dye dissolved in acetone (c=1 mg/mL) was drop-casted on the glass slide surface and the acetone was allowed to evaporate. Then the fresh **8PEG-NH_3** hydrogel was put on the dyed region of the glass. After 0.5h of the reaction, the SH-modified hydrogel was peeled off mechanically for the characterization.

2.2.7 Fabrication of micro-/nano-patterned 8PEG-NH_3 hydrogel replicas

Micro-/nano-patterned silicon wafers were rinsed with acetone, water and isopropanol and dried under a mild stream of nitrogen before use. Prior to the replication the cleaned silicon masters were fluorinated with trichloro(1H,1H,2H,2H-perfluorooctyl) silane 97% (Sigma-Aldrich). The selected viscous liquids of **8PEG** mixed with NH_3 were dispensed on the silicon master, covered with a thin glass cover slip and left to gel for 1h. Following gel formation, the transparent polymeric film, with an inverse relief to that on the silicon master, was peeled off mechanically. The stand-alone film (250-300 μm in thickness) could be handled with tweezers.

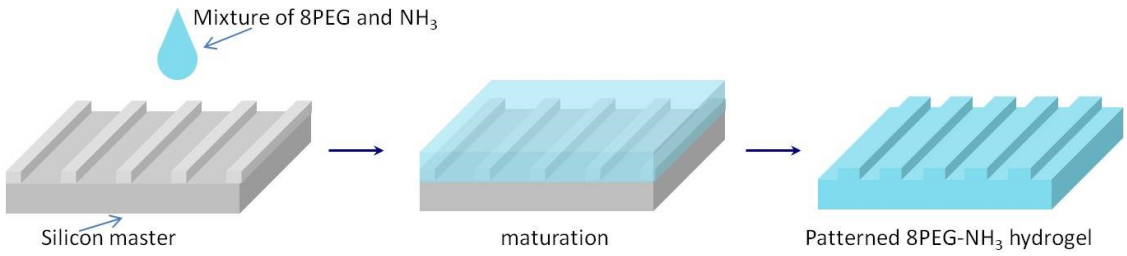

Scheme 2. Preparation of patterned **8PEG-NH_3** hydrogels

2.2.8 Deprinting of dyes on the patterned surface of 8PEG-NH_3 hydrogel

First, the fluorescence dye dissolved in acetone (c=1 mg/mL) was drop-casted on a glass slide surface and the acetone was allowed to evaporate. Then the patterned hydrogel was put on the dyed region of the glass. After 3 seconds of contact, the hydrogel was transferred to a new, clean glass side (in the same configuration with the pattern facing down) in order to let the dye diffuse into the gel. After 2 h of diffusion, the sample was investigated by CLSM.

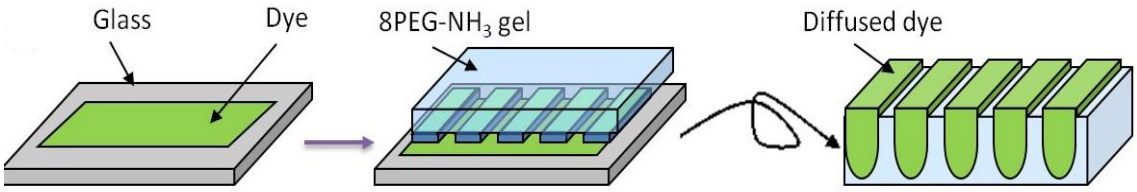

Scheme 3. Dye diffused into the patterned hydrogel matrix

2.2.9 Analysis of degradation products of 8PEG-NH_3 hydrogel

The degradation of the **8PEG-NH_3** was analyzed by immersing the hydrogel in water for hydrolysis at 37 °C. After three days, when the hydrogels had totally degraded, the mixture was filtered. MS spectrum of degradation products were obtained through LTQ Orbitrap XL (Thermo scientific) controlled by XCalibur 2.0.7 Software. Syncronis C18 (Thermo scientific), length 50mm, ID 3mm, 5µm with a

gradient mobile phase of methanol/water with 0,025% HCO2H at 1.3 mL/min was utilized for analytical separation. Optimized settings for the sample ionization by positive ion atmospheric pressure chemical ionization (APCI) were used.

2.2.10 Characterization

^{1}H NMR spectra were recorded on a Bruker Advance DRX-400 spectrometer with trimethylsilane (TMS) as the internal standard and deuterochloroform ($CDCl_3$) as the solvent.

Carbon (C), hydrogen (H), nitrogen (N), and oxygen (O) elemental analysis (EA) of the various samples was carried out with the aid of the elemental analyzer (Perkin-Elmer Series II CHNS/O Analyzer 2400). The C and N contents were determined for the various samples.

Hydrogels modified with fluorescence dye in water were characterized by confocal microscopy (Leica DM IRBE confocal laser scanning microscope (CLSM) with a 30 W UV lamp (λ = 350 nm) as the light source). Data was edited utilizing BioImage XD software.

2.2.11 Swelling tests

As prepared, “dry”, gels were weighed and immersed in deionized water at 37 °C. After appropriate time, the gels were taken out from the water, blotted dry with tissue paper and weighed again immediately. The water uptake was determined according to the equation (1) for calculating the swelling degree (Qm):

$$Qm=Ms/Md \qquad (1)$$

where Ms is the gel mass after swelling and Md is the dry gel mass. Reported results were averages of measurements on three samples. The hydrogels were then dried in an oven at 80 °C for 24 h, and their dry mass (Md) was measured. Reported results were the average of three samples and incubation was continued until the hydrogel samples had insufficient physical integrity to handle.

2.2.12 Rheology measurements

Rheology measurements were conducted using a Gemini 200 HR Rheometer (Malvern Instruments) applying the strain-controlled mode for all experiments performed. Prior to all experiments, the linear elastic range of the samples was determined with the help of the amplitude sweep. This was observed when the when Storage Modulus (G') (indicating the elastic property of the network) and the Loss Modulus (G") (indicating viscous properties of the fluid) were yielding a constant plateau.

Gelation time measurement

A 40 mm plate was used and measurements were conducted at room temperature. A solvent trap was used throughout the measurement to avoid loss of water. Constant frequency sweep was applied and gelation time was recorded at the crossover of G` and G''. Measurements were repeated at least 3 times for each set of samples.

Rheological Measurements of Swollen Network

An 8 mm plate was used and measurements were taken at room temperature. Samples were swollen min. 12 h prior to measurement. During the recording of data of swollen samples were kept in a solvent trap to avoid loss of water during the experimental run. First, the linear elastic range of the samples was determined with the help of the amplitude sweep. This is observed when the when Storage Modulus (G') (indicating the elastic property of the network) and the Loss Modulus (G") (indicating viscous properties of the fluid) are yielding a constant plateau. The value was transferred to the frequency sweep, where the suitable values were ascertained within a range of 0.01 to 10 Hz. 1 Hz as applied frequency and 0.0001 – 0.01 as deformation value (γ) were chosen as appropriate parameters for all measured samples. The value of the observed plateau was recorded and the bulk elasticity was calculated by the following equation as described by Flory,

$$E = 3\,G' \qquad (2)$$

where E is the Young's Modulus and G' is the Storage Modulus. Each material composition was measured at least 3 times.

2.2.13 Raman Spectroscopy

Surface Resonance Raman Spectroscopy (LABRAM, HR Horiba Scientific) was conducted on films dried at ambient conditions with an excitation wavelength of 514 nm. Spectra were recorded between 500 cm^{-1} and 3000 cm^{-1}.

2.2.14 Microscopy

Atomic Force Microscopy (AFM)

An Atomic Force Microscope (JPK instruments, Nanowizard II) was used in order to measure the topography and surface elasticity of samples in dry and swollen state.

Topographical Imaging

Imaging was done in intermittent contact (swollen samples) and contact mode (dry samples) using silicon nitride cantilevers (PNP TR, k ≈ 0.08 N/m, f0 ≈ 17 kHz; Nanoworld Innovative technologies) with a chromium-gold coating. Images were edited with NanoWizard IP Version 3.3a (JPK instruments). Samples measured in swollen state were immersed for at least 12 h in deionized water prior to measuring.

Surface elasticity by Atomic Force Microscopy (AFM)

Surface elasticity was calculated using force-distance curves measured on the same scanning probe microscope (JPK instruments, Nanowizard II). In order to obtain quantitative values for surface elasticity of hydrogel samples, 64 single force-distance curves in a range of 100 µm × 100 µm were recorded and repeated on at least three different areas on the surface. After every set of measurements, the cantilever was newly calibrated (by applying the thermal noise method) before starting with the next set of force-distance measurements. Out of those 64 different values, a mean

value with standard deviation was calculated and from the three values obtained again, a mean value along with the according standard deviation was obtained. This value was then taken as surface-elasticity. Silicon nitride cantilevers (PNP TR tips) with a chromium-gold coating (k ≈ 0.08 N/m, f0 ≈ 17 kHz; Nanoworld Innovative technologies) were used. Images were edited with NanoWizard IP Version 3.3a (JPK instruments). PNP TR tips (Nanoworld) exhibiting a pyramidal tip-shape (face angle 35°) were used and the tip-geometry had been taken into account by applying the Bilodeau formula in order to fit force distance curves. This is a modification of Sneddon's model. The fitting is implemented in the Nanowizard IP software and resulting values for the E-Modulus are accordingly obtained.

2.2.15 Cytotoxicity tests

L-929 cells were used to investigate the cytocompatibility of smooth samples of PEG-NH_3 gels. Hydrogels (0.5 cm x0.5 cm) were washed with ethanol (70%), rinsed in Dulbecco's PBS (DPBS, PAA Laboratories GmbH) and placed in a µ-slide (Ibidi GmbH). 300 µL of a cell suspension containing 50,000 cells were seeded into each well and incubated at 37oC, 5% CO2 atmosphere and 100% humidity. The viability of cells on the gels was calculated after 24 h incubation. Following incubation, cells were stained with 100 µL of a vitality staining solution containing fluorescein diacetate (stock solution 0.5 mg/mL in acetone, Sigma-Aldrich) and propidium iodide (stock solution 0.5 mg/mL in Ringer's solution, Fluka). Viable and dead cells were quantified by fluorescence microscopy.

2.3 Results and discussions

2.3.1 Hydrogel formation

In our work, hydrogels based on poly(ethylene glycol) (PEG) are used, first of all because of the renown bioinertness and biocompatibility of PEG and, second, since the intriguing versatility of PEG macromonomer chemistry facilitates the

incorporation of biochemical cues for cell adhesion and controlled, functional cell behavior [19]. Novel hydrogels composed of star-shaped PEG molecules (having 8 arms with acrylate end groups; **8PEG**) were readily formed in situ by mixing of two aqueous solutions: **8PEG** with 40% water content and an ammonium hydroxide solution (30 wt%), via a Michael-type addition between the acrylate and amine groups (Scheme 4). Although amines, another class of reactive nucleophiles besides thiols, are much slower to react than thiols [10], the incomplete Michael addition reaction between the acrylate and amines groups can be exploited to synthesize a range of hydrogels with different amounts of residual functional end groups, which exhibit tunable mechanical properties and degradation kinetics, simply by adjusting the amount of ammonia added to the reaction. Herein, the different amount of NH_3 solutions (0.75 wt%, 1.5 wt%, 3 wt%, 6 wt% and 12 wt% NH_3 to **8PEG** precursor by weight) were added to the **8PEG** acrylate precursor solution at room temperature, resulting in crosslinking to form a gel network structure, even with 0.4 wt% NH_3.

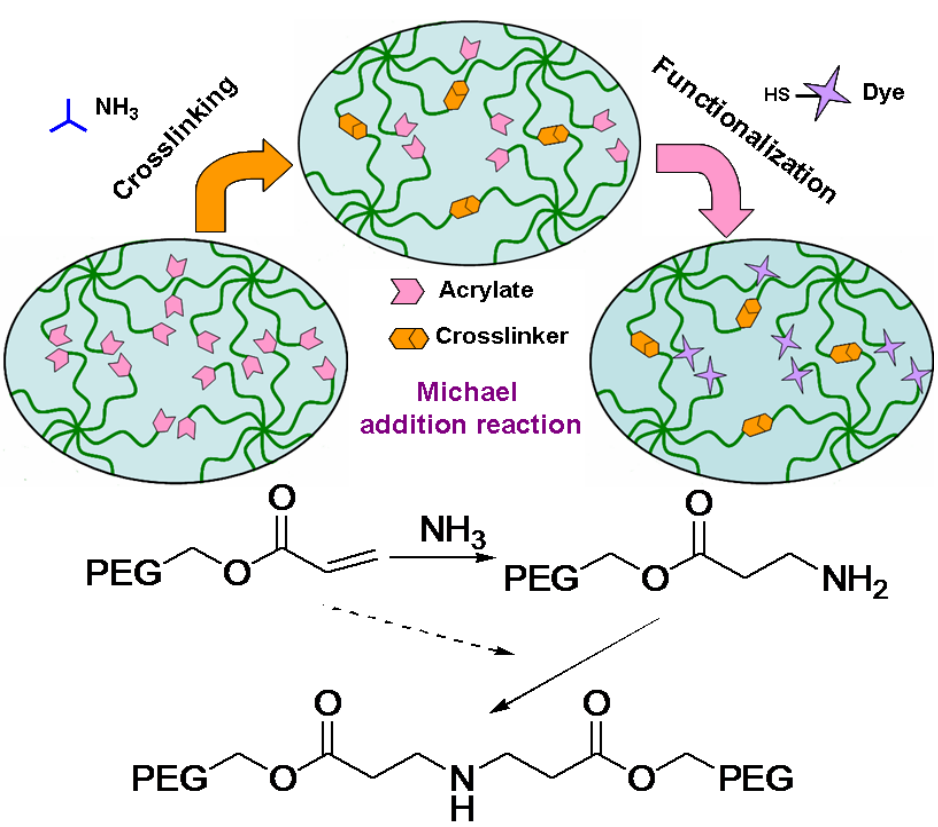

Scheme 4. Schematic representation of novel hydrogel prepared through amine-Michael type addition and modification through sulfur-Michael type addition.

Table 1. Physical and chemical properties of **8PEG-NH_3** hydrogels.

Entry	N content[a] [%]	Relative integrated C=C[c]	Surface elasticity[d] [MPa]	Surface roughness[d] [nm]
1	0.365	0.33	1.55±0.19	20.5
2	0.185	0.57	1.15±0.24	42.2
3	0.130	0.72	0.75±0.23	38.5
4	0.075	0.79	0.15±0.05	57.2
5	-[b]	0.83	0.01±0.01	-[e]

1:**8PEG**-12wt%NH_3; 2:**8PEG**-6wt%NH_3; 3**8PEG**-3wt%NH_3; 4:**8PEG**-1.5wt%NH_3; 5:**8PEG**-0.75wt%NH_3; a) elemental analysis after vacuum drying; b) not detected; c) compared with **8PEG** precursor; d) measured by AFM; e) degraded before measurement was completed.

We have chosen the NH_3-molecule as the crosslinker, which at the same time acts as a catalyst because of its very basic nature. In contrary to the use of free-radical initiators in the most commonly used photopolymerization, the advantage of using NH_3 as crosslinker is the ease to remove its excess after the reaction by evaporation. From elemental analysis (Table 1) after drying, the N contents in all the gels are lower than 0.5% including covalently bound N, indicating that most of the Nitrogen must have been evaporated.

2.3.2 Gelation time

The evolution of storage modulus (G') and loss modulus (G'') are investigated in the course of 900 min (Figure 2). The Storage Modulus (G') refers to the elastic property of the gel network (solid-like behavior) while the Loss Modulus (G") refers to the viscous properties of the gel network (fluid-like behavior).

Both the storage and loss moduli increased with time, confirming that the gel network is progressively stabilized by chemical crosslinking. Furthermore, in the plateau region after the crossover point, the storage modulus became 1-2 times higher than the loss modulus. In the rheological curves, the gel point, defined as the crossover of storage modules and loss modules, can be used to determine the

gelation time. The inset table lists the determined gelation times of the various investigated **8PEG-NH$_3$** hydrogels.

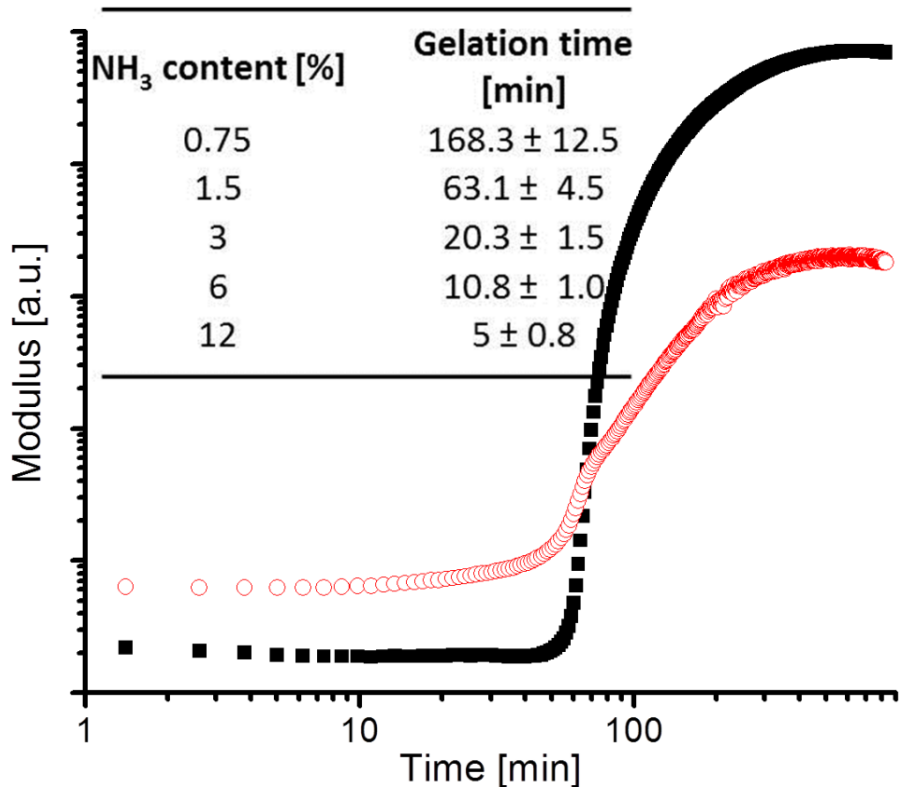

Figure 1. Dynamic rheometry recorded during the gelation reaction of **8PEG**-1.5wt% NH_3 showing the storage modulus G' (solid, black squares) and loss modulus G'' (open, red circles). The gelation time is defined as the time point where the two curves intersect. The inset table shows the gelation time of hydrogels with different content of NH_3.

As displayed in Figure 1, the gelation time is dramatically affected by the amount of NH_3 solution added. This can be understood by taking into account that a higher NH_3 concentration leads to a higher pH value, resulting in more reactive amine groups during gel formation. As the incorporated NH_3 amount decreases from 12 wt% to 0.75 wt%, the gelation time increases accordingly from 5 min to 2.8 h. Thus, the gelation time can be tuned by addition of NH_3 in our system. Moreover, during the gel preparation, the rheological time sweep experiment of **8PEG-NH$_3$** showed no decrease of storage modulus, ruling out hydrolysis or aminolysis, which could otherwise impair the gel network structure [20].

2.2.3 Surface roughness and surface elasticity

Surface morphologies of hydrogels with varying amounts of NH_3 have been determined by atomic force microscopy (AFM) in the swollen state (i.e. measured under water). All hydrogel surfaces showed a uniformly smooth morphology, but exhibited different rms roughness (calculated over an area of 25 μm^2). For example, the surface roughness of **8PEG**-12wt% hydrogel was determined to be 20.5 nm, while in the cases of **8PEG**-6wt%, **8PEG**-3wt% and **8PEG**-1.5wt%, increasingly higher values were found (Table 1). For even lower NH_3 concentrations, i.e. in the case of **8PEG**-0.75wt%, degradation due to the hydrolysis of ester groups was observed to be fast with respect to the duration of the measurement, so that surface analysis could not be performed reliably.

In addition, the surface elasticity (E) of completely hydrated **8PEG**-NH_3 hydrogel samples was determined via force spectroscopy and subsequently evaluated according to the Bilodeau formula [21]. The values are reported in Table 1, in relation to the amount of NH_3 addition. In general, the surface elasticity of **8PEG-NH_3** hydrogels is found to lie within the range of 0.5 - 1.6 MPa. The gel prepared with 0.75% NH_3 was notably softer (10 kPa) but not stable enough to work with. The surface elasticity of the different **8PEG-NH_3** hydrogels could be precisely tuned by varying the amount of NH_3 addition. Similar to the bulk elasticity (although the absolute values cannot be directly compared due to the inherently different techniques), vide infra, more NH_3 addition lead to a higher value of surface elasticity, apparently due to the increased crosslinking density.

Interestingly, there appears to be a direct correlation between the surface roughness of hydrogels and their surface elasticity. We observed for the crosslinked gels that the smaller the surface elasticity (hence lower cross-linking density) the larger the surface roughness (the values are listed in Table 1). This can be attributed to polymer strands that are not integrated firmly in the gel network and are more or less freely moving above the network surface. These dangling polymer chains are

therefore assumed to contribute to the surface roughness as measured. However, it could be just as well that the observed increased roughness is due to disparities in the height profile, a regular swelling phenomenon of hydrogels. The more chemical crosslinks that are provided (e.g. by means of an increased NH_3 content), the more polymer strands are chemically bound into the gel network and therefore the gels exhibit a smaller surface roughness and an increased elastic (Young's) modulus.

2.3.4 Bulk elasticity

In addition, frequency-dependent rheological characterizations of hydrogels with different amounts of NH_3 addition were carried out in order to determine the bulk elasticity of the gels (Figure 2; G'' not shown for the sake of clarity). The data obtained for all gels were characterized by G' exhibiting an almost constant value in the lower frequency range (0.10-10 Hz) with a slight increase when applying higher frequencies. The reason for the observed increase in modulus with increasing frequency may be the partially fluidic viscoelastic nature of the gels. The increasing frequency allows less time for polymer relaxation and this incomplete relaxation may lead to a pre-stressed state of the gels with a corresponding higher Young's Modulus. The lower the crosslinking density, the more fluidic the nature of the gels becomes, resulting in a more pronounced deviation from the ideal behavior, as observed in Figure 2.

The storage modulus is proportional to the hydrogel crosslinking density [22]. The larger amount of NH_3 added leads to higher storage moduli; the G' values of **8PEG**-12wt%NH_3 and **8PEG**-6wt%NH_3 hydrogels are more than 10 times larger than that of **8PEG**-1.5wt%NH_3 hydrogel, suggesting that the **8PEG**-1.5wt%NH_3 hydrogel has quite a low crosslinking density. This result is in agreement with the Raman results (vide infra; Figure 4), which demonstrated that most of acrylate groups in fact do not participate in the crosslinking reaction and thus remain available for further photo-initiated crosslinking and/or (bio)chemical functionalization after gel formation.

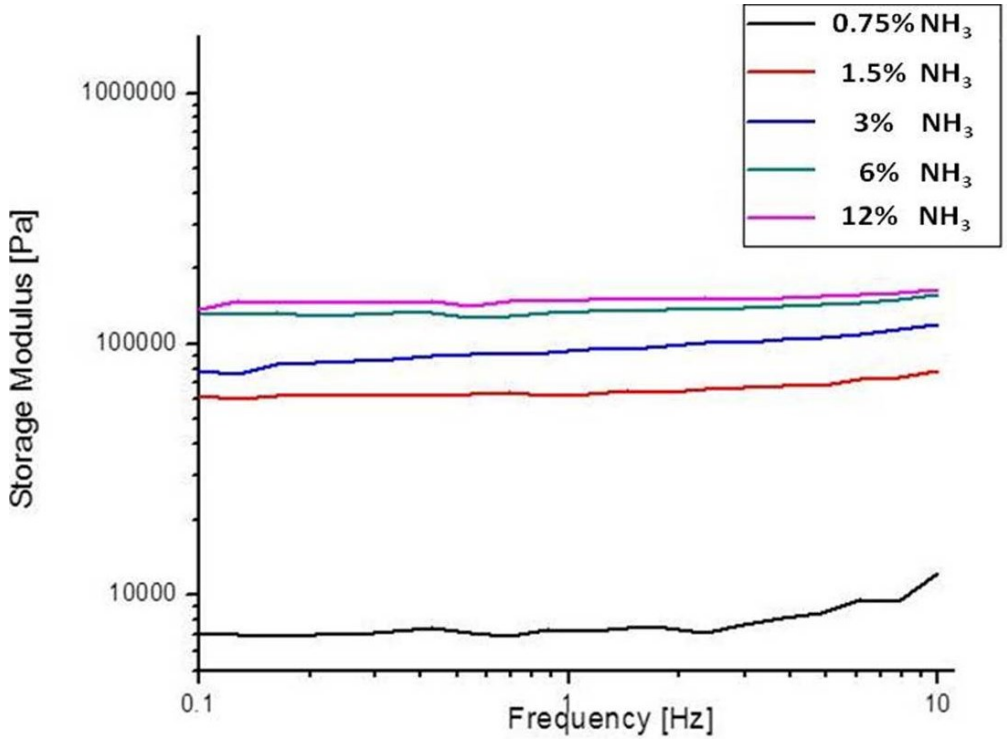

Figure 2. Storage moduli of **8PEG**-NH_3 hydrogels obtained from a frequency sweep performed at 0.5% strain.

2.3.5 Swelling tests and observation of gel degradation

As part of the physicochemical characterization of our hydrogels, we investigated their swelling behavior. For this, at regular time intervals, the swelling ratio (Qm) was calculated by dividing the weight of the swollen hydrogel (after incubation at 37 ºC in deionized water) by the initial weight of the gel. The swelling tests (Figure 3) revealed that the softest hydrogels (i.e. those with the smallest amount of NH_3 added; **8PEG**-0.75wt% NH_3) swelled the most, and almost twice as much as the other gels, which have proven to more stable in the other experiments. In fact, these very loosely crosslinked gels had disintegrated after 9 h. That is why this gel could not be studied any further in the swelling tests. The other **8PEG-NH_3** hydrogels were stable for at least 24h. Thereafter, however, **8PEG**-1.5%wt NH_3 and **8PEG**-3wt% NH_3 gels were also found to disintegrate; after 5 days and 7 days, respectively, while **8PEG**-6%wt NH_3 and **8PEG**-12wt% NH_3 gels remained stable up until 9 days. This result can be easily understood on the basis of the observation that higher NH_3

addition leads to more crosslinks in the bulk of the gels, which require more time for hydrolysis of the ester groups, in turn leading to longer degradation time. It is interesting to note that the different gels showed quite comparable swelling behavior; the softer gels did not swell significantly more than the more tightly crosslinked ones.

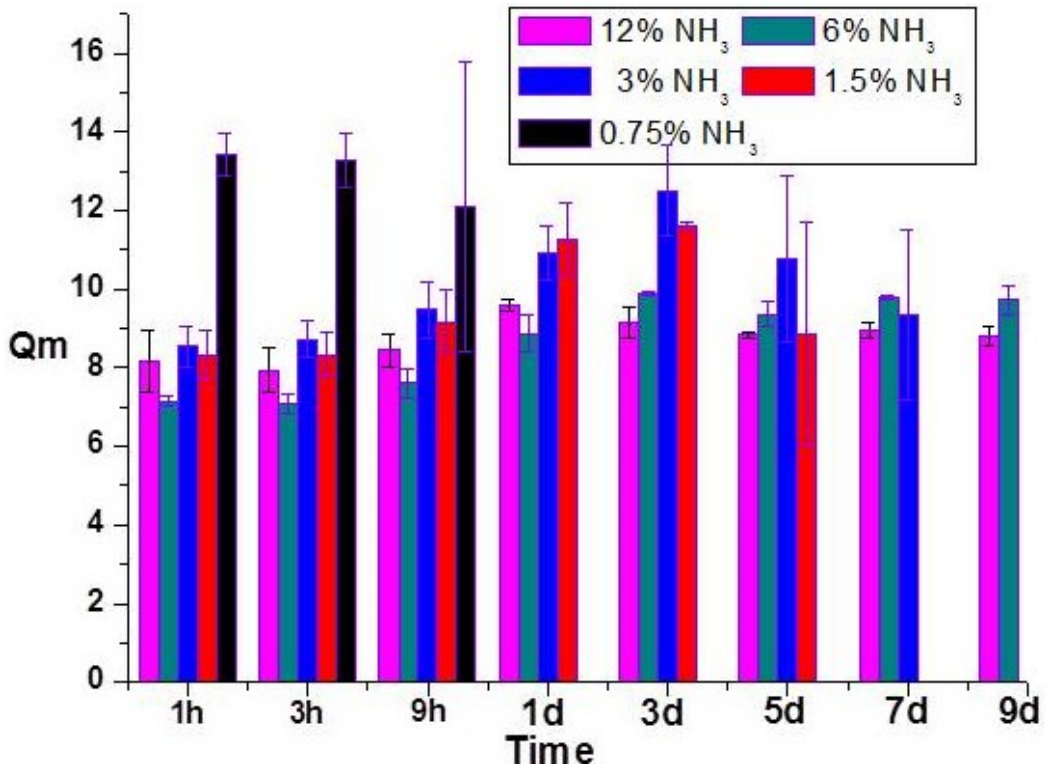

Figure 3. Swelling degree of different kinds of **8PEG-NH$_3$** gels at 37 ºC, in deionized water. Data are shown as average (n=3).

2.3.6 Analysis of gel degradation by chromatography

Due to the presence of ester moieties in the gel, hydrolysis and aminolysis can occur, which lead to the observed degradation of the gels. In fact, the degradation products resulting from the hydrolysis are useful in identifying and explaining the gel network structure and possible reaction mechanisms. Analysis of the degradation products of **8PEG-NH$_3$** gels via Liquid Chromatography Mass Spectroscopy (LC-MS) allows us to determine the molecular weight and distribution of the degradation products. A typical mass spectrum with designation of the degradation products is shown in the Supporting Information (Figure 4). The Michael-type addition products

can be easily detected, and there are no peaks corresponding to degradation products, which could have been formed via chain polymerization, e.g. indicative of poly(acrylic acid). These results demonstrate that the gel network forms via Michael addition chemistry, and not by chain polymerization. In addition, size exclusion chromatography was performed.

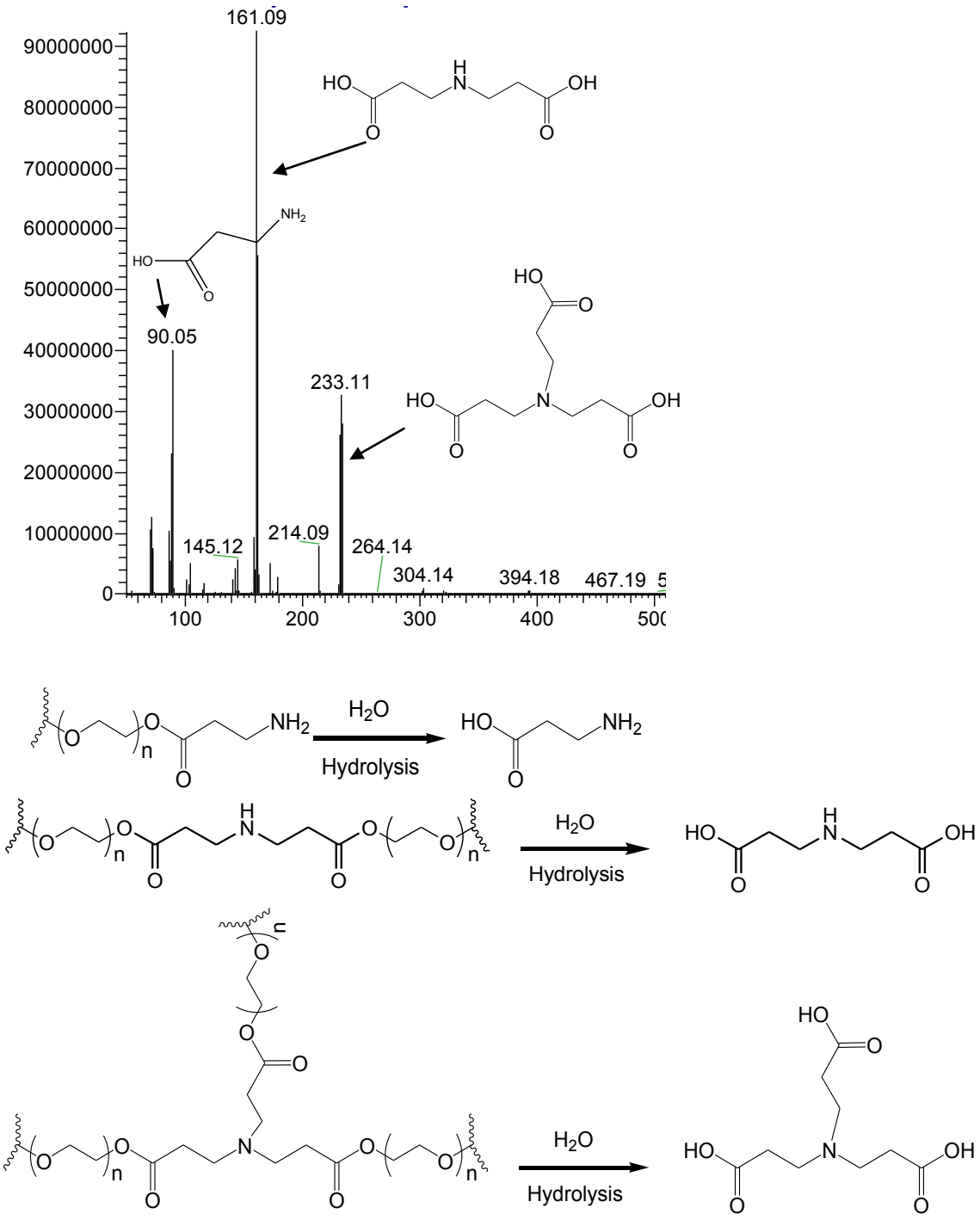

Figure 4. Proposed reaction scheme of hydrolysis of **8PEG-NH$_3$** hydrogels and the MS spectrum revealing the degradation products of **8PEG-NH$_3$** hydrogels.

Comparison of the SEC traces of the **8PEG** precursor and the degradation products of the **8PEG**-0.75wt% NH_3 hydrogel (Figure 5) revealed that they had nearly the same retention time. This result implies that the degradation products are of comparably high molecular weight as **8PEG** building blocks, and thus most likely are derivatives of **8PEG**, which further supports our conclusion that the degradation is due to the hydrolysis of ester moieties in the crosslinking group, and not of the **8PEG** backbone.

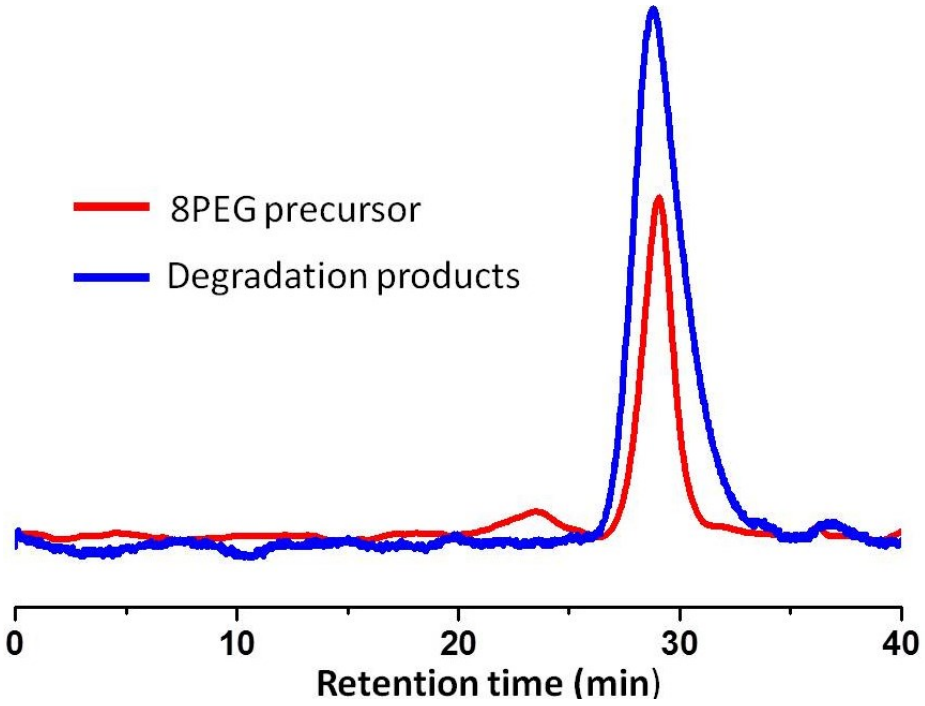

Figure 5. Size exclusion chromatograms of **8PEG** precursor and the degradation products of **8PEG**-NH_3 hydrogel.

2.3.7 Quantification of residual acrylate groups by Raman spectroscopy

In the spectral region of interest, the **8PEG**-NH_3 hydrogels show peaks at 1061 cm^{-1}, 1140 cm^{-1} and 1480 cm^{-1}, which correspond to C-O vibrations, (Figure 6) and peaks at 1640 cm^{-1}, corresponding to C=C vibrations, which are also highlighted in Figure 7. Due to the polymeric backbone of PEG maintaining practically the same within these hydrogels, the spectra could be normalized such that the peak intensity at 1480 cm^{-1}, corresponding to C-O vibrations, i.e. of the ether moieties on the PEG polymer chain,

remained constant. Table 1 listed the fraction of residual acrylate groups in dependence on the added amount of NH_3 and shows the clear and expected trend that a higher amount of NH_3 addition resulted in fewer residual acrylate groups. Nevertheless, even when 12wt% NH_3 was added, so that the ratio of NH_3 to acrylate became around 13:1, after gel formation, still around 33% of the unreacted acrylate groups were left (Table 1). As a comparison, it is interesting to note that Michael addition chemistry between thiols and acrylates have been reported to exhibit complete consumption of acrylates, when the two reactants are combined in a 1:1 ratio or higher, underlining that thiol groups are more reactive than amine groups [7].

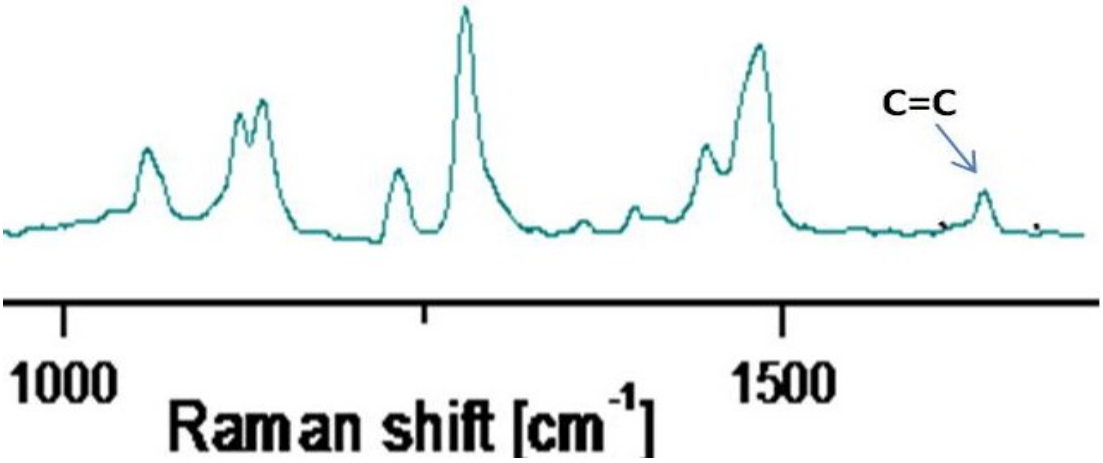

Figure 6. Raman spectrum of **8PEG**-3wt%NH_3 hydrogel

2.3.8 Gel stabilization by UV-curing

The residual acrylate groups can be photopolymerized to further stabilize the **8PEG-NH_3** gels. As shown in Figure 7, after UV-exposure, the peaks corresponding to acrylate groups disappeared from the Raman spectra, indicating that the new network structure indeed formed via polymerization of residual acrylate groups.

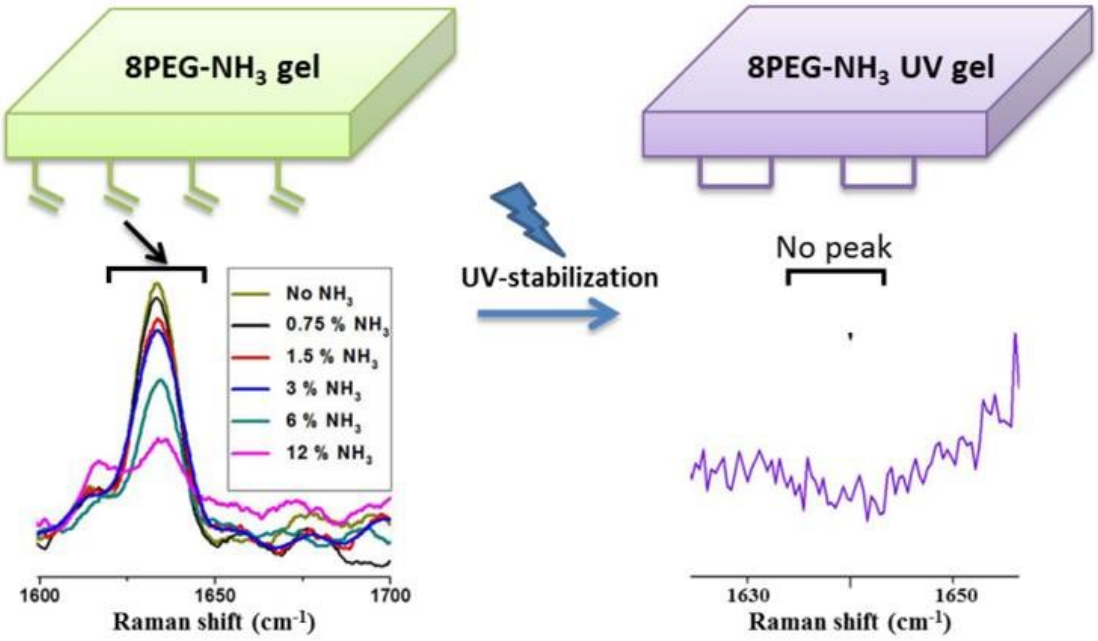

Figure 7. a) cartoon of an **8PEG-NH$_3$** gel formed by amine-Michael type addition and Raman spectra of the residual acrylate groups of gels with different amount of NH_3 addition; b) cartoon of an **8PEG-NH$_3$** hydrogel after UV-curing and part of the Raman spectrum showing the absence of the signal corresponding to the acrylate groups.

Remarkably, hydrogels still form even though more than 70% of the acrylate groups remain unreacted, i.e. when the amount of NH_3 is lower than 3 wt%. In this case, some **8PEG** molecules may have only one or two acrylate groups reacted, and thereby become tethered to the gel. These results reveal that the amount of residual acrylate groups can be tuned by controlling the addition of NH_3, which benefits the here presented post-gelation UV-curing applications such as soft-lithography in order to fabricate nanometer-precise 3D-structures (Figure 8) or further functionalization with biomolecules (Figure 9). Even though surface nano-patterning could already be successfully achieved without further curing, the application of UV-curing resulted in even more stable, high-precision 3D structures, also in fully hydrated state as demonstrated in Figure 8b.

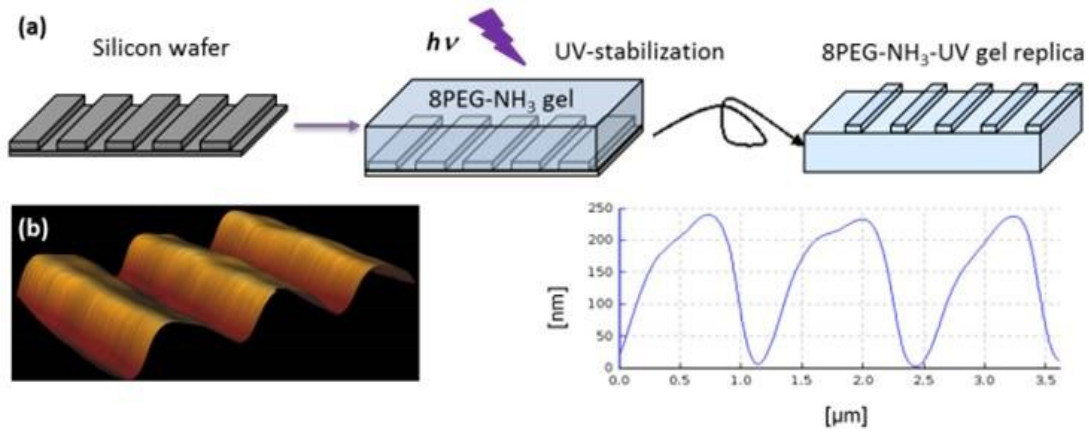

Figure 8. a) Schematic representation of the molding process to fabricate a hydrogel replica and further UV-stabilization of the imprint; b) AFM image and cross-section profile of UV-stabilized **8PEG**-3wt%NH_3 hydrogel replica in fully hydrated state (silicon master pattern: width of grooves 400 nm, spacing 400 nm, depth 200 nm).

2.3.9 Gel functionalization

Taking advantage of post-network formation reactivity due to plenty of unreacted, pendant acrylate groups present in the gel, a second Michael-type addition between thiol and acrylate groups has enabled facile modification of the gel; not only on the gel surface, but also throughout the gel matrix (the concept was schematically depicted in Scheme 4). The proof of principle is demonstrated here, employing a thiol-containing fluorescent dye (Scheme 1). In order to facilitate the discrimination between the surface and the bulk of the hydrogel, topographically micro-patterned stamps of the gels are fabricated and placed into contact with the reactive dye molecule on a flat substrate. In other words, a micrometer sized pattern fabricated via molding of an **8PEG**-3wt%NH_3 hydrogel is “inked” by contacting a glass slide, on which a drop of dye was placed (Figure 9a). After 3 seconds of contact and 2 h of consequent diffusion time, the hydrogel was investigated by confocal laser scanning microscopy (CLSM). While the regions conjugated by the dye were observed to be highly fluorescent, other regions where the dye had not reached showed no fluorescence (Figure 9b).

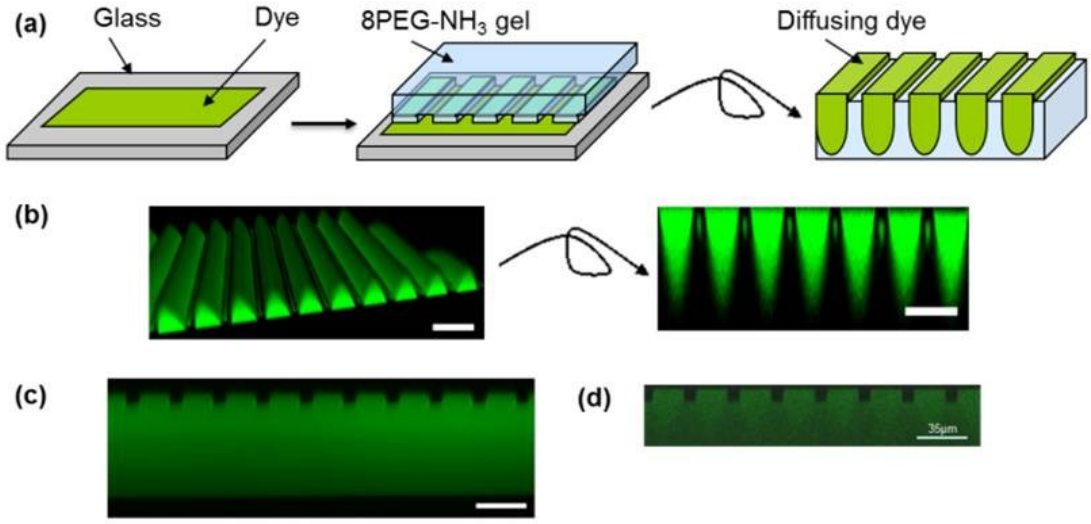

Figure 9. a) Schematic representation of the inking process introducing reactive dye molecules to functionalize micro-patterned **8PEG**-3wt%NH_3 hydrogel; b) CLSM 3D fluorescence image and cross sectional image of **8PEG**-3wt%NH_3 micro-patterned hydrogel showing the reactive dye diffusion profile (silicon master pattern: width of grooves 10 µm, spacing 20µm, depth 5µm); c) and d) Cross sectional images of the same experiment but using in c) a UV-cured **8PEG**-3%NH_3 hydrogel (all the acrylate groups have reacted), and in d) a reactive **8PEG**-3%NH_3 hydrogel using a non-thiolated dye; both showing unrestricted dye diffusion troughout the micro-patterned gels. Scale bars represent 35 µm.

This simple experiment very nicely demonstrated that the reactive dye can only diffuse into the gel matrix until it reacts with pendant acrylate groups; the shape of the fluorescent profile in the gel exactly represents the reactive diffusion pathway of the dye. Apparently, the covalent bonding of the dye to the gel leads to immobilization of the dye within the gel matrix, which makes it very difficult for the dye molecules from the reservoir to travel to the front when the reactive positions are occupied and the mesh has become blocked. As a result, a clear edge between the conjugated dye region and the areas where the dye could not penetrate further, was observed (Figure 9b). On the contrary, for the hydrogel without pendant acrylate groups the dye could diffuse unrestrictedly and thoroughly into the gel matrix within 2h of otherwise similar conditions (Figure 9c). Likewise, when a non-functionalised (no thiol group present) dye molecule was used, the dye diffused throughout the gel as well (Figure 9d).

2.3.10 Gel surface modification

The **8PEG**-NH_3 gels that were surface-modified (with a thiol-containing fluorescent dye before UV curing) were characterized by AFM, in terms of surface roughness and elasticity, and the results (Figure 10) were compared with those for non-functionalized, but merely UV-cured, **8PEG**-NH_3 gels (**8PEG**-NH_3 UV gel; Figure 10a).

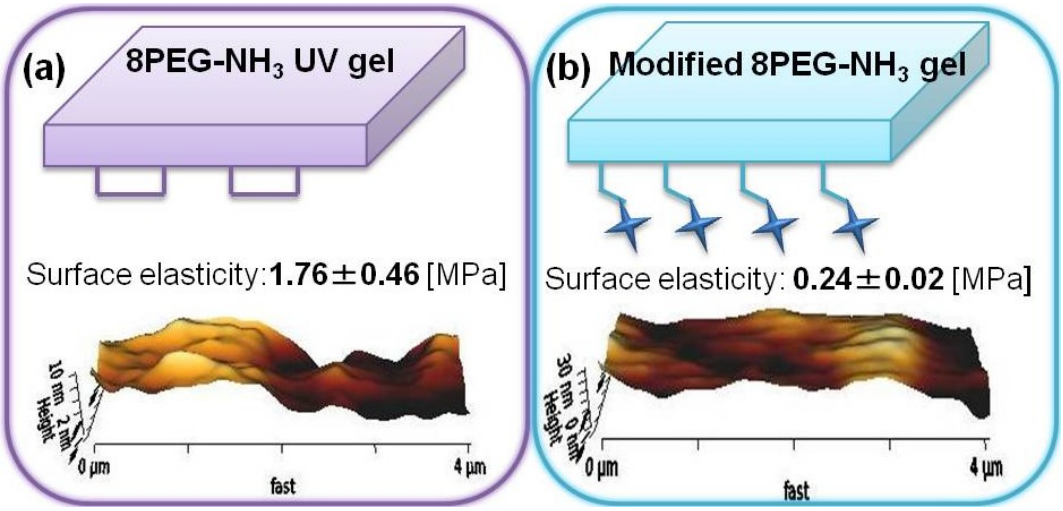

Figure 10. AFM characterisation of hydrogels that were just UV-cured (a) or surface modified and then UV-cured (b), revealing significant differences in surface roughness and elasticity.

It was found that the surface roughness of the surface modified **8PEG**-NH_3 gel was significantly larger (7.0 nm) than that of the **8PEG**-NH_3 UV gel (2.3 nm). Correspondingly, as was the case for the hydrogels with different crosslinking density (vide supra; Table 1), the surface elasticity of the UV stabilized **8PEG**-NH_3 hydrogels was higher than that of the surface-functionalized hydrogels. Thus, surface-modified hydrogels have smaller surface elasticity and higher roughness values (it should be noted that AFM measurements were performed in hydrated state). This can be rationalized by considering that after surface modification, the residual acrylate groups have been consumed and very few acrylate groups remained available for photopolymerization via UV-curing. Therefore, a greatly diminished crosslinking density compared to UV-stabilized hydrogels without surface-modification was

observed. This is another proof that the residual acrylate groups can be modified by other molecules, or UV-photo polymerized, which could be very useful for bioactive substance attachment for biomedical applications.

This active hydrogel and the application of the versatile patterning techniques will be particularly useful in cell guidance and tissue engineering research, when biofunctional molecules, e.g. cell adhesion molecules, antibodies or growth factors, are employed to react with the pendant acrylate groups.

2.3.11 Cytocompatiblity

For the eventual use in biomedical applications, it is indispensable to test the gels' potential cytotoxicity. To verify the cytocompatibility of **8PEG-NH_3** hydrogels, we have performed a live-dead assay via direct contact of cells (fibroblast cell line L-929) with gels after 24h of incubation (TCPS as control). In this test, dead cells appear red, whereas living cells appear green when observed with a fluorescence microscope. It can be seen in Figure 11 that there was no apparent in vitro cytotoxicity originating from the contact with **8PEG-NH_3** hydrogels; the viability of the cells in the medium containing **8PEG-NH_3** hydrogels is very high, and similar to that of cells cultured on the TCPS control, i.e. >98% via the quantitative analysis, for all samples. Thus, although ammonia could be regarded as a potential toxic substance, in our gel system, even in the case where as much as 12wt% of NH_3 was involved in the gel formation process, cells still remained viable after 24 h of incubation. We attribute the very good cytocompatiblity of the new gels to the fact that the excess ammonia was readily eliminated from the gel matrix after the (amine Michael type addition) reaction.

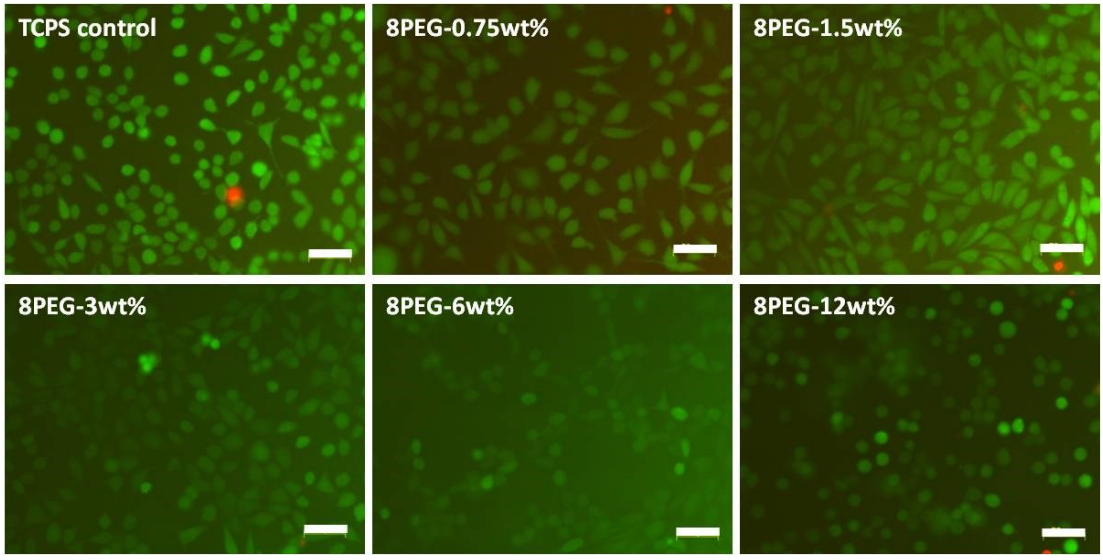

Figure 11. Live-dead assay indicating viable (green) and dead (red) L-929 cells on TCPS control and **8PEG-NH_3** hydrogels after 24h of incubation. Scale bar represents 50 µm.

As discussed earlier, during swelling tests we observed that **8PEG**-0.75wt%NH_3 hydrogels degraded in less than 24h (in deionized water at 37°C). This degradation process was also observed in the cell culture experiments, nevertheless, the high cell viability (after 24 h) demonstrates that the degradation products derived from **8PEG**-0.75wt%NH_3 hydrogels apparently have no influence on cell viability either. Therefore, these cytocompatible hydrogels with degradable properties are very promising for use as tissue engineering and drug delivery matrices.

2.4 Conclusions

In summary, the synthesis of a new class of PEG-NH_3 hydrogels formed by Michael-type addition reaction between acrylate and amine functional groups has been described. This crosslinking reaction of acrylate terminated 8-arm PEG -macromonomers with NH_3 allows the formation of hydrogels with well controlled molecular structure, mechanical properties, gelation time and residual acrylate end-groups for chemical functionalization. Such flexible functionalized surfaces represent a significant advance to enable applications in such areas as catalysis, biofunctionalization, or sensors development. Moreover, this active hydrogel and the

application of the versatile patterning techniques will be particularly useful in cell guidance and tissue engineering research, when biofunctional molecules, e.g. cell adhesion molecules, antibodies or growth factors, are employed to react with the pendant acrylate groups. Since biochemical and biomechanical cues both play an important role in the interaction between cells and their ECMs, such chemical and structural control of the gel's architecture is of paramount importance for the performance of the material in biomedical applications.

References

[1] Hirst, A.R. Escuder, B.; Miravet, H.F.; Smith, D.K.; High-Tech Applications of Self-Assembling Supramolecular Nanostructured Gel-Phase Materials: From Regenerative Medicine to Electronic Devices. *Angew.Chem. Int. Ed.* **2008,** 47, 8002-8018.

[2] Seliktar, D. Designing Cell-Compatible Hydrogels for Biomedical Applications *Science* **2012,** 336, 1124-1128.

[3] Kiyonaka, S.; Sada, K.; Yoshimura, I.; Shinkai, S.; Kato, N.; Hamachi, I. Semi-wet peptide/protein array using supramolecular hydrogel. *Nat. Mater.* **2004**, 3, 58-64;

[4] Lee, K. Y.; Yuk, S. H. Polymeric protein delivery systems. *Prog. Polym. Sci.* **2007**, 32, 669-697.

[5] Lutolf, M. P.; Hubbell, J. A. Synthetic biomaterials as instructive extracellular microenvironments for morphogenesis in tissue engineering. *Nat. Biotechnol.* **2005**, 23, 47-55.

[6] Lutolf M. P.; Hubbell, J. A. Synthesis and Physicochemical Characterization of End-Linked Poly(ethylene glycol)-co-peptide Hydrogels Formed by Michael-Type Addition. *Biomacromolecules* **2003**, 4, 713-722.

[7] Rizzi, S. C.; Ehrbar, M.; Halstenberg, S.; Raeber, G. P.; Schmoekel, H. G.; Hagenmuller, H.; Muller, R.; Weber F. E.; J. Hubbell, A. Recombinant protein-co-PEG networks as cell-adhesive and proteolytically degradable hydrogel matrixes. Part II: biofunctional characteristics. *Biomacromolecules*, **2006**, 7, 3019-3029.

[8] Kloxin, A. M.; Kloxin, C J.; Bowman, C. N.; Anseth K. S. Mechanical Properties of Cellularly Responsive Hydrogels and Their Experimental Determination. *Adv. Mater.* **2010**, 22, 3484-3494.

[9] Slaughter, B. V.; Khurshid, S. S.; Fisher, O. Z.; Khademhosseini, A.; Peppas, N. A. Hydrogels in Regenerative Medicine. *Adv. Mater.* **2009**, 21, 3307-3329.

[10] Elbert, D. L.; Pratt, A. B.; Lutolf, M. P.; Halstenberg, S.; Hubbel, J. A. Protein delivery from materials formed by self-selective conjugate addition reactions. *J. Controlled Release* **2001**, *76*, 11-25.

[11] Lutolf, M. P.; Raeber, G. P.; Zisch, A. H.; Tirelli, N.; Hubbell, J. A. Cell-Responsive Synthetic Hydrogels. *Adv. Mater.* **2003**, *15*, 888-892.

[12] Hiemstra, C.; van der Aa, L. J.; Zhong, Z. Y.; Dijkstra, P. J.; Feijen, J. Rapidly in situ-forming degradable hydrogels from dextran thiols through Michael addition. *Biomacromolecules* **2007**, *8*, 1548-1556.

[13] Vernon, B.; Tirelli, N.; Bächi, T.; Haldimann, D.; Hubbell, J. A. Water-borne, in situ crosslinked biomaterials from phase-segregated precursors. *J. Biomed. Mater. Res. A* **2003**, 64, 447-456.

[14] Lin C. C.; Anseth, K. S. PEG Hydrogels for the Controlled Release of Biomolecules in Regenerative Medicine. *Pharm. Res.* **2009**, 26, 631-643.
[15] Nie, Z. H.; Kumacheva, E. Patterning surfaces with functional polymers. *Nat. Mater.* **2008**, 7, 277-290.
[16] Altin, H.; Kosif I.; Sanyal, R. Fabrication of "Clickable" Hydrogels via Dendron−Polymer Conjugates. *Macromolecules* **2010**, *43*, 3801-3808.
[17] Polizzotti, B. D.; Fairbanks, B. D.; Anseth, K. S. Three-Dimensional Biochemical Patterning of Click-Based Composite Hydrogels via Thiolene Photopolymerization. *Biomacromolecules* **2008**, 9, 1084-1087.
[18] DeForest, A.; Polizzotti, B. D.; Anseth, K. S. Sequential click reactions for synthesizing and patterning three-dimensional cell microenvironments. *Nat. Mater.* **2009**, 8, 659-664.
[19] Hern D. L.; Hubbell, J. A. Incorporation of adhesion peptides into nonadhesive hydrogels useful for tissue resurfacing. *J. Biomed. Mater. Res.* **1998**, 39, 266-276.
[20] Censi, R.; Fieten, P.J.; di Martino, P.; Hennink, W. E.; Vermonden, T. In Situ Forming Hydrogels by Tandem Thermal Gelling and Michael Addition Reaction between Thermosensitive Triblock Copolymers and Thiolated Hyaluronan. *Macromolecules* **2010**, 43, 5771-5778.
[21] Bilodeau, G. G. Regular Pyramid Punch Problem. *Journal of Applied Mechanics* **1992**, 59, 519-523.
[22] Kloxin, A. M.; Kasko, A. M.; Salinas, C. N.; Anseth K. S. Photodegradable Hydrogels for Dynamic Tuning of Physical and Chemical Properties. *Scienc**e*** **2009**, 324, 59-63.

Chapter 3.

Restricted crystallization of PEG-based hydrogels synthesized by different cross-linking chemistry

Collaboration with Prof. Zhiqiang Su's group from Beijing University of Chemical Technology

Abstract

In this chapter, three kinds of hydrogels based on star-shaped poly(ethylene glycol) molecules (having 8 arms with acrylate end groups; **8PEG**) as synthesized by different methods have been investigated; (I) UV-cured **8PEG**-based hydrogels (**8PEG-UV**) formed by photoinitiated radical cross-linking; (II) novel hydrogels that are chemically cross-linked via a Michael-type addition between the acrylate and amine groups (**8PEG-NH_3**) (III) **8PEG-NH_3** gels that are further UV-stabilized (**8PEG-NH_3-UV**). Besides, the **8PEG** polymer material consisting of the pure **8PEG** precursor without chemical cross-linking, is investigated for comparison. The crystallization of hydrogels is facilitated by a solvent drying process to obtain a thin hydrogel membrane. The microstructures and crystallization behaviors of as-prepared hydrogels and **8PEG** polymer have been studied in terms of cross-polarizing optical microscopy (POM), differential scanning calorimetry (DSC), wide-angle X-ray diffraction (WAXD), scanning electron microscopy (SEM) and atomic force microscopy (AFM). Variable-scale structures have been observed in these hydrogels, with different network structures ranging in size from a few hundred nanometers to several micrometers. WAXS studies show no significant difference among the crystal structures of the three kinds of hydrogel membranes. However, POM results reveal that in contrary to the nano-scaled crystallites observed in the **8PEG-UV** gel membrane, the **8PEG-NH_3** and **8PEG-NH_3-UV** hydrogel membranes both show a framework of giant crystalline domains with spherulite sizes ranging from 30 μm to 500 μm. And compared with **8PEG-NH_3,** more and smaller PEG spherulites are observed in **8PEG-NH_3-UV**. SEM and AFM results further confirmed the results.

3.1 Introduction

In nature, many biological materials such as bone, nacre, sea sponge exoskeletons, diatoms and spider silk are built up from ordered and multi-scale hierarchical structures [1-3]. In fact, structural hierarchy is a rule of nature. Biological tissue with excellent mechanical toughness and functionality possesses these ordered and multi-scale hierarchical structures, selected to ensure tolerance of material/structural flaws, as exemplified by tissues such as bone and cartilage. On the contrary, synthetic materials have serious problems, such as mechanical weakness restraining their application. Therefore, biomimetic and bioinspired materials, into which ordered and hierarchical structure can be introduced, are receiving increasing attention because of their robust functionality and potential applications as artificial tissue [4, 5].

Synthetic hydrogels, i.e. crosslinked polymer networks capable of imbibing water, have been widely used in a diverse range of applications [6-8], such as drug delivery, biosensors, tissue engineering and wound healing, owing to their excellent biocompatibility, tunable chemical and physical properties and capability of incorporating bioactive molecules. With the similarity to biological soft tissue, hydrogels, which are also soft and contain water, could be an ideal substitute for biological soft tissue. Nevertheless, unlike most biological tissues such as muscular tissue, which contain well-ordered aggregates that may arrange themselves regularly in a continuous length beyond the micrometer scale and allow living materials to be of sufficient mechanical toughness, synthetic hydrogels generally have poor functionality. This inherent drawback is primarily due to the biological tissue having a sophisticated, multifunctional structure, whereas most synthetic hydrogels are simple and amorphous [9, 10].

Recently, self-assembly, i.e. the spontaneous organization of discrete components into organized structures, has received widespread attention as a method for developing materials with self-organized structures. These efforts have succeeded in

designing various functional materials based on the formation of self-assembled structures in solutions, elastomers, gels and hard materials. Within these self-organized materials, structured hydrogels are of particular significance because they possess properties similar to biological soft tissue (both are soft and wet) and therefore have important potential applications in artificial tissues and optical sensing [11–14]. In order to obtain hydrogels with long range ordered structures, self-organized structures have been introduced into synthetic physical or chemical hydrogels via intermolecular noncovalent interactions, such as ionic bonding and hydrophobic interactions [15–21]. However, so far the ordered hydrogel structures could only be constructed by self-assembled molecules, such as block copolymers and liquid crystal molecules. In this study, we developed a novel gel formation method, with which homopolymers without self-assembly properties can also be assembled into ordered structures.

Among various types of homopolymers, poly(ethylene glycol) (PEG) is one of the most popular, non-toxic, biologically inert polymers, which owes its inertness to the fact that it is hydrophilic, electrically neutral and highly hydrated [22, 23]. The crystallization and melting behavior of PEG homopolymer has been extensively studied [24-27]. The crystallization behavior of well-defined star-shaped PEG and linear PEG has been studied by He et. al [28]. Their results revealed that although the crystallization growth rates are different between linear PEG and star-shaped PEG, there is no change in crystal structure. The spherulites formed in star-shaped PEG are much smaller than those formed in linear PEG. However, the crystallinity of chemically crosslinked PEG-based hydrogels has not been reported, probably due to the heterogeneous nanoscale structure of hydrogels fabricated via the commonly used chain growth polymerization, which only leads to the nanoscaled crystal structure formation [29, 30].

In Chapter 2, novel PEG-based hydrogels (**8PEG-NH$_3$**) with different amounts of residual functional end groups, which exhibit tunable mechanical properties and degradation kinetics, have been formed by the Michael-type addition reaction

between the acrylate and amine groups. **8PEG-NH_3** hydrogels are crosslinked via step growth polymerization, which, compared with chain growth polymerization, often leads to superior mechanical integrity. Unlike the resultant hydrogels of chain growth polymerization having heterogeneous nanoscale structure [29, 30], the corresponding hydrogels formed via step growth polymerization possess more homogeneous nanoscale network structures [31]. Herein, only the nanoscale crystallites have been found in the PEG hydrogels synthesized via common and robust photoinitiated chain polymerization (**8PEG-UV**). On contrary, the long-rang ordered (microscale) crystalline structures in the hydrogels, formed via Michael addition reaction between the acrylate and amines groups (**8PEG-NH_3**), have been observed and studied in terms of cross-polarizing optical microscopy (POM), differential scanning calorimetry (DSC), wide-angle X-ray diffraction (WAXD), scanning electron microscopy (SEM) and atomic force microscopy (AFM).

3.2 Materials and Methods

3.2.1 Materials

All chemicals were purchased from Aldrich and used as received unless stated otherwise. Solvents were at least analytical grade quality. 8arm poly(ethylene glycol) (**8PEG**-OH) was purchased from Jenkem technology USA with a molecular weight of 15 KDa. AFM measurements were performed following the same procedure described in Chapter 2. **8PEG** with acrylation end-group macromonomer was prepared via the same procedure as described in Chapter 2.

3.2.2 Hydrogels preparation

Three kinds of hydrogels based on star-shaped poly(ethylene glycol) (PEG) molecules (having 8 arms with acrylate end groups; **8PEG**) were synthesized by three different methods:

3.2.2.1. 8PEG-UV hydrogel

8-PEG, aqueous solutions (50 wt%) containing 1% of PI (1 wt% with respect to the amount of the precursor) were prepared. Subsequently, 50 µl of the **8PEG** precursor mixtures were dispensed on the clean glass slide, capped with a cover glass (18 mm × 18 mm; Carl Roth GmbH & Co. KG) and exposed to UV light (λ = 365 nm, Vilber Lourmat GmbH) for 15 min using a working distance of 10 cm, in a nitrogen-filled glovebox. The cured transparent gels were peeled off with tweezers. And then the samples were put on the clean glass slide. The water was evaporated and further dried until constant weight.

3.2.2.2. 8PEG-NH_3 hydrogel

8PEG, aqueous solutions (40 wt%) containing 1% of PI (1 wt% with respect to the amount of the precursor) were prepared. 15 µl of ammonium solution (30% NH_3 in H_2O) were added to 100µl of the **8PEG** precursor mixtures at room-temperature under vigorous magnetic stirring until the solution turned into a viscous liquid. The resulting liquids were deposited on the clean glass slide, capped with a cover glass (18 mm × 18 mm; Carl Roth GmbH & Co. KG). After 0.5h, the **8PEG-NH_3** hydrogel were formed. The cured transparent gels were peeled off with tweezers. And then the samples were put on the clean glass slide. The water was evaporated and further dried until constant weight.

3.2.2.3. 8PEG-NH_3-UV hydrogel

In order to obtain UV stabilizing hydrogels, after same process with in situ **8PEG-NH_3** gel formation, the gels were exposed to UV light (λ = 365 nm, Vilber Lourmat GmbH) for 15 min using a working distance of 10 cm, in a nitrogen-filled glovebox. The cured transparent gels were peeled off with tweezers to obtained **8PEG-NH_3-UV** gel. And then the samples were put on the clean glass slide. The water was evaporated and further dried until constant weight.

3.2.2.4. 8PEG Polymer Film Preparation

8PEG were dissolved in water with 50% of polymer by weight containing 1% of PI (1 wt% with respect to the amount of the precursor). The solution was stirred at room temperature over 1h, then casted on the clean glass slide. The water was evaporated and further dried until constant weight.

3.2.3 Differential scanning calorimetry (DSC)

Differential scanning calorimetric analysis was employed with a Mettler-Toledo DSC 822e. Samples with 3~5mg in weight were encapsulated in aluminum pans. The calibration was performed with indium and hexatriacontane and an ultra pure nitrogen atmosphere was employed as circulating atmosphere for all tests. The Measurement was performed at the Heating rate 10 ºC/min.

3.2.4 Wide-angle X-ray diffraction (WAXD)

Wide-angle X-ray diffraction analyses were carried out using a D/Max 2500 XB2+/PC X-ray diffractometer (Rigaku). The scanning angle 2θ was from 5 ºC to 90 ºC. Annealed samples having 50 μm thickness were prepared for WAXD measurements, and all the experiments were carried out at room temperature, 25 ºC. The casting films on sheet glasses were fixed on the equipment. The data were collected in every 0.02s.

3.2.5 Cross-polarizing optical microscopy (CPOM)

Polarization microscope morphology observations of the hydrogels were performed with an Olympus optical microscope (Olympus, BX51), equipped with a Canon EOS40D camera system. The whole processes were carried out in a nitrogen atmosphere.

3.2.6 Scanning electron microscopy (SEM)

For scanning electron microscopy (SEM) the samples were sputtered with gold

using a sputter coater (SCD 030, Balzers). Scanning electron images were taken with a Hitachi S-520 using an acceleration voltage of 20 kV and a working distance of 10 mm. Pictures were taken using the Digital Image Processing System (2.6.20.1, Point Electronic).

3.3 Results and discussion

3.3.1 Hydrogel formation

According to the crosslinking reaction mechanism, the crosslinked polymer networks can be formed from (a) chain-growth polymerization mechanism, (b) step-growth polymerization mechanism, and (c) mixed-mode chain and step growth mechanism. Generally, compared with photoinitiated chain polymerization, the Michael-type addition reaction, one type of step-growth polymerization mechanisms, processes better control of the crosslinking network structures and consequently better hydrogels properties [32,33]. In our study, three kinds of hydrogels based on star-shaped poly(ethylene glycol) (PEG) molecules (having 8 arms with acrylate end groups; **8PEG**) have been synthesized by different methods: (I) UV-curing **8PEG**-based hydrogels with 50% water content (**8PEG-UV**) have been synthesized via photoinitiated chain polymerization (chain-growth polymerization); (II) Novel hydrogels composed of **8PEG** (**8PEG-NH_3**) have been obtained by simply mixing **8PEG** with 40% water content with an ammonium hydroxide solution (30 wt%). The mechanism is a Michael-type addition between the acrylate and amine groups (step-growth polymerization). (III) **8PEG-NH_3-UV** hydrogels have been obtained by further UV stabilizing of **8PEG-NH_3** to photoinitiate chain polymerization of the residual acrylate end groups of **8PEG**s (mixed-mode chain and step growth mechanism). Besides, **8PEG** polymer membranes without any chemical cross linking were created for comparison with the films of the crosslinked polymers.

3.3.2 Observation of crystallinity

In order to study the crystalline morphology of **8PEG** and its corresponding hydrogels, polarized optical microscopy (POM) measurements were firstly conducted. The crystal morphologies are shown in Figure 1. Spherulites are a morphological feature of crystallized polymers and consist of a large number of chain-folded lamellar crystallites, radiating in all directions from a central nucleus with molecular chains oriented tangentially [26]. For **8PEG** polymer (Fig. 1a), it forms large spherulites with sizes of hundreds of microns, but without the typical Maltese cross. In Fig. 1b, it has shown the spherulites with sizes of 50-500 μm, and the apparent Maltese crosses in **8PEG-NH_3** hydrogel. This spherulite pattern indicates that the continuous radial variation of the orientation of the polymer crystal axes is not inhibited by crosslinking points. The spherulites formed in the **8PEG-NH_3-UV** hydrogels are much smaller but still with a definite boundary, as is seen in Fig. 1c. It is possible that the backbone kinetic chains (polyacrylates) generated during polymerization serve as a nucleating agent for the crystallization, resulting in lower crystallinity compared to **8PEG-NH_3**.

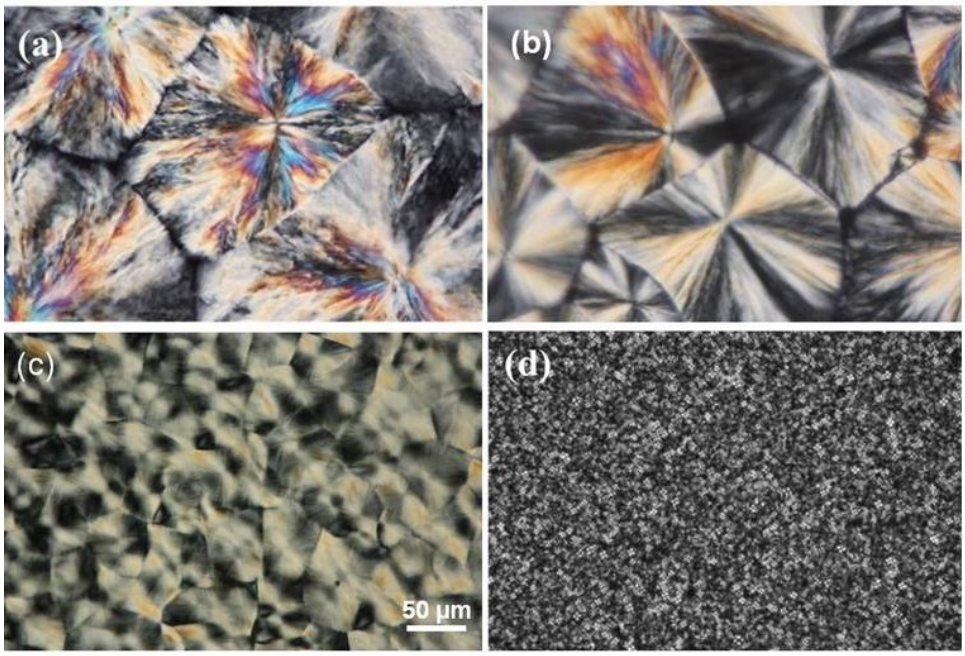

Figure 1. Spherulite morphologies of (a) **8PEG**; (b) **8PEG**-NH_3; (c) **8PEG**-NH_3-UV; (d) **8PEG**-UV.

Different from all the other samples, no large spherulites but a large number of nano-crystals are observed in **8PEG-UV** (Fig. 1d). Similar nano-sized crystalline domains have also been reported to form in partially crystallized hydrogels such as regenerated cellulose and polyacrylates with long alkyl side chains [34].

In order to investigate the crystallization process of **8PEG-NH_3** hydrogels, representative crystal morphologies that developed with time, have been studied. Figure 2 shows the evolution of crystallinity of PEG segments in **8PEG-NH_3** hydrogel membrane with increasing crystallization time (crystallization temperature is 25 °C). At the early stage, spherulites with Maltese crosses appear in the dark phase and the crystallites grow outward from the nucleus and appear as a spherical shape (Fig. 2(a)). A progression of a growing spherulite is shown in Fig. 2(b, c), and as water evaporate, the size of the spherulite increases. The color difference with the cross-polarizer corresponds to the rotation of the PEG chain orientation about the nucleus. Fig. 2(d) shows the completion of PEG crystallization in a short period of time (1 min).

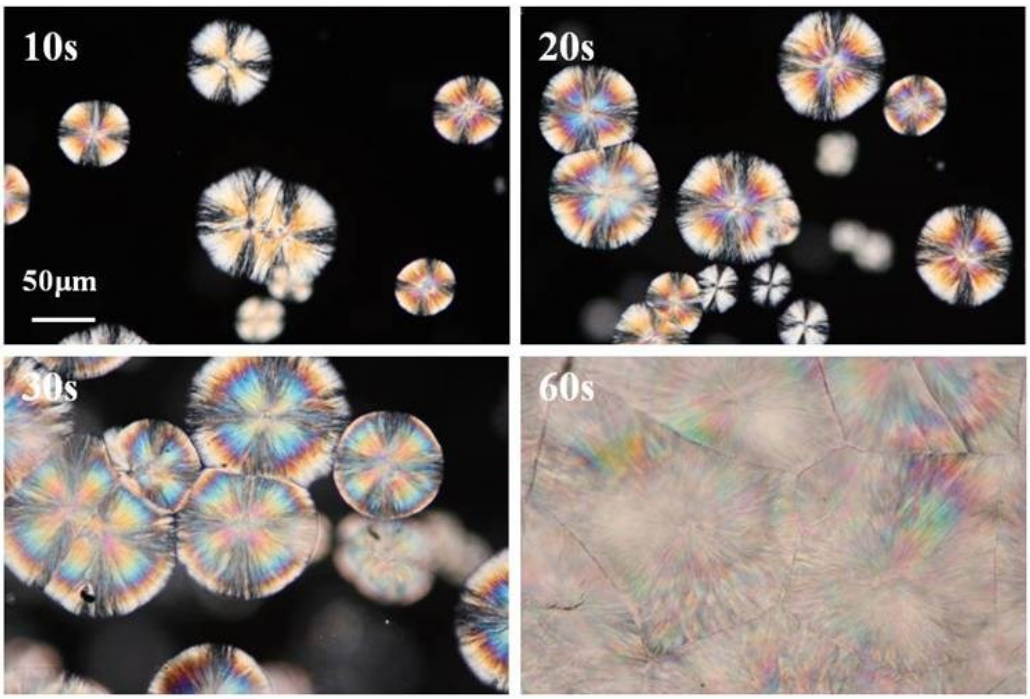

Figure 2. Spherulite morphology observation with increasing time during **8PEG-NH_3** drying process.

3.3.3 Crystal Characterization

The crystallization states of **8PEG** polymer, 8PEG-UV, **8PEG-NH_3** and **8PEG-NH_3-UV** hydrogels have been investigated by WAXD. From the patterns in Figure 3, different diffraction peaks for the PEG crystals can be detected, which correspond to the (120) and (032) planes of PEG crystallites [27], indicating the existence of a monoclinic phase. These diffractions are characteristic to PEG crystals where the PEG chains form a 72 helix structure with 6 Å per cycle [35]. The two typical peaks suggest that PEG chains in the three hydrogels are all able to crystallize and form separate crystalline phases. The almost identical spectra indicate that no significant difference of the PEG crystal structure was formed in the three hydrogels. However, the intensity of the (032) diffraction peaks decrease successively in the order of **8PEG**, **8PEG-UV**, **8PEG-NH_3** and **8PEG-NH_3-UV** hydrogels, which reflects the decreasing regularity of PEG crystals in the hydrogels.

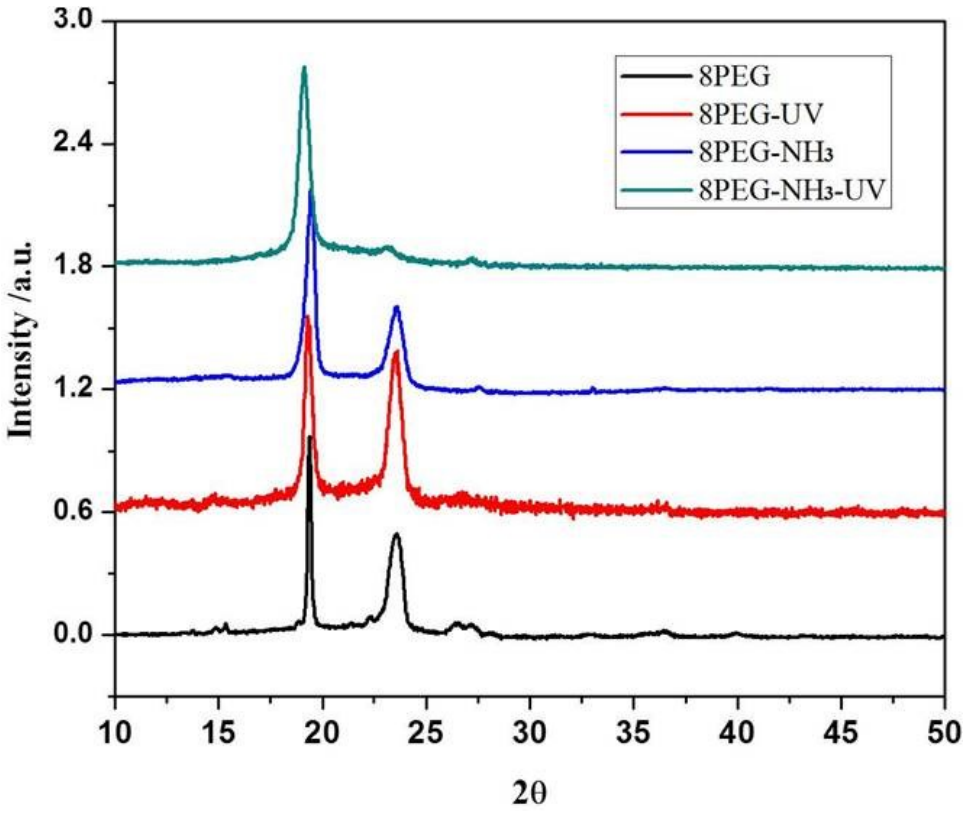

Figure 3. WAXD patterns of **8PEG**; **8PEG**-NH_3; **8PEG**-NH_3-UV; and **8PEG**-UV.

Figure 4 shows the DSC thermographs for the **8PEG** polymer and its corresponding hydrogels during heating processes with a heating rate of 10 °C/min. Sharp exothermic peaks are observed and are assigned to the melting temperatures (Tm). Tm of the pure **8PEG** polymer is 52.4 ± 0.2 °C (Fig. 4). It is interesting to note that the melting temperatures of the as-formed hydrogels are all lower. The low values of crystallinity and corresponding melting temperatures can be ascribed to the non-perfect crystal formed in the hydrogels and the irregular crystal folding. During the gel formation processes, the PEG chains are limited in a confined space till they are fixed in the gel network. Gel network formation leads to lower crystallinity, and consequently decreased melting temperatures.

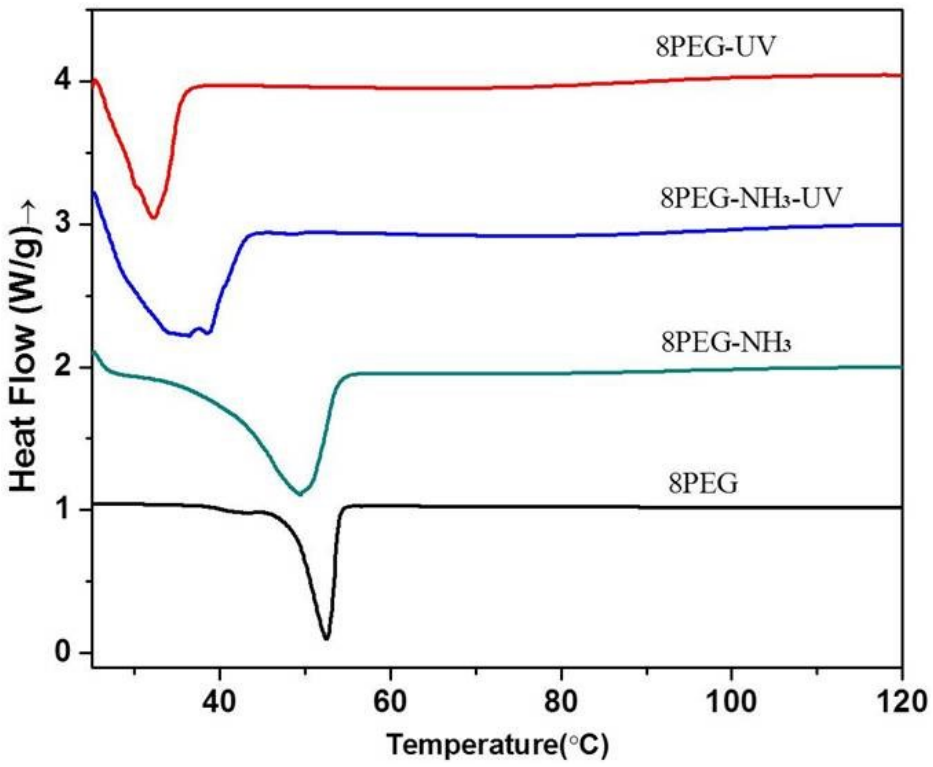

Figure 4. Representative DSC curves for **8PEG**; **8PEG-NH$_3$**; **8PEG-NH$_3$-UV**; and **8PEG-UV**, obtained at a rate of 10 °C/min.

Moreover, 8PEG-UV hydrogels show the lowest melting temperature, while the Tm of **8PEG-NH$_3$** hydrogels is closest to that of **8PEG** polymers, and the value for **8PEG-NH$_3$-UV** lies in between. This can be understood by taking into account that in

the photocrosslinked **8PEG-UV** gel matrix most of the PEG chains are cross-linked and lose their mobility. In contrast, as described in Chapter 2, due to incomplete reaction, about 60% of PEG chains in **8PEG-NH_3** gel matrix are not cross-linked, leaving many residual acrylate end group [29]. These unbound chains possess more mobility, which explains the higher degree of crystallinity and correspondingly higher melting temperature. In addition, unlike polyacrylate chains in **8PEG-UV**, which form during the chain polymerization process and lead to a tightly crosslinked network, the crosslinking points in **8PEG-NH_3** (formed according to a step-growth mechanism) hardly have any influence on crystallite growth. The consequent UV-initiated crosslinking will lead to shorter and/or fewer polyacrylate chains in the **8PEG-NH_3-UV** gel, which explains the intermediate degree of crystallinity and melting temperature.

3.3.4 Morphology investigation

We further investigated the morphology on the hydrogels' surfaces with SEM, and the corresponding photographs of **8PEG-NH_3**, **8PEG-UV** and **8PEG-NH_3-UV** hydrogels are shown in Figure 5.

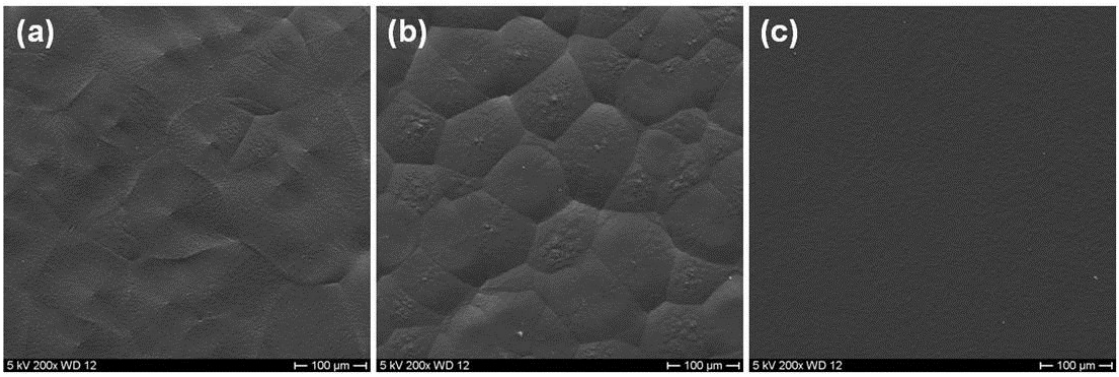

Figure 5. SEM images of (a) **8PEG-NH_3**, (b) **8PEG-NH_3-UV** and (c) **8PEG-UV** hydrogels with same magnification factor.

In Figure 5(a), regular spherulites, ranging from around 50 µm to hundreds of µm, with radial stripes are observed, showing that **8PEG-NH_3** hydrogel can form large spherulites. In addition, patterns appear mainly in the diagonal directions and

propagated from the center. This coincides with the appearance under POM as shown in Fig. 1b. However, on **8PEG-UV** hydrogel surface (Fig. 5c), no microscale structure of crystalline can be found via SEM, indicating only nano-scale crystals are formed. For **8PEG-NH_3-UV** hydrogel (Fig. 5b), large spherulite structures with clear boundaries can be observed, but the spherulite surfaces are much rougher than those of **8PEG-NH_3**, and many dots distribute on the surface. These indicate that nano-scale crystals are formed, due to the inhibition of cross-linked polyacrylate chains introduced via UV radiation into the hydrogel.

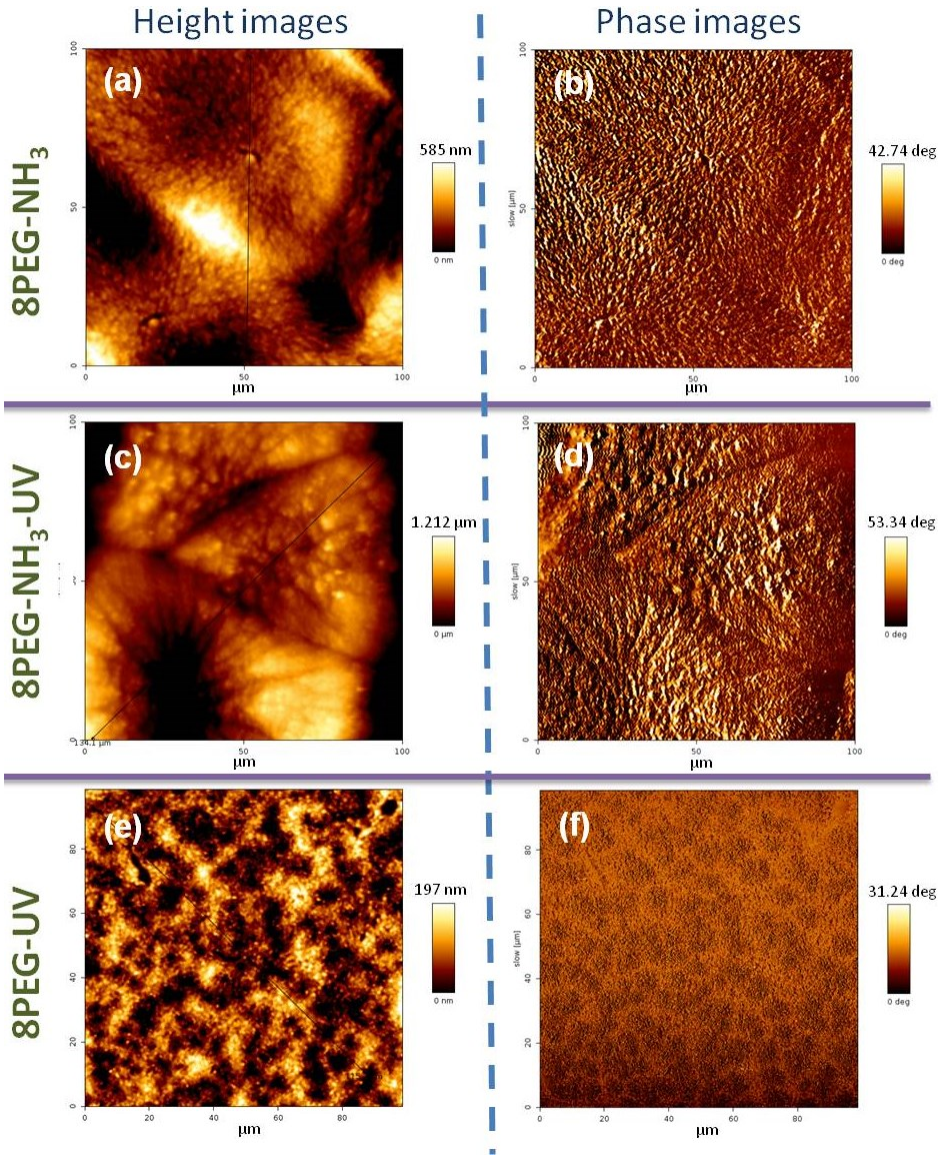

Figure 6. Representative AFM height images and phase images of **8PEG-NH_3**, **8PEG-NH_3-UV** and **8PEG-UV** hydrogels with same lateral scale.

AFM is a good method to provide further structural details of crystallization at a substantially higher resolution than that can be achieved by optical and electron microscopy. Figure 6 shows the AFM results of the **8PEG-NH_3**, **8PEG-NH_3-UV** and **8PEG-UV** hydrogels crystallized at room temperature for 12 h.

Both height and phase images clearly show the difference of the crystal structure among the three kinds of hydrogels. Figure 6(a, b) show that **8PEG-NH_3** hydrogel forms regular, large spherulites. In contrast, the crystals formed in **8PEG-UV** hydrogel are irregular, small and with more defects, as shown in Figure 6(e, f). Moreover, compared with Fig. 6e we can find that the surface topography of **8PEG**-NH_3 varies much greater in Fig. 6a, which is caused by the more flexible polymer chains in **8PEG-NH_3**. In addition, the crystal structure of **8PEG-NH_3-UV** (Figure 6(c, d)) is similar to that of **8PEG-NH_3**, while the surfaces of **8PEG-NH_3-UV** become much rougher. This indicates that after UV radiation a large number of crosslinking points are introduced, which disturb the crystallization process of PEG segments, and lead to many small dots formation. It should be noted that the AFM shows the surface images of the hydrogel films, while the POM shows the bulk images of the hydrogel between two glass slides. However, the morphological observation in Figure 6 is in agreement with the result obtained by POM in Figure 1.

3.3.5 Discussion of the crystallization mechanism

For all three kinds of gels, the chemical constitution of the gels and resultant crystalline phases are almost the same, while the main difference is the gel network structure. To clearly explain the difference we propose a model here to schematically illustrate the different crystalline formation mechanisms in the three kinds of gels (Fig. 7).

According to the crosslinking reaction mechanism [32], Fig. 7 illustrates the network structures resulting from the chain-growth polymerization (**8PEG-UV**), step-growth polymerization (**8PEG-NH_3**) and mixed-mode polymerization

(**8PEG-NH$_3$-UV**) of **8PEG** precursors. In Fig. 7b for chain-growth polymerization (**8PEG-UV**), the propagation of free radicals through multiple carbon-carbon double bonds on the constituting PEG monomers results in covalently crosslinked, uncontrolled and high molecular weight kinetic chains, leading to irregularly distributed cross-linked points and consequently network imperfections, such as cycles and dangling chain ends [29,30]. Meanwhile the polymer chains are tightly bonded with each other, so the crystallization process is confined in nano-scaled space, leading to the formation of nanocrystals (Fig 7b).

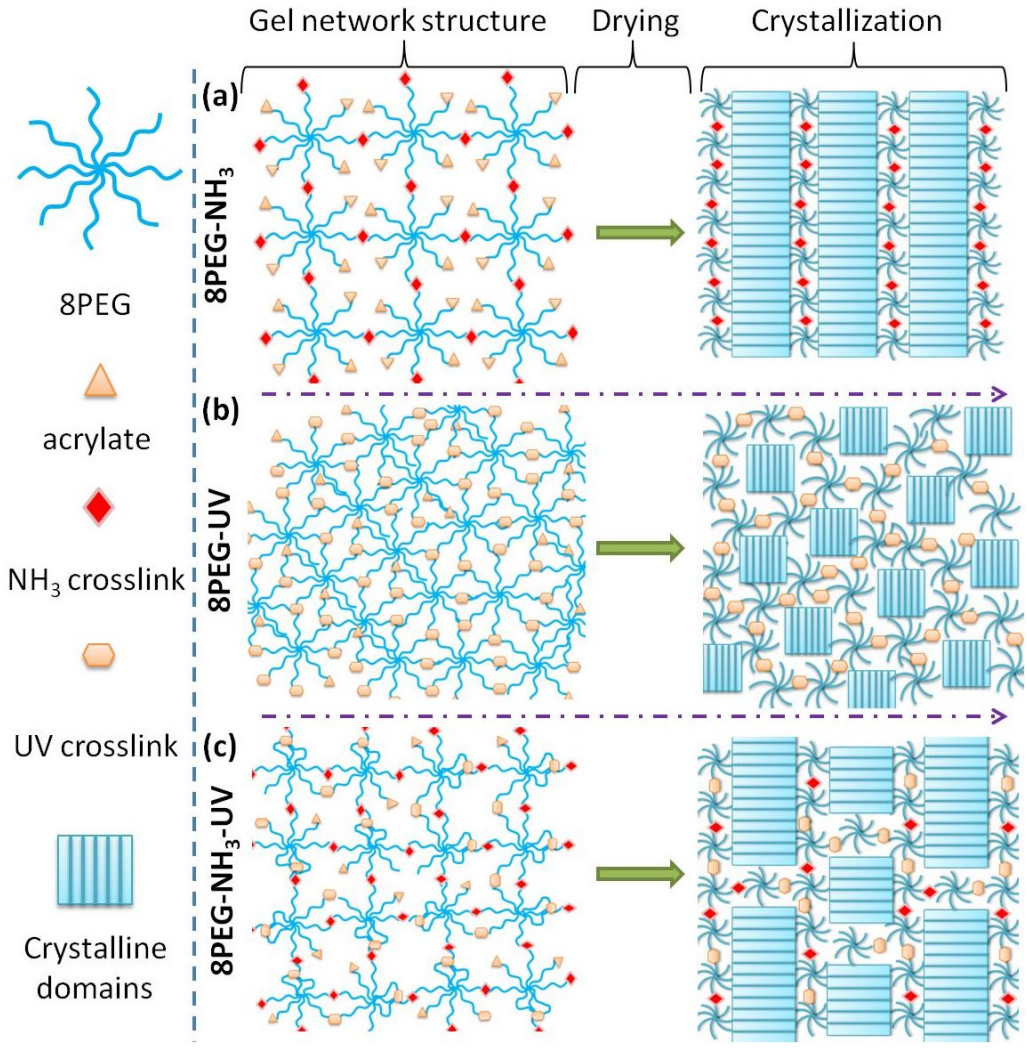

Figure 7. A scheme of proposed mechanism for the crystallization structure formed due to different type of gel network structure. Three kinds of gel network structure are shown on the left, after drying process, the resultant crystalline patterns are shown on the right .

On the contrary, the networks of **8PEG**-NH_3 form through a step-growth polymerization of amines and conjugated unsaturated vinyl groups (Fig. 7a), and two multifunctional monomers with mutually reactive chemical groups are reacted to form one crosslink point, producing fewer structural defects during network formation and more flexible polymer networks, so that the resulting hydrogels possess homogeneous network structures [31,33]. The hydrated and flexible polymer chains and crosslink points are both regularly distributed. When drying, the crystallites can easily propagate from the center, resulting in the long-range ordered structure in the gel matrix (Fig 7a).

In addition, as shown in Fig. 7c the **8PEG-NH_3-UV** hydrogels, formed from the mixed-mode polymerization mechanism, exhibit intermediate network characteristics between chain and step-growth polymerizations. On one hand, due to the regularly distributed crosslink points formed through the acrylate and amine groups, the regular gel network structure can still be maintained so that the similar ordering structure in microscale merged after drying; however, on the other hand, the polyacrylate chains introduced via further UV radiation disturb the propagation of crystallites and decrease the flexibility of polymer chains, leading to much rougher surface.

3.4 Conclusions

In conclusion, the crystallization of three kinds of chemically cross-linked PEG-based hydrogels, evolved from chain-growth polymerization (**8PEG-UV**), step-growth polymerization (**8PEG-NH_3**), and mixed-mode chain and step growth polymerization (**8PEG-NH_3-UV**) respectively, has been compared and investigated. POM, SEM and AFM studies confirm that the **8PEG-NH_3** and **8PEG-NH_3-UV** have a framework of crystalline domains sized in 30 µm-500 µm, in contrast to only nanoscaled crystalline domains in **8PEG-UV**. Moreover, DSC is utilized to determine crystalline states and thermal properties of **8PEG** and their hydrogels, the results indicate that less crystallinity leads to the decrease of the melting temperatures of

hydrogels. Moreover, WAXD spectra of **8PEG** polymer and three **8PEG**-based hydrogels reveal that there is almost no change in crystalline phases between **8PEG** polymer and the corresponding hydrogels. However, the sizes of crystalline domains are different. The relationship between the formation of ordered structures in hydrogels and the gel network structures is proposed and elucidated, which reveals that the regular molecule's orientation in nano-scale scope can lead to the ordering structure formation in micro-scale scope.

References

[1] Fratzl, P.; Weinkamer, R. Nature's hierarchical materials. *Progress in Materials Science* **2007**, 52, 1263–1334.

[2] Aizenberg, J. *et al.* Skeleton of Euplectella sp.: Structural hierarchy from the nanoscale to the macroscale. *Science,* **2005**, 309, 275–278.

[3] Thiel, B. L.; Guess, K. B.; Viney, C. Non-periodic lattice crystals in the hierarchical microstructure of spider (major ampullate) silk. *Biopolymers* **1997**, 41, 703–719.

[4] Sanchez, C.; Arribart, H.; Guille, M. M. G. Biomimetism and bioinspiration as tools for the design of innovative materials and systems. *Nat. Mater.* **2005**, 4, 277-288.

[5] Whitesides, G. M.; Grzybowski, B. Self-assembly at all scales. *Science* **2002**, 295, 2418-2421.

[6] Hirst, A.R. Escuder, B.;, Miravet, J.F.; Smith, D.K. High-tech applications of self-assembling supramolecular nanostructured gel-phase materials: from regenerative medicine to electronic devices. *Angew.Chem. Int. Ed.* **2008**, 47, 8002-8018.

[7] Seliktar, D. Designing cell-compatible hydrogels for biomedical applications. *Science* **2012**, 336, 1124-1128.

[8] Lee, K. Y.; Yuk, S. H. Polymeric protein delivery systems. *Prog. Polym. Sci.* **2007**, 32, 669-697.

[9 Wu, Z. L.; Gong, J. P. Hydrogels with self-assembling ordered structures and their functions. *NPG Asia Mater.* **2011**, 3, 57–64.

[10] Clark, A. H.; Ross-Murphy, S. B. Structural and mechanical properties of biopolymer gels. *Adv. Polym. Sci.* **1987***, 83*, 57.

[11] Zhang, S. Fabrication of novel biomaterials through molecular self-assembly. *Nat. Biotechnol* **2003**, 21, 1171–1178.

[12] Hirst, A. R.; Escuder, B.; Miravet, J. F.; Smith, D. K. High-tech applications of self-assembling supramolecular nanostructured gel-phase materials: from regenerative medicine to electronic devices. Angew. Chem., Int. Ed. **2008**, 47, 8002–8018.

[13] Lutolf, M. P.; Hubbell., J. A. Synthetic biomaterials as instructive extracellular microenvironments for morphogenesis in tissue engineering. *Nat. Biotechnol.* **2005**, 23, 47–55.

[14] Zhang, S.; Greenfield, M. A.; Meta, A.; Palmer, L. C.; Bitton, R.; Mantei, J. R.; Aparicio, C.; de la Curz, M. O.; Stupp, S. I. A self-assembly pathway to aligned monodomain gels. *Nat. Mater.* **2010**, 9, 594–601.

[15] Kang, K.; Walish, J. J.; Gorishnyy, T.; Thomas, E. L. Broad-wavelength-range chemically tunable block-copolymer photonic gels. *Nat. Mater.* **2007**, 6, 957–960.

[16] Huang, Z.; Lee, H.; Lee, E.; Kang, S. K.; Man, J. M.; Lee, M. Responsive nematic gels from the self-assembly of aqueous nanofibres. *Nat. Commun.* **2011**, 2, 459.
[17] Um, S. H.; Lee, J. B.; Park, N.; Kwon, S. Y.; Umbach, C. C.; Luo, D. Enzyme-catalysed assembly of DNA hydrogel. *Nat. Mater.* **2006**, 5, 797–801.
[18] Kaneko, T.; Yamaoka, K.; Gong, J. P.; Osada, Y. Liquid-crystalline hydrogels. 1. Enhanced effects of incorporation of acrylic acid units on the liquid-crystalline ordering. *Macromolecules* **2000**, 33, 412–418.
[19] Kaneko, T.; Yamaoka, K.; Osada, Y.; Gong, J. P. Thermoresponsive shrinkage triggered by mesophase transition in liquid crystalline physical hydrogels. *Macromolecules* **2004**, 37, 5385–5388.
[20] Kato, T.; Hirai, Y.; Nakaso, S.; Moriyama, M. Liquid-crystalline physical gels. *Chem. Soc. Rev.* **2007**, 36, 1857–1867.
[21] Kaneko, T.; Tanaka, S.; Ogura, A.; Akashi, Mitsuru. Tough, thin hydrogel membranes with giant crystalline domains composed of precisely synthesizedmacromolecules. *Macromolecules* **2005**, 38, 4861-4867
[22] Hennink, W. E.; van Nostrum, C. F. Novel crosslinking methods to design hydrogels. *Advanced Drug Delivery Reviews* **2002**, 54, 13-36.
[23] Zalipsky, S.; Harris, J. M. *Poly(Ethylene Glycol)* **1997**, 680, 1-13.
[24] Cheng, S. Z. D.; Zhang, A.; Barley, J. S.; Chen, J.; Habenschuss, A.; Zschack, P. R. Isothermal Thickening and Thinning Processes in Low Molecular Weight Poly(ethylene oxide) Fractions. 1. From Nonintegral-Folding to Integral-Folding Chain Crystal Transitions. *Macromolecules* **1991**, 24, 3937-3944.
[25] Alfonso, J. C.; Russell, T. P. Kinetics of crystallization in semicrystalline/amorphous polymer mixtures. *Macromolecules* **1986**, 19, 1143-1152.
[26] Cheng, S. Z. D.; Wu, S. S.; Chen, J.; Zhuo, Q.; Quirk, R. P.; Meerwall, E. D. V.; Hsiao, B. S.; Habenschuss, A.; Zschack, P. R. Isothermal thickening and thinning processes in low-molecular-weight poly (ethylene oxide) fractions crystallized from the melt. 4. End-group dependence. *Macromolecules* **1993**, 26, 5105-5117.
[27] Cheng, S. Z. D.; Zhang, A.; Chen, J.; Heberer, D. P. Nonintegral and integral folding crystal growth in low-molecular mass poly(ethylene oxide) fractions. I. Isothermal lamellar thickening and thinning. *Journal of Polymer Science Part B: Polymer Physics*. **1991**, *29*, 287-297.
[28] Mya, K.Y.; Pramoda, K.P.; He C.B. Crystallization behavior of star-shaped poly (ethylene oxide) with cubic silsesquioxane (CSSQ) core. *Polymer* **2006**, 47, 5035–5043.
[29] Lin-Gibson, S.; Jones, R. L.; Washburn, N. R.; Horkay, F. Structure-property relationships of photopolymerizable poly (ethylene glycol) dimethacrylate hydrogels. Macromolecules 2005 , 38 , 2897-2902.
[30] Flory, P. J.; Rehner, J. Statistical Mechanics of Cross-Linked Polymer Networks I. Rubberlike Elasticity. *J. Chem. Phys.* **1943**, 11, 512-521.
[31] Lutolf, M. P.; Hubbell, J. A. Synthesis and physicochemical characterization of end-linked poly (ethylene glycol)-co-peptide hydrogels formed by Michael-type addition. *Biomacromolecules* **2003**, 4, 713-722.
[32] Lin, C. C.; Anseth, K. S. PEG Hydrogels for the Controlled Release of Biomolecules in Regenerative Medicine *Pharm. Res.* **2009**, 26, 631–643.
[33] Rydholm, A. E.; Bowman, C. N.; Anseth. K. S. Degradable thiol-acrylate photopolymers:

polymerization and degradation behavior of an in situ forming biomaterial. *Biomaterials* **2005**, 26, 4495–4506.
[34] Osada, Y.; Matsuda, A. Shape memory in hydrogels. *Nature* **1995**, 376, 219-220.
[35] Tadokoro, H.; Chatani, Y.; Yoshimura, T.; Tahara, S.; Murahashi, S. Structural studies on polyethers, [-(CH2)m-O-]n. II. Molecular structure of polyethylene oxide. *Makromol. Chem.* **1964**, 73, 109-127.

Chapter 4.

In situ Synthesis of Nanocomposites from Poly(Ethylene Glycol)-Based Hydrogels and Calcium Phosphates; Characterisation and Investigation of their Mechanical and Bioactive Properties

Abstract

Bioactive polymer/inorganic (nano) composites in which the elastomeric properties of for instance hydrogels are combined with hard components of ceramics have been intensively investigated; such nanocomposite gels are promising materials to promote tissue regeneration and reconstruction. Here we present a novel *in situ* synthetic procedure to prepare nanocomposite hydrogels consisting of poly(ethylene glycol) (PEG) and homogeneously dispersed crystalline hydroxyapatite (HAp) nano-domains (nHAp) . The addition of mixtures of calcium and phosphorous salt-solutions with ammonium hydroxide to the PEG-precursor solution leads to spontaneous gelation. The resulting hydrogels can be further stabilized through covalent cross-linking via photo polymerization of the acrylate groups. Rheological measurements were conducted in order to assess the spontaneous gelation time in dependence of the salt content. The perfect homogeneity of nHAp was proved by scanning electron microscopy (SEM) elemental mapping. Transmission electron microscopy (TEM) analysis revealed crystalline regions distributed throughout the hydrogels which mainly exhibit an amorphous nature. Nevertheless, Raman-spectroscopy as well as X-ray diffraction (XRD) verified the formation of HAp domains and allowed us to distinguish these domains from other potential calcium phosphate phases. Thermogravimetric analysis (TGA) measurements were evaluated, suggesting that a concentration of 20wt% nHAp within the gel matrix reveals the strongest interaction between the organic and inorganic phase. The incorporation of nHAp into PEG hydrogels via chemical mixing resulted in highly interesting physical and chemical hydrogel properties and provided significant bioactivity, as highlighted by specific osteoblast cell adhesion.

4.1 Introduction

Hydrogels are hydrophilic polymer chain networks containing large quantities of water. Because of their efficient mass transfer, stimuli- and cell-responsiveness due to hydrophilicity, porous structure and often found cytocompatible nature they have been utilized for various applications, such as surface modification, soft tissue engineering scaffolds, drug/cell delivery vehicles, stem cell cultures, biosensors, and tissue fillers [1-4]. Poly(ethylene glycol)(PEG)-based hydrogels are one of the most important types of hydrogels and act as promising materials for various biomedical applications, because of their very useful properties, such as good biocompatibility, non-immunogenicity, and resistance to protein adsorption [5-8]. Despite the many advantages provided by PEG-based hydrogels, they display insufficient mechanical rigidity. They are therefore limited concerning applications such as 3D matrices for tissue repair or scaffolds for bioactive molecule delivery [9]. Some applications need to introduce biological activity to the non-adhesive nature of PEG chains [10]. Therefore, there is growing interest to incorporate a variety of nanoparticles (NPs) into the hydrogels to improve their mechanical and biological properties [11-13].

Recently, Pek et al. fabricated PEG-based nanocomposite hydrogels with silicate nanoparticles as a three-dimensional cell culture material [14]. The aggregation of nano- and micrometer-sized nanoparticles led to a high porosity of these hydrogels. It was demonstrated that not only the proliferation of Human mesenchymal stem cells was enhanced due to good permeability of nutrients and gases through the gels, but also the differentiation of cells could be controlled by changing the rheological properties of the gel. Another study by Schmidt et al. reported on the synthesis and formulation of injectable silicate-PEG nanocomposite precursor solutions that can be covalently cross-linked to form transparent, highly elastic and tough hydrogels. The incorporation of silicate NPs to the covalently cross-linkable PEG network improved the elastic properties, induced adhesion (stickiness) to soft and hard surfaces and promoted mammalian cell adhesion [15]. In a different study, Chang et al.

synthesized biocompatible poly(ethylene glycol) diacrylate (PEGDA)/Laponite nanocomposite hydrogels [16]. Incorporation of those inorganic nanoparticles significantly enhanced both the compressive and tensile properties of PEGDA hydrogels without severely compromising their ability to imbibe water. Simultaneously, these hydrogels supported cell adhesion and subsequent spreading in a 2D culture, as well as 3D cell encapsulation.

Among the most prominent inorganic NPs, hydroxyapatite (HAp) NPs have been studied extensively because of their excellent biocompatibility, bioactivity and osteoconductivity as well as their similarities to biological apatite, the main mineral component of bone [17-20]. Moreover, HAp has been widely used as a bioactive phase in composite materials, coatings on metal implants, and as granular fillers for direct incorporation into human tissues [21]. The bioactive characteristics of HAp NPs [22-24] strongly affect the final polymer-HAp composite systems. These systems find special interest in hard tissue engineering related to bone or tendons [25-27]. However, it is difficult to synthesize HAp in the complex forms required for bone treatment. The hardness and brittleness，as well as the poor compressive strength limits the applicability of HAp. Moreover, HAp (in the form of) powders, used for the treatment of bone defects, easily leaks out of the implanted sites [28, 29]. To mimic natural organic/inorganic biocomposites with excellent mechanical and biological properties, such as those found in shells and pearls, one wide spread strategy uses HAp NPs as inorganic phase for reinforcement and thus forming nanocomposite (NC) hydrogels with enhanced mechanical properties such as elongation, toughness and tensile strength. For example, Gaharwar et al. developed a range of photo-cross-linked poly(ethylene glycol) (PEG) nanocomposites with enhanced extensibilities, fracture stress, compressive strength, and toughness via physical mixing of PEG with HAp NPs [30]. This literature report already indicated that the combination of PEG and HAp may significantly improve the physical and chemical hydrogel properties as well as biological characteristics such as mammalian cell adhesion.

Herein we present an *in situ* nucleation process of HAp in an 8-arm poly(ethylene glycol) (**8PEG**) hydrogel matrix for the spontaneous gelation of a bioactive nanocomposite material. The benefits of this approach are on the one hand the secondary interactions between organic/inorganic phases with improved mechanical properties, and on the other hand the avoidance of the common agglomeration problem accompanying nanocomposites consisting of an inorganic and organic phase [31]. Furthermore it is possible to precisely tune the mechanical, biological and degradation properties.

In this study, the crystal phase of the calcium phosphate (CP), i.e. the quality of the HAp that is formed, and the morphologies of the composite hydrogels are characterized by scanning electron microscopy (SEM), transmission electron microscopy (TEM), X-ray diffraction (XRD) and RAMAN spectroscopy. The inorganic contents are determined by thermogravimetric analysis (TGA). Mouse connective tissue fibroblasts (L-929) and MC3T3-E1 osteoblasts are utilized for cell adhesion tests, verifying the specific bio-interaction between osteoblasts and (**8PEG**-HAp based) composite hydrogels. The unique property combinations of the hydrogels and HAp reported in this Chapter offer new approaches for complex composite biomaterials engineering.

4.2 Materials and Methods

4.2.1 Materials and Measurements

All chemicals were purchased from Sigma-Aldrich and used as received unless stated otherwise. 8-arm PEG-OH with a molecular weight of 15 KDa was purchased from Jenkem technology USA. Solvents were analytical grade quality minimum. The silicon masters were purchased from Amo GmbH (Aachen). The synthesis of macromonomer of 8arm PEG with acrylated end-groups, AFM measurements, Raman spectroscopy and rheological measurements were performed following the same procedure described in Chapter two.

4.2.2 8PEG Composite Synthesis

Composites made of **8PEG** and HAp were obtained as shown in Fig. 1. As prepared salt solutions of $Ca(NO_3)_2$ and $(NH_4)_2HPO_4$ were added to the precursor solution of 8arm PEG complemented with 1 % PI at room-temperature under vigorous magnetic stirring. Maturation time was 24 h constantly. Compositions were varied in order to receive 10 wt%, 20wt%, and 40 wt% HAp in the **8PEG** composites (**8PEG** 10HAp, **8PEG** 20HAp and **8PEG** 40HAp, respectively).

For the cell adhesion tests, in order to avoid complete degradation of the gels, the obtained gels need to be further stabilized by UV curing (wavelength 365 nm) in the hydrated state for 15 min. For comparison, **8PEG** 20wt% $(NH_4)_2HPO_4$ UV stabilized hydrogels were prepared using the same procedure as for **8PEG** 20HAp hydrogel preparation, without the addition of a calcium containing solution.

4.2.3 X-ray diffraction (XRD)

A X'Pert Pro, PANalytical powder-diffractometer was used for XRD measurements in the range of 5 to 80 ° 2θ. Samples were vacuum-dried at room temperature and grinded into powder prior to measurements. The X-ray generator was operated at a voltage of 40 kV and 40 mA producing Cu*Kα* radiation with a wavelength λ of 0.154 nm. The scanning speed was kept at 2300s degree^{-1} for all measurements.

4.2.4 Electron microscopy

Scanning electron microscopy (SEM) images were taken with a Hitachi S-520 using an acceleration voltage of 20 kV and a working distance of 10 mm. In-situ electron Energy dispersive x-ray spectroscopy (EDX) was performed on a Hitachi SEM S-520, EDX-Horiba Link instrument, which was used to identify elemental composition (in particular Ca/P ratios) and elemental mapping in defined areas of the corresponding sample. Prior to image recording, samples were carbon-coated. An acceleration

voltage of 8 keV was applied yielding EDX spectra with a penetration depth of approximately 2.0 µm.

Transmission electron microscopy (TEM) (TECNAI G²20) was used to identify and quantify the crystalline character of PEG-HAp composites. In order to analyze the elemental composition in-situ EDX was utilized. Prior to measurements, samples were frozen in LN2 and subsequently grinded using small amounts of ethanol. For their observation, the samples were mounted on holey-carbon coated 300 mesh copper grids. As a final step the suspension on the copper grid was dried at ambient conditions. The instrument was operated at 200 keV acceleration voltage with a LaB6-cathode and 0.24 nm point-resolution.

4.2.5 Thermogravimetric Analysis (TGA)

Dry hydrogel films were characterized by TGA and differential thermal analysis (DTA) with a TA Instrument, a TGA 2050 thermogravimetric analyzer. The temperature was raised from room temperature to 800 °C at a heating rate of 5 °C min^{-1} under air. Sample weight was 100 mg each .The dry films were cut into small pieces. Alumina powder was used as standard.

4.2.6 Cell Culture

Mouse connective tissue fibroblasts (L-929) were kindly provided by Dr. J. Lehmann (Fraunhofer Institute for Cell Therapy and Immunology IZI, Leipzig). L-929 cells were cultured in RPMI 1640 containing 10 % fetal bovine serum (FBS) and 1 % penicillin/ streptomycin (PS; all obtained from PAA Laboratories GmbH) at 37 °C and 5 % CO_2 in a humidified incubator. The cells were grown in 75 cm^2 cell culture flasks (SPL Life Sciences Inc.) until confluence, washed with Dulbecco's phosphate buffered saline solution (DPBS, PAA Laboratories GmbH) and treated with trypsin-EDTA (PAA Laboratories GmbH).

MC3T3-E1 osteoblast like cells (further denoted as osteoblasts), originally derived

from mouse calvaria, were kindly provided by Prof. Z. Su (Beijing University of Chemical Technology, China). MC3T3- cells were grown in 75 cm^2 cell culture flasks containing minimum essential medium (Sigma-Aldrich) supplemented with 10 % FBS and 1 % PS at 37 °C and 5 % CO_2 in a humidified incubator. The cells were grown until confluence, washed with DPBS and treated with trypsin-EDTA.

4.2.7 Cell adhesion and viability tests

Samples were washed with ethanol (70 %), rinsed in DPBS and placed in 24 well-plates (Becton Dickinson). 50.000 cells/ ml were seeded on top of the samples and incubated for 24 h at 37 °C, 5 % CO2 and 100 % humanity. After 24 h the cells were washed with DPBS to remove unattached cells as well as remaining medium components and fixed for 30 min with 4 % formaldehyde at pH 7 (Carl Roth GmbH). Optical images were taken with the Axio Oberserver. Z1(Carl Zeiss).

In order to assess the cells' viability, after incubation and DPBS washing, the cells were stained with 100 µl of a vitality staining solution containing fluorescein diacetate (stock solution 0.5 mg ml^{-1} in acetone, Sigma-Aldrich) and propidium iodide (stock solution 0.5 mg ml^{-1} in Ringer's solution, Fluka). Attached cells were observed by fluorescence microscopy.

4.3 Results and Discussion

4.3.1 Hydrogel synthesis

The **8PEG** composite hydrogels were synthesized via the following procedure (Fig 1a). The salt solutions were added dropwise (slowly) to the **8PEG** precursor solutions. The mixed solution was vigorously stirred until the slightly opaque, almost transparent hydrogels form. The hydrogels were easy processible and can be readily shaped into any desired form. The initial contents of these reagents were adjusted to yield the final **8PEG**/Ca+PO_4 salt weight ratios of 10%, 20% and 40%. The different

salt solutions used here to test if gelation occurred under different conditions are listed in Figure 1b.

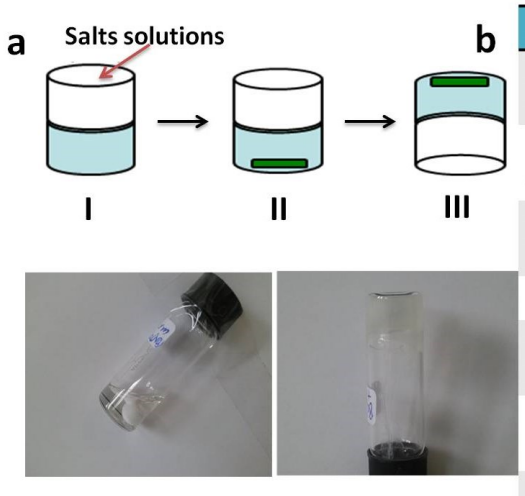

b

Salts solutions	Gel formation
8PEG+$Ca(NO_3)_2$+$(NH_4)_2HPO_4$/NH_3(PH=9.8)	Stiff gel
8PEG-OH+$Ca(NO_3)_2$+$(NH_4)_2HPO_4$/NH_3(PH=9.8)	No gel formation
8PEG+$Ca(NO_3)_2$+$(NH_4)_2HPO_4$/NH_3(PH=9.5)	Viscous liquid(no gel formation)
8PEG+$Ca(NO_3)_2$	No gel formation
8PEG+$(NH_4)2HPO_4$/NH_3 (PH=9.8)	Soft gel
8PEG+$(NH_4)_2HPO_4$	Jelly like gel formation after 2day
8PEG+Na_2HPO_4	No gel formation

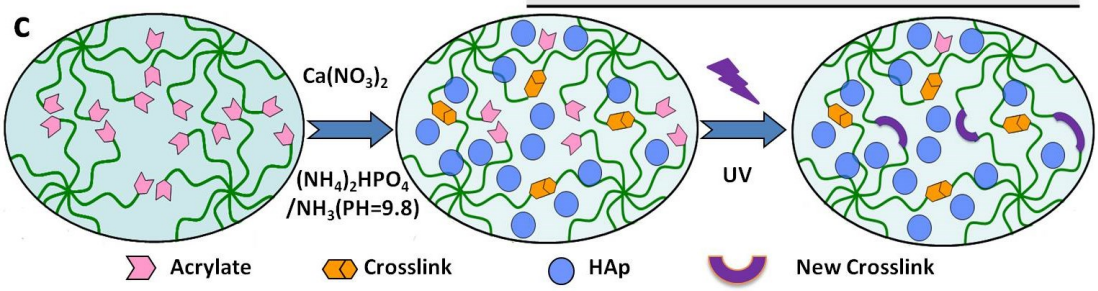

Figure 1. Gel formation process (a) gel formation during the reaction: (I) addition of salt solutions to an aqueous solution of **8PEG** (II) maturation under constant magnetic stirring (III) gelled **8PEG** HAp composite hydrogel; (b) The table lists for which formulations gels are formed; (c) proposed gelation reaction schemes detailing the Michael type addition chemistry of the gelation reaction and UV stabilization.

As depicted in Fig. 1b, **8PEG** with the unsaturated carbon double bonds and NH_3 are essential for gel formation via amine Michael type addition chemistry. Based on our previous study described in Chapter 2, the amine-type Michael addition reaction leads to the crosslinked network formation. The pH is adjusted to 9.8 with NaOH solution to generate enough of the nucleophilic reactant, amine anions (NH_2^-), for a stable hydrogel network formation. Nevertheless, incorporation of CP also leads to strengthened gel networks. The much stiffer gels are obtained via in situ CP formation within the gel matix, compared with $(NH_4)_2HPO_4$/NH_3(PH=9.8) addition without CP formation. It demonstrates that the stiff nature of the nanocomposite

networks can be attributed to sufficiently long and flexible PEG chains between cross-linking points but also to physical interactions between polymer and the inorganic phase.

Fig. 1c sketches the proposed reaction scheme based on Michael type addition chemistry, in which HAp nucleates and matures in the **8PEG** precursor matrix. The in-situ HAp formation process leads to homogenous distribution of the inorganic phase within the polymer matrix. In addition, HAp formation improves the hydrogel composites mechanical properties due to the interaction between the inorganic phases and polymer chains. Subsequent UV radiation is utilized for the polymerization of the residual acrylate groups in order to stabilize the hydrogels in aqueous conditions.In fact, UV radiation proved crucial to prevent gel degradation due to the cleavage of ester groups on the polymer backbone in aqueous solution after 24 h.

4.3.2 Mechanical properties of the hydrogels

Rheological measurements are performed to access the gelation time in dependence of the CP content (see inset table in Fig 2a). In the following, CP will be denoted as HAp, since this is the desired phase that is formed, and also detected (vide infra). Figure 2a depicts a representative example of a gelation time recording of **8PEG** 20HAp, which is determined as the crossover-point of the storage modulus (G') and the loss modulus (G"). Surprisingly, there is no clear trend for gelation times with rising or falling CP content. **8PEG** 20HAp (20 wt% HAp) shows the shortest gelation-time, which indicates strongest interactions between the mineral and the precursor **8PEG** network. This is quite remarkable, since the concentration of calcium- and phosphate-ions is considerably lower than in composite gels containing 40 wt% HAp (**8PEG** 40HAp); it could be expected to have shorter gelation times for higher CP contents. The results furthermore demonstrate that a minimum concentration of salt ions must be present in order to facilitate gel formation. A nearly 4 times longer gelation time is needed for hydrogels with only 10 wt% HAp

(**8PEG** 10HAp). Those resulting hydrogels were very soft in comparison to gels with higher CP content.

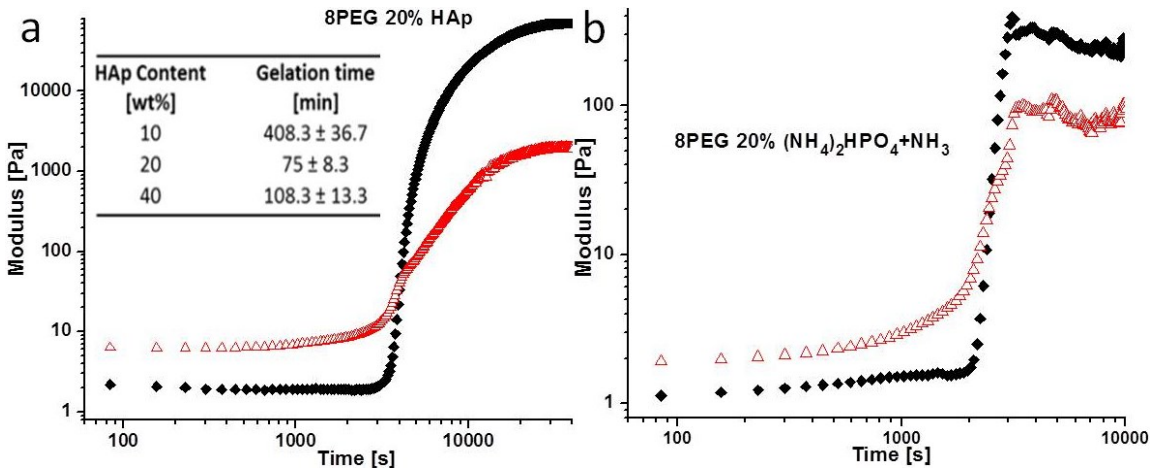

Figure 2. a: representative crossover recording of storage and loss modulus during rheological measurements of **8PEG** with 20%HA, inset table shows gelation times for the different **8PEG** HAp hydrogel composites; b: representative crossover recording of storage and loss modulus during rheological measurements of **8PEG** 20wt%$(NH_4)_2HPO_4$ gel without Calcium ions.

In addition, the same amount of $(NH_4)_2HPO_4/NH_3$(PH=9.8) as for **8PEG** 20HAp, but without the calcium-ion containing salt solution is used for gel formation, and the gelation process is monitored via rheological measurements in Figure 2b. The gelation time is around 45mins, much less than **8PEG** 20HAp, nevertheless, the storage modulus, corresponding to stiffness of gels, is more than 100 fold lower than **8PEG** 20HAp, which is in good agreement with Figure 1b. It could be reasoned that the faster gelation process is attributed to the higher pH value in the absence of a calcium solution. However, the lack of calcium ions lead to a hydrogel without HAp formation and therefore to weak mechanical properties. This indicates that HAp phase interactions with the polymer chains, as well as crosslinking reactions, mutually play crucial roles in the formation of these stiff yet flexible gels.

4.3.3 Characterization of the nanocomposite gels

In order to analyze the morphology of the as prepared nanocomposite gels, TEM images were conducted with selected area electron diffraction (SAED) modes and

furthermore with an in-situ EDX and in-situ XRD analysis as shown in Fig. 3. The crystallographic net-planes representing crystalline domains (white circle) of the composite can be clearly identified. Electron diffraction helped allocating the corresponding net-planes assigned from the according Miller index reflections (002) and (211) and determining the respective net-plane distance to be 2.84 Å and 3.41 Å [32]. However, most areas shown in the TEM image exhibit an amorphous character as depicted in the X-ray diffraction pattern. Therefore it can be concluded, that although a general amorphous morphology prevails, local highly crystalline domains exist, explaining the extraordinary properties of these nanocomposite hydrogels. In-situ EDX analysis confirms the presence of both calcium and phosphorous, which can be attributed to the inorganic CP phase, as well as carbon and oxygen at high levels belonging to the PEG polymer chains.

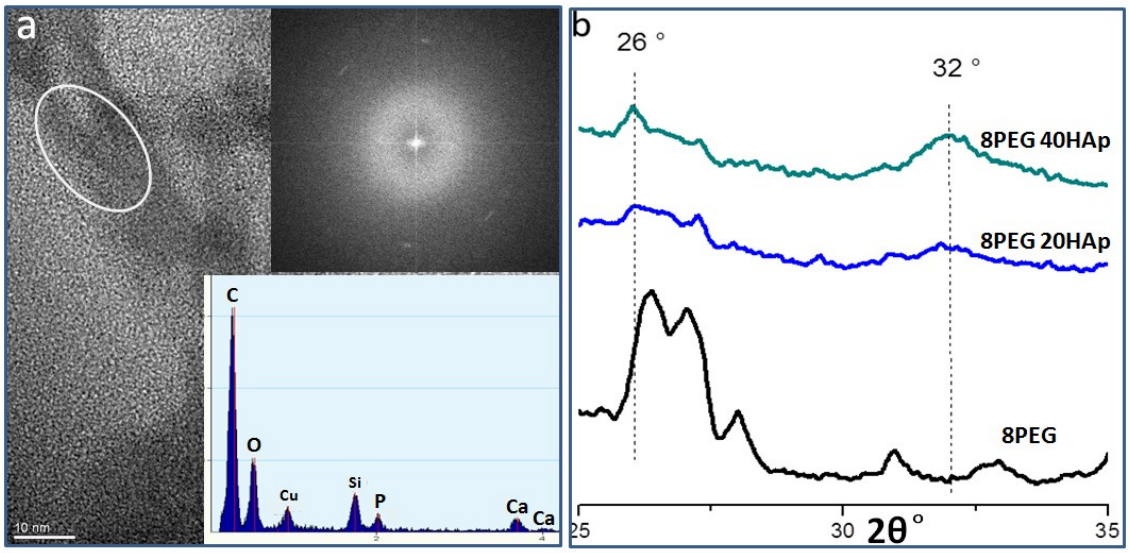

Figure 3. Chemical characterization of **8PEG** HAp nanocomposites with varying composition. (a) TEM image of **8PEG** 20HAp depicting crystalline areas (white circle) with its corresponding-in-situ XRD pattern, and EDX spectrum; (b) Powder XRD patterns displaying **8PEG** 20HAp and **8PEG** 40Hap and pure **8PEG** for comparison.

XRD measurements (Figure 3b) can be used to verify phase purity [32]. Here, it proves the presence of reflections typically assigned to HAp at 26 ° 2θ and 32 ° 2θ. This supports the results from TEM diffractions, verifying HAp presence in the nanocomposites. **8PEG** 10HAp is not depicted due to the very low intensity of

reflections in the according spectrum. The intensity of the reflections increases with HAp content. Furthermore, the spectra demonstrate that an increased mineral content also results in rising crystallinity of the CP phase. However XRD analysis and in-situ TEM electron diffraction patterns with only two visible reflections imply very low crystallinity, untypical for HAp. Therefore, the Ca/P ratio of the composite hydrogels was determined, which is generally considered a helpful tool discerning the different calcium phosphate phases. EDX revealed a Ca/P ratio of 1.35 ± 0.09 (n = 5), which is lower than what is expected for the crystalline HAp phase (Ca/P ratio of 1.67). Hence, the observed low crystallinity of the composite hydrogel samples might be attributed to the additional presence of an amorphous calcium phosphate (ACP) phase. ACP exhibits low Ca/P ratios down to 1.18, as reviewed by Nancollas et al [20]. ACP is a precursor-phase for the formation of HAp during the nucleation process. The hydrogel nanocomposites might therefore be considered to display an early stage of HAp formation.

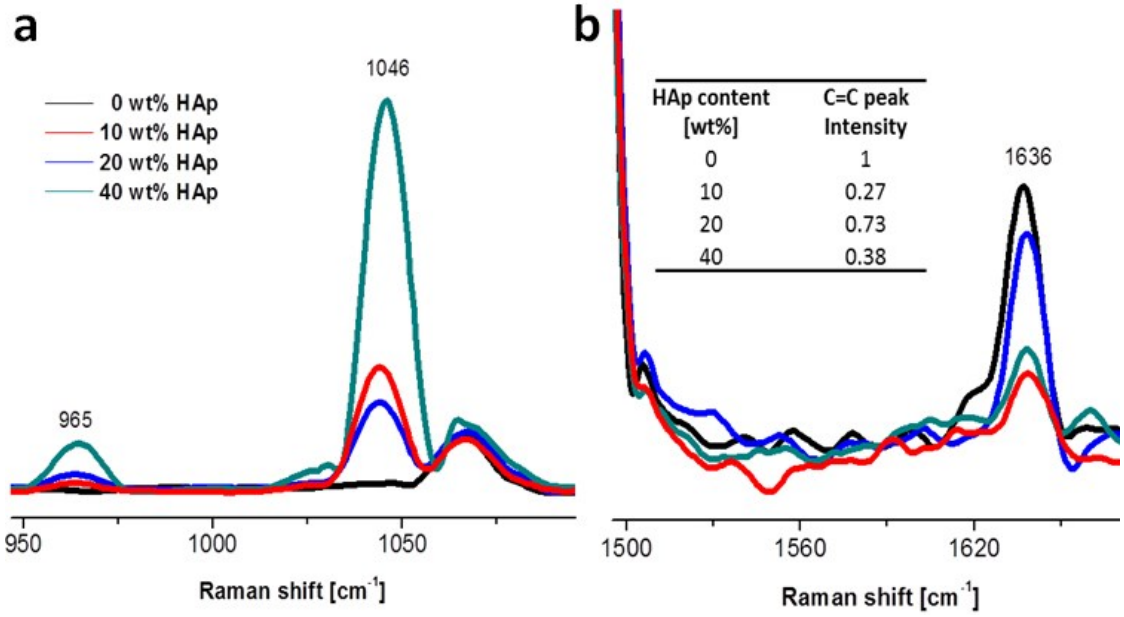

Figure 4. (a) RAMAN analysis of PEG HAp composite materials, demonstrating the existence of the HAp phase; Table in (b) states the residual quantities of C=C double bonds available for further post-gelation functionalization.

Chemical characterization was achieved by Raman spectroscopy, which enabled the identification of distinctive peaks for HAp formation as depicted in Fig. 4a. The

spectrum of pure **8PEG** is given for comparison. All hydrogels show peaks at 842 and 853 cm^{-1}, which correspond to the CH_2 rocking, peaks at 1061 and 1071 cm^{-1}, which correspond to C-O vibrations and CH_2 rocking and peaks at 1125 and 1140 cm^{-1}, which correspond to C-C and C-O vibrations [30]. All these peaks can be attributed to the PEG polymers. Figure 4a compares the Raman spectra of pure **8PEG** and all three **8PEG**-HAp hydrogels in the region of 940-1150 cm^{-1}. The spectra are normalized through that the intensity of C-O vibrations and CH_2 rocking, and peaks at 1125 and 1140 cm^{-1} from **8PEG** polymer chains remain constant. Two main bands existing at 965 cm^{-1} attributed to HAp for symmetric stretching of phosphate (υ_1) and 1046 cm^{-1} attributed to ACP for asymmetric stretching of phosphate (υ_3) confirm the formation of HAp in all three **8PEG** composite hydrogels [33-34]. The recorded RAMAN spectra exhibit a rising peak at ca. 965 cm^{-1} with augmenting HAp content. This peak derives from a totally symmetric non-degenerated stretching mode of free tetrahedral phosphate ions. This is in agreement with literature, where this peak is used as an identification site for the presence of HAp [32-34]. It is interesting to see that the intensity of the υ_3 PO_4^{3-} bands for **8PEG** 10HAp and **8PEG** 40HAp increased, compared to those for **8PEG** 20HAp. It can be suggested that more ACP component is generated, due to the (increased) interaction with polymer chains during the reaction [35]. Therefore, **8PEG** 20HAp would be the optimum choice for bone tissue engineering, because it exhibits better HAp phase formation.

Raman spectroscopy also allows for quantification of residual C=C double-bonds represented by a peak at 1636 cm^{-1}, which is absent in pure HAp powder. The amount of remaining C=C double-bonds is decisive for post gelation reactivity (Figure 4b). For **8PEG** 20Hap, 73 % of its initial C=C -double bond amount is still accessible after gelation of the nanocomposite hydrogel. The accessibility of C=C double bonds demonstrates the superb potential to specifically tailor this unique nanocomposite material after gelation. Moreover, the C=C functional groups can be utilized in a further polymerization step (that is, chemical coupling of residual acrylate groups) to stabilize the gel matrix and make them applicable as polymeric biomaterials for cell

culture studies.

4.3.4 TGA tests of the hydrogels

TGA (Figure 5) reveals different amounts of chemically bound water for varying HAp contents. The weight loss at approximately 150°C may be due to physical transitions such as vaporization or desorption of gaseous substances. The fact that **8PEG** 20HAp displays the highest degree of mass loss at approximately 150 °C can be explained by the greatest degree of bound water. It is presumed that this is caused by the presence of HAp, which due to its inherent polar character can interact with molecular water and promote adsorption of physically bound water. This is supported by exhibiting the only polymer degradation for pure 8PEG, and further underlined by the observation of the reduced weight loss of 8PEG 10HAp. In addition, it reveals that the more homogeneous distribution of HAp in 8PEG 20HAp than in 8PEG 40HAp leads to the larger HAp particles surface area, which can bound more water, which lose during TGA measurement.

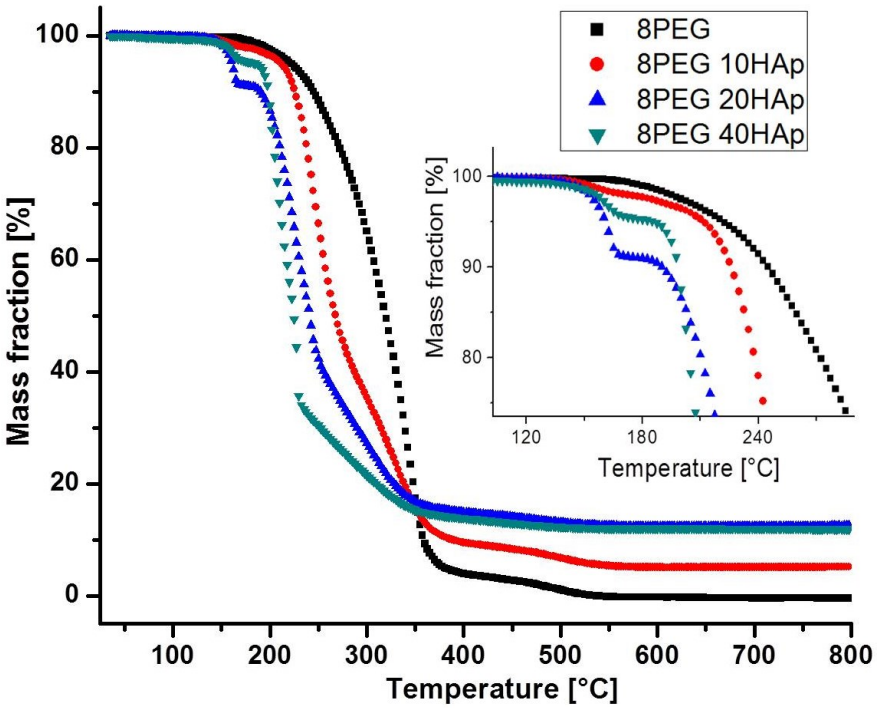

Figure 5. TGA measurements of **8PEG** HAp hydrogel composites with varying HAp content.

Interestingly, **8PEG** 20HAp also exhibits the highest amount of residual mass after complete combustion at approximately 600 °C. **8PEG** 40HAp theoretically designed with a stoichiometric amount of 40 wt% HAp, exhibit a lower mass fraction after complete combustion. It seems that due to the homogeneity and at the same time the strongest interaction of HAp in **8PEG** 20HAp, after combustion, the highest amount of components of gel has been preserved. Otherwise, the residual HAp of 8PEG 40HAp after combustion should be higher than that of 8PEG 20HAp. TGA analysis support RAMAN data, stating that **8PEG** 20HAp seems to be the hydrogel composite exhibiting greatest homogeneity and the highest degree of **8PEG**-HAp interaction

4.3.5 Morphological characterization of the hydrogels

In order to characterize the elemental distribution of calcium and phosphorous, scanning electron microscopy (SEM) including EDX mapping was performed; the results are depicted in Figure 6. The EDX maps show that both elements are found rather inhomogeneously dispersed within the samples. Regions of brighter colour display areas of higher calcium or phosphorus concentration.

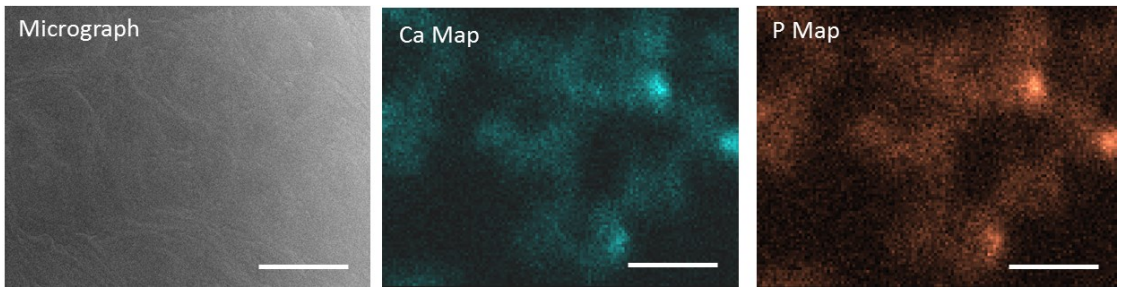

Figure 6. SEM image and EDX mapping of Ca and P in 8PEG 20HAp; Scale bars are 10 µm.

The observed result may be attributed to the interactions between Ca^{2+} and PO_4^{2-} ions with the polymeric matrix during HAp maturation from ACP. However, no huge inorganic particles or regions without calcium and phosphorus are detected. This is a characteristic, which underlines the novelty of our synthetic route. The in situ synthesis of CP prevents the inorganic phase from clustering in the produced

composites, which is commonly observed in composites produced by physical mixing techniques.

4.3.6 Cell culture test

To evaluate cell-biomaterial interactions, cell adhesion and viability tests were performed. Prior to cell culture on the flat **8PEG** 20HAp hydrogels, the surface roughness of such samples was characterized via AFM (RMS 3.0 ± 0.7 nm over 160 μm^2 in fully hydrated state) in order to exclude topography as dominant cause for eventual cellular adhesion.

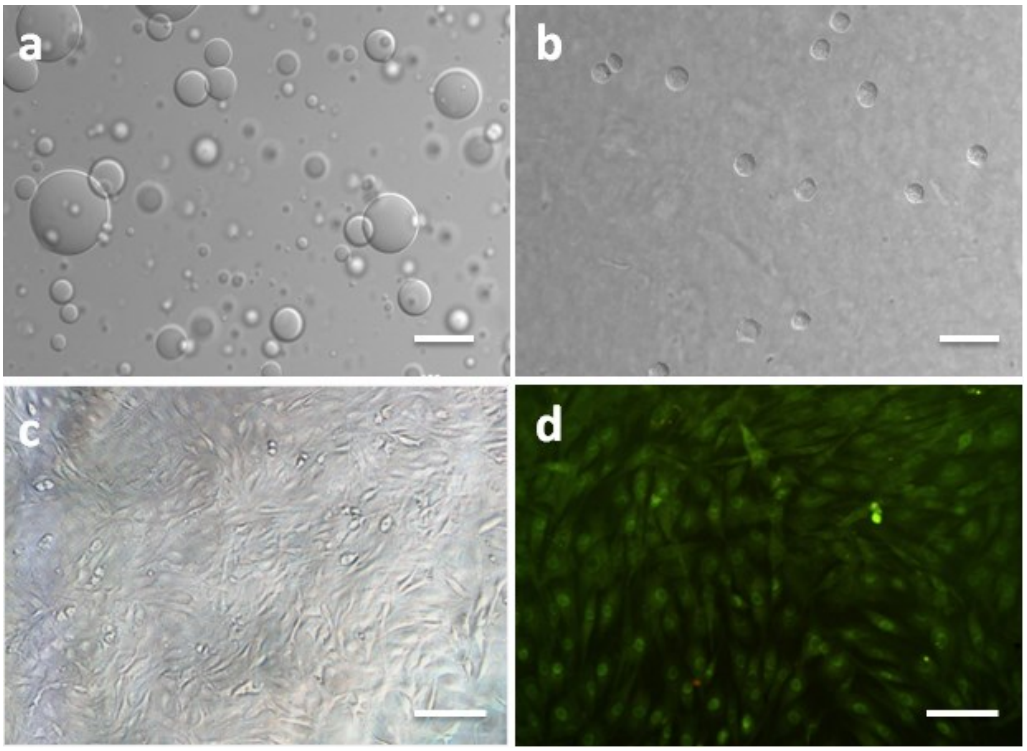

Figure 7. Cell culture experiments show no cell adhesion on **8PEG** 20wt% $(NH_4)_2HPO_4$ gels (a); the adherence of few fibroblasts (L-929) to **8PEG** 20HAp composite gel (b); in contrast to fibroblasts, the much more significant adherence of MC3T3-E1 osteoblasts to **8PEG** 20HAp composite gel in optical microscopy image (c) and fluorescence microscopy image(d). (scale bars represent 50µm)

The flat, pure PEG-based hydrogels, consisting of highly hydrophilic polymer chains, are known for having low protein adsorption and no cell adhesion properties [8, 36]. As expected, the **8PEG** 20wt% $(NH_4)_2HPO_4$ hydrogel does not promote cell adhesion or spreading (Figure 8a), due to the similarity with pure PEG gels where

phosphate ions can easily dissolve in the medium. However it is well known that bioactive nanoparticles can be incorporated within the PEG hydrogel to enhance cell adhesion and spreading [15, 30]. Fig. 7 b, c and d. demonstrate the enhancement of cell adhesion and spreading of both fibroblasts and osteoblasts on **8PEG** 20HAp composite gels compared to **8PEG** 20wt% $(NH_4)_2HPO_4$/ NH_3 control gel.

Figure 7 b, c and d show varying adhesion of different cell-lines. Fibroblasts and osteoblasts exhibit varying affinity towards calcium phosphates and different spreading pattern. A significantly higher number of adhered osteoblasts are observed as shown in Figure 7 c and d, compared to fibroblast adhesion in Figure 7 b. Figure 7c. and 7d. reveal significant osteoblast spreading and elongation on the nanocomposite hydrogels surface., which suggests strong affinity of osteoblasts to these surfaces containing HAp, in contrast to the round shape showing minimal attachment of fibroblasts (Figure 7b) on **8PEG** 20HAp composite gels. And Anselme's research has also shown that hydroxyapatite promotes adhesion of osteoblasts cells [37]. This can be explained by the widely recognized affinity of osteoblasts towards calcium phosphates.

4.4 Conclusions

We have developed 8-arm Poly(ethylene glycol) (PEG)-based calcium phosphate nanocomposite hydrogels with homogeneously dispersed crystalline hydroxyapatite (HAp) nanodomains that are very promising as synthetic mimics for bone tissue engineering applications. Spontaneous gelation upon mixing of the calcium and phosphorus salt-solutions to the PEG-precursor solution indicates the formation of strong polymer-nanoparticle interactions. The *in situ* process is responsible for the homogeneity and enhanced mechanical properties of the resulting composite material.

In-situ TEM-XRD analysis reveals crystalline regions in the generally amorphous system. Techniques such as RAMAN-spectroscopy and X-ray diffraction were utilized

to verify the formation of HAp domains and to distinguish from other potential calcium phosphates phases. TGA measurements seem to show that composite hydrogels containing 20 wt% HAp (**8PEG** 20HAp) exhibit greatest homogeneity and the highest degree of **8PEG**-HAp interaction.

Ultraviolet (UV) radiation is applied to stabilize the nanocomposite hydrogel network under physiological conditions. Cell culture experiments revealed significant adhesion and spreading of osteoblast cells on the nanocomposite **8PEG** 20HAp gels, while fibroblasts hardly adhered and remained round in shape. Live dead staining further highlighted the cytocompatibility of the gels. Therefore, the combination of PEG and nHAp nanoparticles significantly improves the physical and chemical hydrogel properties as well as biological characteristics such as osteoblast adhesion. It could be demonstrated that chemical functionalization by HAp incorporation yields a direct effect on cellular reaction, demonstrating the feasibility of this approach and the potential for specific application in bone or cartilage tissue engineering.

References

[1] Hoffman, A.S. Hydrogels for biomedical applications. *Annals of the New York Academy of Sciences* **2001,** 944, 62-73.

[2] Peppas, N. A.; Hilt, J. Z.; Khademhosseini, A.; Langer, R. Hydrogels in Biology and Medicine: From Molecular Principles to Bionanotechnology. *Advanced Materials* **2006,** 18, 1345-1360.

[3] Khademhosseini, A.; Langer, R.; Borenstein, J.; Vacanti, J.P. Microscale technologies for tissue engineering and biology. PANS **2006,** 103, 2480-7.

[4] West, J. L.; Hubbell, J. A. Reactive polymers Photopolymerized hydrogel materials for drug delivery applications. *Science* **1995,** 25, 139-147 ().

[5] Iza, M.; Stoianovici, G.; Viora, L., Grossiord, J.L.; Couarraze, G. Hydrogels of poly(ethylene glycol): mechanical characterization and release of a model drug. *Journal of controlled release* **1998,** 52, 41-51

[6] Harris, J. Poly(Ethylene Glycol) Chemistry: Biotechnical and Biomedical Applications. (Plenum Press: New York and London, **1992**).

[7] Kim, B.; Peppas, N.A. Poly (ethylene glycol)-containing Hydrogels for Oral Protein Delivery Applications. *Drug Delivery* **2003,** 5, 333-341.

[8] Schulte, V.A.; Diez, M.; Moller, M.; Lensen, M.C. Surface Topography Induces Fibroblast Adhesion on Intrinsically Nonadhesive Poly (ethylene glycol) Substrates. *Biomacromolecules* **2009,** 10, 2795-2801.

[9] Kopecek, J. Hydrogel Biomaterials: A smart Future? *Biomaterials* **2008,** 28, 5185-5192.

[10] Lee, J.H.; Lee, H.B.; Andrade, J.D. Blood compatibility of polyethylene oxide surfaces. *Prog*

Polym Sci **1995,** 20, 1043-1079.
[11] Haraguchi, K. Synthesis and properties of soft nanocomposite materials with novel organic/inorganic network structures. *Polymer Journal* **2011,** 43, 223-241.
[12] Schexnailder, P.; Schmidt, G. Nanocomposite polymer hydrogels. *Colloid and Polymer Science* **2008,** 287, 1-11.
[13] Wu, C.J.; Gaharwar, A.K.; Schexnailder, P.J.; Schmidt, G. Development of Biomedical Polymer-Silicate Nanocomposites: A Materials Science Perspective. *Materials* **2010,** 3, 2986-3005.
[14] Pek, Y. S.; WanAndrew, C. A.; Shekaran, A.; Zhuo, L.; Ying, J. Y. A thixotropic nanocomposite gel for three-dimensional cell culture. *Nat. Nanotechnol.* **2008,** 3, 671–675.
[15] Akhilesh, K. G.; Christian, P. R.; Wu, C.J.; Schmidt, G. Transparent, elastomeric and tough hydrogels from poly(ethylene glycol) and silicate nanoparticles. Acta Biomaterialia **2011,** 7, 4139-4148.
[16] Chang, C.W.; van Spreeuwel, A.; Zhang, C.; Varghese, S. PEG/clay nanocomposite hydrogel: a mechanically robust tissue engineering scaffold. Soft Matter, **2010,** 6, 5157–5164
[17] Cazalbou, S.; Combes, C.; Eichert, D.; Rey, C. Adaptative physico-chemistry of bio-related calcium phosphates. *Journal of Materials Chemistry* **2004,** 14, 2148.
[18] Neira, I. S.; Kolen'ko, Y. V.; Lebedev, O. I.; Tendeloo, G. V.; Gupta, H.S.; Guitia, F.; Yoshimura, M. An Effective morphology control of hydroxyapatite crystals via hydrothermal synthesis. *Crystal Growth& Design* **2009,** 9, 466–474.
[19] Padilla, S.; Izquierdo-Barba, I.; Vallet-Regi, M. High Specific Surface Area in Nanometric Carbonated Hydroxyapatite. *Chem Mater* **2008,** 20, 5942-5944.
[20] Wang, L.; Nancollas, G.H. Calcium orthophosphates: crystallization and dissolution. Chemical reviews **2008,** 108, 4628-69.
[21] Suchanek, W. L.; Shuk, P.; Byrappa, K.; Riman, R. E.; TenHuisen, K. S.; Janas, V. F. Mechanochemical-hydrothermal synthesis of carbonated apatite powders at room temperature. *Biomaterials* **2002,** 23, 699-710.
[22] Tsurushima, H. et al. Enhanced bone formation using hydroxyapatite ceramic coated with fibroblast growth factor-2. *Acta biomaterialia* **2010** 6, 2751-2759.
[23] Kaito, T. et al. Potentiation of the activity of bone morphogenetic protein-2 in bone regeneration by a PLA-PEG/hydroxyapatite composite. *Biomaterials* **2005,** 26, 73-79.
[24] Cai, L.; Guinn, A.S.; Wang, S. Exposed hydroxyapatite particles on the surface of photo-crosslinked nanocomposites for promoting MC3T3 cell proliferation and differentiation. *Acta biomaterialia* **2011,** 7, 2185-99.
[25] Fu, S. et al. Injectable biodegradable thermosensitive hydrogel composite for orthopedic tissue engineering. 1. Preparation and characterization of nanohydroxyapatite/poly(ethylene glycol)-poly(epsilon-caprolactone)-poly(ethylene glycol) hydrogel nanocomposites. *The journal of physical chemistry. B* **2009,** 113, 16518-25.
[26] Zhou, Z.; Ren, Y.; Yang, D.; Nie, J. Performance improvement of injectable poly(ethylene glycol) dimethacrylate-based hydrogels with finely dispersed hydroxyapatite. *Biomedical materials* **2009,** 4, 035007 .
[27] Neffe, A.T. et al. Gelatin functionalization with tyrosine derived moieties to increase the interaction with hydroxyapatite fillers. *Acta Biomaterialia* **2011,** 7, 1693-1701.
[28] Snyders, R.V.; Eppley, B.L.; Krukowski, M.; Delfino, J.J. Enhancement of repair in experimental calvarial bone defects using calcium sulfate and dextran beads. *J. Oral. Macillofac. Surg.* **1993,** 51.

517-524.
[29] Yamaguchi, I.; K. Tokuchi,; Fukuzaki, H.; Koyama, Y.; Takakuda, K.; Monma, H.; Tanaka, J. Preparation and microstructure analysis of chitosan/hydroxyapatite nanocomposites *J.Biomed. Mater. Res.* **2001,** 55. 20-27.
[30] Gaharwar, A.K.; Dammu, S.A.; Canter, J.M.; Wu, C.J.; Schmidt, G. Highly extensible, tough, and elastomeric nanocomposite hydrogels from poly(ethylene glycol) and hydroxyapatite nanoparticles. *Biomacromolecules* **2011,** 12, 1641–1650.
[31] Supová, M. Problem of hydroxyapatite dispersion in polymer matrices: a review. Journal of materials science. *Materials in medicine* **2009,** 20, 1201-1213.
[32] Uskoković, V.; Uskoković, D.P. Nanosized hydroxyapatite and other calcium phosphates : Chemistry of formation and application as drug and gene delivery agents. *J Biomed Mater Res B Appl Biomater.* **2011,** 96, 152-91.
[33] Muller, F.; Muller, L.; Caillard, D.; Conforto, E. Preferred growth orientation of biomimetic apatite crystals. *Journal of Crystal Growth* **2007,** 304, 464-471.
[34] Seah, R.K.H.; Garland, M.; Loo, J.S.C; Widjaja, E. Use of Raman Microscopy and Multivariate Data Analysis to Observe the Biomimetic Growth of Carbonated Hydroxyapatite on Bioactive Glass. *Anal Chem.* **2009**, 81, 1442-1449.
[35] Haque, S.; Rehman, I.; Darr, J.A. Synthesis and characterization of grafted nanohydroxyapatites using functionalized surface agents. *Langmuir* **2007,** 23, 6671-6676.
[36] Ratner, B. D. Biomaterials Science: An Introduction to Materials in Medicine; Academic Press: New York, **1996.**
[37] Anselme, K. Osteoblast adhesion on biomaterials. *Biomaterials* **2000,** 21, 667–681.

Chapter 5.

Fabrication of hydrogels from star-shaped and hyperbranched polyether macromonomers with tuneable degradation properties via click chemistry

Collaborations with Prof. Rainer Haag's group from Freie Universität Berlin

Abstract

In this chapter, we present a versatile method of creating hydrogel networks from bioinert polyethers, such as 8-arm poly(ethylene glycol) (**8PEG**) and hyperbranched polyglycerol (**hPG**), where the level of swelling and degradation of the gel network is precisely controlled. Three methods for gel formation are evaluated; the first is the traditional method of photopolymerization of precursors with acrylate groups (Method A); the other two are recently developed click chemistry methods which use an in situ copper(II) salt reduction to produce the active catalyst, (copper(I)), for the crosslinking reactions. The first of these click chemistry methods involves the reduction of the copper (II) by sodium ascorbate (Method B) and the second uses a photochemical (UV) reduction (Method C) to generate the active catalyst. Furthermore, two different hydrogels have been produced via the click chemistry crosslinking using photochemical (UV) reduction method (Method C); 1) a hydrogel based on pure **8PEG**, (**8PEG**-**8PEG**) and 2) a hybrid hydrogel consisting of **hPG** and **8PEG** building blocks (**hPG**-**8PEG**). The controlled degradation of the gels is managed by tuning the ratios of **8PEG** terminated with alkyne groups with and without a degradable ester linkage, which reacts with **8PEG** or **hPG** terminated with azide groups for gel formation; the result is a series of gels of different compositions, each with their own distinct swelling, elastic and degradation properties, containing a specific amount of ester linkages present. Herein, the synthesis, as well as swelling, degradation and rheological properties of a series of **8PEG** and **hPG** based hydrogels have been studied. Finally, we have shown that these gels are non-cytotoxic and maintain their cell-repellent property, thus having great potential as tissue engineering and drug delivery matrices.

5.1 Introduction

Polymer biomaterials are an important class of materials that have found use in biomedical applications ranging from scaffolds for tissue engineering to drug delivery vehicles. For many of these applications, the physical properties (e.g. swelling ability and elasticity) of the polymeric materials are key to their successful integration. The use of materials of different stiffness can help direct the migration and differentiation of stem cells and swelling is essential for the controlled release of drugs from vesicles [1-5]. Aside from the cytocompatible properties of the materials, the ability of the materials to degrade in situ (in the body) is one of the most desired features of polymeric biomaterials. On top of the ability for these materials to degrade safely in the body, control over this breakdown is vital for many biomedical purposes. For example, sutures made of polylactic acid must reabsorb at the correct rate if they are to aid wound repair, orthopaedic fixtures (e.g. pins for the fixation of fractures) do not need to be removed after insertion if they are resorbable; materials used as tissue engineering scaffolds degrade and reabsorb as new tissue grows and replaces the scaffolds [6-10].

Our aim is to fabricate a series of cytocompatible hydrogels where the crosslinking system integrates a hydrolysable, degradable bond, the cleavage of which can be controlled under varying conditions e.g. pH, temperature and chemical environment. For application in tissue engineering scaffolds，it is desirable for successful long-term tissue regeneration that the biomaterial can be degraded and remodelled, so that cells can migrate and form a new extracellular matrix [11]. In addition，hydrogels are highly hydrated networks formed by the crosslinking of polymer chains via various chemical bonds and physical interactions. They can be processed under relatively mild conditions and have mechanical and structural properties similar to many biological tissues [12-14]. Our hydrogels are based on multi-arm (8-arm) polyethylene glycol (**8PEG**) and hyperbranched polyglycerol (**hPG**). PEG is one of the most popular non-toxic, biologically inert biomaterials; it owes its

inertness to the fact that it is hydrophilic, electrically neutral and highly hydrated [15,16]. Nevertheless, it has been shown by us and others that when PEG surfaces are functionalised (chemically)[17,18] or patterned (elastically and with topography)[19-22] they in fact do support cell adhesion and promote cell proliferation; this enables PEG to be used as an inert background upon which the effect of pre-determined, specific cues on cell behavior can be investigated. Moreover, **hPG** has recently drawn great attention due to its non-cytotoxic yet cell-repellent properties, which makes it an interesting alternative to PEG as a cytocompatible polymer. For example, **hPG** with molecular weight of 6000 gmol-1 has been shown to exhibit superior biocompatibility when compared to PEG and other clinical polymers both in vitro and in vivo [23-25]. Additionally, the multivalent hydroxyl functionality of **hPG** allows facile fabrication of hydrogels and modification with bioactive substances [26,27].

Multivalent polymers (**8PEG** and **hPG**) offer some significant advantages over their linear counter-parts, specifically 1) increased functionality and 2) different physicochemical properties. With these molecules, there are a large number of functional groups available for crosslinking reactions in a small volume; this leads to the formation of more crosslinking points with respect to the molecular weight (MW) when compared with the linear molecule of the same MW; subsequently, polymer networks with a higher crosslinking density can be formed. If a step-polymerization method for crosslinking is used (e.g. Michael addition or click chemistry), linear compounds cannot form a network unlike their multi-arm equivalents; in the case of linear polymers, the two-point junctions formed just results in polymerization to form longer chains [28,29]. The unique branched structure of polymers is also responsible for the production of hydrogels with a homogenous, “ideal” structure; such structures are not obtained from linear polymers [30-32].

The use of multi-arm PEG terminated with acrylate in the formation of hydrogels was first reported by Peppas et. al. in 1999 [33]. This work described the production of gels from high molecular weight (Mn > 250,000 Da) polymers via both gamma

irradiation and the UV-polymerised crosslinking of acrylate-terminated macromolecules. They observed that hydrogels prepared from star PEG polymers containing a smaller number of short arms produced a more highly crosslinked structure than hydrogels produced from multi-arm PEG polymers containing a large number of longer arms. Low molecular weight (< 20,000 Da) 8-arm PEG macromolecules have been used previously in hydrogel fabrication, namely in the formation of photoscissile hydrogels that incorporate nitrocinnamate crosslinking moieties and more recently as the basis of cyclodextran- and cholesterol-functionalised self-assembling hydrogels.[34,35] Hybrid microgels based on PEG and **hPG**, crosslinked via bio-orthogonal thiol-ene click chemistry and through photoinitiated free-radical polymerization for encapsulating cells, were reported recently [36,37].

In this study, we have utilized three methods for the crosslinking of our gels; A) photopolymerisation of acrylate groups, B) click chemistry, and C) "UV-click". Method A used the tried and tested method of photopolymerisation, a reaction we have previously used in the synthesis of biocompatible hydrogels. The use of the non-toxic photoinitiator, Irgacure 2959, ensured that these gels remain non-toxic after formation. The samples from this method were used as a standard to which the other gels could be compared. Methods B and C employed click chemistry reactions as the crosslinking method. Click chemistry reactions are high yielding, highly atom efficient reactions which result in the formation of a very stable triazole group [38-41]. Recently, Bowman et. al. have reported the discovery of the copper-catalyzed alkyne–azide cycloaddition (CuAAC) reaction via photochemical reduction of Cu(II) to Cu(I) (Method C), and it has been demonstrated that this technique can be applied for small molecule synthesis, patterned material fabrication and patterned chemical modification [42]. In contrary to the commonly used click reaction (Method B), Method C ensures there are much fewer toxic copper ions involved in the reaction as well as a homogenous distribution of Cu(I) generated, leading to a more ideal network structure.

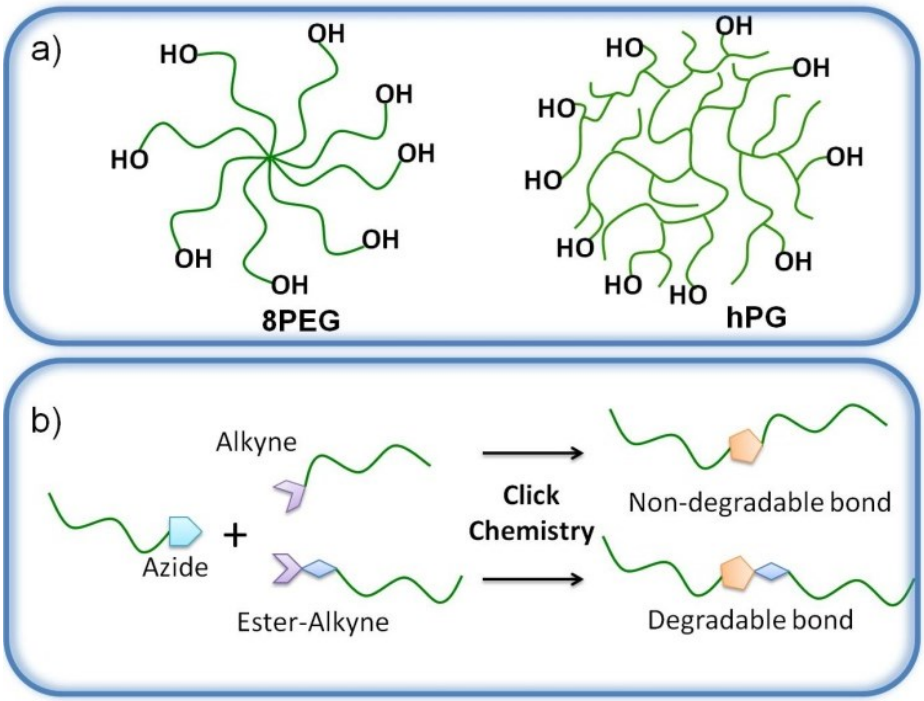

Figure 1. a) The chemical structures of **8PEG** and **hPG** macromonomers; b) schematic outline of the reactions that will introduce degradable bonds into our gels via click chemistry

For the hydrogel building blocks we have used 8-arm star–shaped PEG (having a hexaglycerol core and a MW of ~ 15,000 Da; **8PEG**) and hyperbranched polyglycerol (**hPG**) (Fig. 1a). The hydroxyl end groups on the macromolecules have been converted into mutually reactive, functional groups, i.e. azide (Az) and alkyne (Alk) end-groups, which undergo a 1,3-cycloaddition click reaction which resulted in the formation of a covalent network. The special feature of our crosslinking strategy (Fig. 1b) is that the alkyne functionality was connected to the macromolecules either directly (Alk) or via a linker fragment containing an ester moiety (E-Alk). By altering the ratio of Azide:Alk:E-Alk we have been able to control the percentage of crosslinks that contain the ester bond; this bond is responsible for the degradation of these hydrogels in aqueous conditions. Two kinds of hydrogels with controlled degradable properties, **8PEG**-**8PEG** and **hPG**-**8PEG**, were crosslinked via this strategy.

5.2. Materials and Methods

5.2.1 Materials and measurements

All chemicals were purchased from Aldrich and used as received unless stated otherwise. 8arm PEG-OH with a molecular weight of 15 KDa was purchased from Jenkem technology USA. Solvents were at least analytical grade quality. The silicon masters were purchased from Amo GmbH (Aachen). ^{1}H NMR spectra were recorded on a Bruker Advance DRX-400 spectrometer with trimethylsilane (TMS) as the internal standard and deuterochloroform ($CDCl_3$) as the solvent. Swelling test and Rheological Measurements were performed with same procedure as Chapter 2.

5.2.2. Precursor synthesis

5.2.2.1. Synthesis of 8PEG-OTs (Compound 2)

8PEG-OH (Compound 1) (5 g, MW = 15,000) was dried in vacuum oven 100^{o}C for 4h. To the PEG was added triethylamine (3 eq) and 4-Dimethylaminopyridine (4-DMAP) (20 mg) in dry dichloromethane (DCM) (40 mL) under nitrogen and placed into an ice bath. Tosyl chloride (3 eq) was dissolved in dry DCM (10 mL) under nitrogen and was slowly added to the PEG solution. The solution was allowed to warm to room temperature and was stirred for 2 days. The solution was filtered, poured into ice-cold diethyl ether then separated to get the crude product. The crude product was dissolved in 50mL DCM and insoluble impurities were removed by filtration. The filtrate was washed with saturated $NaHCO_3$ solution, dried over $MgSO_4$ and filtered. After filtration, the solvent was removed under reduced pressure and the yellow oil was purified by column chromatography (stationary phase SiO_2, eluent DCM: ethanol 20:1), and after drying to obtain a yellowish solid (63% isolated yield). ^{1}H NMR (Ar-C**H$_3$** 2.45ppm (6H), OC**H$_2$**C**H$_2$**O 3.64ppm (288H), (C=O)OC**H$_2$** 4.15ppm (4H), =CH=CC**H$_3$**7.34ppm (4H), C**H**=CCO 7.80ppm (4H)).

5.2.2.2. Synthesis of 8PEG-Az (Compound 3)

8PEG-OTs (**2**) (1 eq, 5.0g) was dissolved in 15 mL DMF, to which NaN_3 (20 times) was added. The reaction was stirred at 80^{o}C for 20 h. The solution was filtered, poured into ice-cold diethyl ether then separated to get the crude product. The resulting intermediate was dissolved in 50 mL DCM and insoluble impurities were removed by filtration. The filtrate was washed with saturated NaCl, dried over $MgSO_4$ and filtered. Solvent was removed under reduced pressure to yield a white solid (64% isolated yield). ^{1}H NMR ($N_3C\mathbf{H_2}$ 3.38ppm (4H), $OC\mathbf{H_2}C\mathbf{H_2}O$ 3.64ppm (288H)).

5.2.2.3. Synthesis of 8PEG-Alk (Compound 4)

8PEG (**1**) (7.8g, 1 eq) was dissolved in dry THF (150 mL), to which NaH (420 mg as a 60%-suspension in mineral oil, 10.5 mmol, 2.5 eq per arm) was added and the reaction mixture was stirred for 15 min at room temperature. Then, propargyl bromide (600 μL as an 80% solution in toluene, 5.4 mmol, 1.3 eq per arm) was added and the resulting reaction mixture was stirred for 16 h at room temperature. The solution was filtered, poured into ice-cold diethyl ether and separated to get the crude product. The resulting intermediate was dissolved in 50 mL DCM and insoluble impurities were removed by filtration. The filtrate was washed with saturated NaCl, dried over $MgSO_4$ and filtered. The solvent was removed under reduced pressure to yield a white solid (60% isolated yield).^{1}H NMR (C**H**≡C 2.40 ppm, $OC\mathbf{H_2}C\mathbf{H_2}O$ 3.64 ppm, CH≡C-C$\mathbf{H_2}$-O 4.17 ppm).

5.2.2.4. Synthesis of 8PEG-Acr (Compound 5)

8PEG (**1**) (5g) and K_2CO_3 (30 eq) were dried in a vacuum oven at 100^{o}C for 4 h before being dissolved in 50 mL CH_2Cl_2 under nitrogen and cooled in an ice bath. Acryloyl chloride (20 eq) was added dropwise and the mixture was stirred at 60^{O}C for 4 days. The solution was filtered and poured into ice-cold petroleum ether. The solution was stirred for 10 min then separated to get the crude product. The crude product was dissolved in 50 mL DCM then extracted with saturated NaCl solution (x3). The organic layers were collected and dried over $MgSO_4$ overnight. The $MgSO_4$ was

filtered off and the solvent was removed under reduced pressure to yield a white solid (72% isolated yield). ^{1}H NMR (OC**H$_2$**C**H$_2$**O 3.64 ppm (1496H), (C=O)OC**H$_2$** 4.31 ppm (16H)**, =**C-**H** trans 5.83 ppm (8H), C**H**=C 6.15 ppm (8H), **=**C-**H** cis 6.42 ppm (8H)).

5.2.2.5. Synthesis of 8PEG-E-Alk (Compound 6)

8PEG-**Acr** (**5**) (1 eq, 0.5g) was dissolved in 15 mL methanol and propargylamine (2 eq) was added and the solution was stirred at room temperature for 24 h. The solution was then filtered and poured into ice-cold diethyl ether and then separated to get the crude product. The solvent was removed under reduced pressure to yield a white solid (69% isolated yield). ^{1}H NMR (C**H**≡C 2.23 ppm, N-C**H$_2$**CH$_2$CO 2.55 ppm, N-CH$_2$C**H$_2$**CO 2.97 ppm, CH≡C-C**H$_2$**-N 3.43 ppm, OC**H$_2$**C**H$_2$**O 3.64 ppm, (C=O)OC**H$_2$** 4.24 ppm).

5.2.2.6. Synthesis of hPG-Az (Compound 7)

Hyperbranched Polyglycerol terminated with azide groups (**hPG-Az**) was synthesized according to the literature [43], which came from Prof. Rainer Haag's group. Briefly, **hPG**-OH (301 mg, 0.74 mmol equivalents of epoxide group) and sodium azide (200 mg, 3.08 mmol, excess) were dissolved in 5 mL DMF and stirred for 16 h at 60 °C. After the reaction mixture was quenched by 10 mL water, it was dialyzed in water to yield the desired azide-terminated **hPG-Az** (185 mg, 60 % recovery) as a highly viscous, clear yellowish oil.

5.2.3. Gel formation

8PEG Hydrogels, fabricated via photopolymerisation of acrylate groups (Method A), and **8PEG-8PEG** hydrogels, fabricated via click chemistry with ascorbate (Method B), were prepared to compared with the hydrogels made via click-UV (Method C). In addition, a series of **8PEG-8PEG** and **hPG-8PEG** hydrogels with different percentages of **8PEG-E-Alk** (100%, 90%, 75% and 50%) which contained ester group, were prepared via click-UV (Method C).

5.2.3.1. Method A - Photopolymerization

50 µl of the **8PEG-Acr** precursor mixtures with Irgacure 2959 (1% w/v) were dispensed on fluorinated silicon wafers (CrysTec GmbH), capped with a cover glass (18mm x 18mm; Carl Roth GmbH & Co. KG) and exposed to UV light (λ_{365nm}, Vilber Lourmat GmbH) for 30min using a working distance of 10 cm, in a nitrogen-filled glovebox. Finally, the cured transparent gels were peeled off with tweezers and kept in clean petri dishes (VWR International GmbH) until further use.

5.2.3.2. Method B – Click chemistry with ascorbate

To a small vial was added **8PEG-Az** (100 mg), **8PEG-Alk** (100 mg) and 150 mg of water. To the vial was added 15 mg of sodium ascorbate and the mixture was stirred to give a clear solution. The mixture was then drop cast onto a silicon master or on a glass slide. Copper sulfate (10 mg) solution (0.2 mg/µL) was then dispensed on top and the sample was covered with a glass coverslip. The solution was allowed to react for 20 min and upon separation of the plates a uniform click gel was formed.

5.2.3.3. Method C (for 100% ester) UV-click

To a small vial was added **8PEG-Az** (100 mg), **8PEG-E-Alk** (100 mg) and 150 mg of water. To the vial was added Irgacure 2959 (1% w/v, 2mg) and copper sulfhate (1 mg) solution (0.1mg/µL) and the mixture was stirred to give a clear solution. After mixing thoroughly, the mixture was drop cast onto a silicon master or a glass slide and covered with a glass coverslip on top. The polymer was cured under nitrogen for 20 min under a UV-lamp (distance of 10 cm from a 365 nm lamp).

5.2.4 Cell experiments

5.2.4.1. Optical microscopy

Light microscopy images were taken with an inverted Axiovert 100A Imaging microscope (Carl Zeiss, Göttingen, Germany) using an AxioCam MRm digital camera and analysed using the AxioVisionV4.8.1 software package (Carl Zeiss, Göttingen, Germany).

5.2.4.2. Cell Culture

Mouse connective tissue fibroblasts (L-929) were kindly provided by Dr. J. Lehmann (Fraunhofer Institute for Cell Therapy and Immunology IZI, Leipzig). L-929 cells were cultured in RPMI 1640 containing 10% **F**etal **B**ovine **S**erum (FBS, PAA Laboratories GmbH) and 1% **P**enicillin/ **S**treptomycin (PS, 100x, PAA Laboratories GmbH) at 37^{o}C, 5% CO_2 atmosphere and 100% humidity. The cells were grown in 75cm^2 cell culture flasks (Greiner Bio-One) until confluence, washed with Dulbecco's **P**hosphate **B**uffered **S**aline solution (Dulbecco's PBS, PAA Laboratories GmbH) and treated with Trypsin-EDTA (PAA Laboratories GmbH). After incubation for 2 min at 37^{o}C, detached cells were suspended in cell culture medium. The cell suspension was transferred into a falcon tube (VWR International GmbH) and centrifuged for 5min at 1300 rpm, 4^{o}C. Finally, the cell pellet was re-suspended in fresh medium and cells were counted using a haemocytometer (Paul Marienfeld GmbH & Co. KG). In this work, L-929 cells were used between passages 9 and 40; cell culture medium was refreshed every second day.

5.2.4.3. Cytocompatibility

L-929 cells were used to investigate the cytocompatibility of smooth samples of PEG-based polymer gels. Cytotoxicity was determined as colony forming ability using varying amounts of crosslinker (1% PI; 0% CL and 10% CL).

Hydrogels (1 cm x 1 cm) were washed with ethanol (70%), rinsed in Dulbecco's PBS (DPBS, PAA Laboratories GmbH) and placed in a µ-slide (Ibidi GmbH). 300 µL of a cell suspension containing 50,000 cells were seeded into each well and incubated at 37^{o}C, 5% CO_2 atmosphere and 100% humidity. The viability of cells on the gels was calculated after 24 h incubation. Following incubation, cells were stained with 100 µL of a vitality staining solution containing fluorescein diacetate (stock solution 0.5 mg/mL in acetone, Sigma-Aldrich) and propidium iodide (stock solution 0.5 mg/mL in Ringer's solution, Fluka). Viable and dead cells were quantified by fluorescence microscopy.

5.3. Results and Discussions

5.3.1 Precursor synthesis

Synthesis of PEG-hydrogel pre-cursors started with the functionalisation of **8PEG** (1) (Scheme 1). From this hydroxyl compound, the **8PEG-Az** component (3) was first synthesised via the reaction of tosylated alcohol (2), with sodium azide. 20 equivalents of sodium azide were needed in this reaction to drive the functionalisation to completion. Meanwhile, according to our previous work, a facile route to azide functionalized **hPG-Az** (7) with the same end group structure as **8PEG-Az** (3) was obtained through epoxide groups undergoing a ring-opening reaction with sodium azide (scheme not shown). The corresponding alkynes, with which this azide would react in the cycloaddition, were made as two different variations; 1) non-degradable and 2) degradable (with ester linkage). The synthesis of the non-degradable alkyne, **8PEG-Alk** (4), was completed via deprotonation of the hydroxyl compound using sodium hydride and subsequent reaction with propargyl bromide.

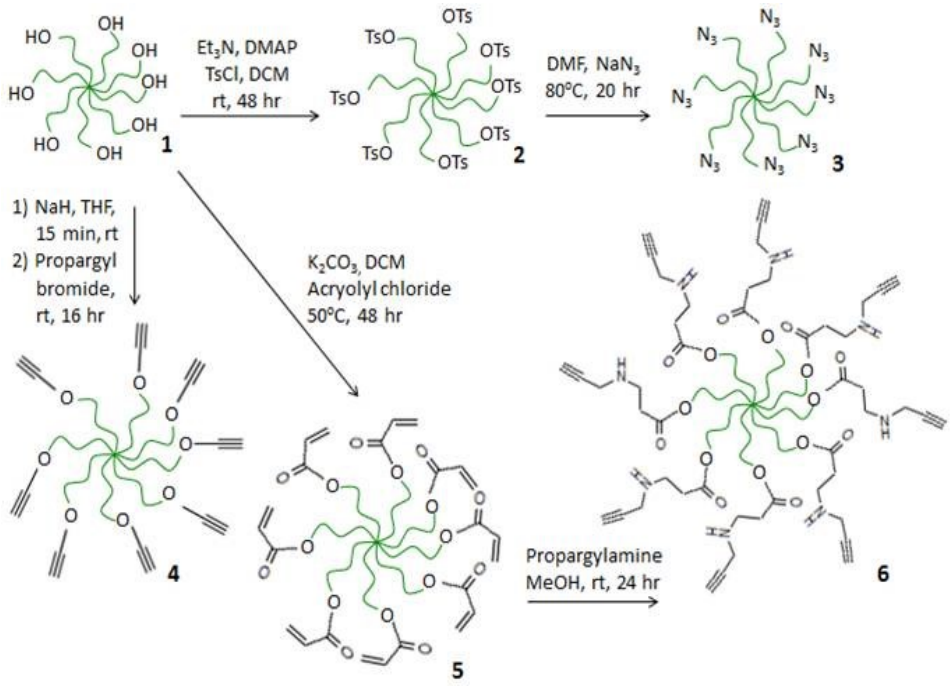

Scheme 1. Functionalization of **8PEG** building blocks.

The introduction of the degradable ester linkage at the terminal-end of the polymer was carried out in a two-step manner. To begin, the **8PEG**-OH (1) was reacted with acrylolyl chloride under mildly basic conditions. When the usually standard base for this reaction, Et_3N, was used, the final product was found to have an unusual yellow colour instead of being colourless [44]. However, when K_2CO_3 was employed, a colourless liquid was produced. The **8PEG-Acr** (5) is also, in its own right, a suitable substrate for use in UV-polymerization crosslinking reactions (Method A) for the formation of hydrogels by radical crosslinking. Having worked with this acrylated 8-arm PEG previously, we have used it as standard with which to compare the physical properties of our new click chemistry gels.

Reaction of **8PEG-Acr** (5) with propargylamine gave the final product **8PEG-E-Alk** (6) in good yield. The percentage of functionalization of the 8-arm structures was regulated by controlling the amount of reagent used in the reaction. In the case of 6, it was shown that the partial functionalization of the substrate was possible, when less than 2 equivalents of propargylamine were used with respect to the acrylate 5 (Fig. 2).

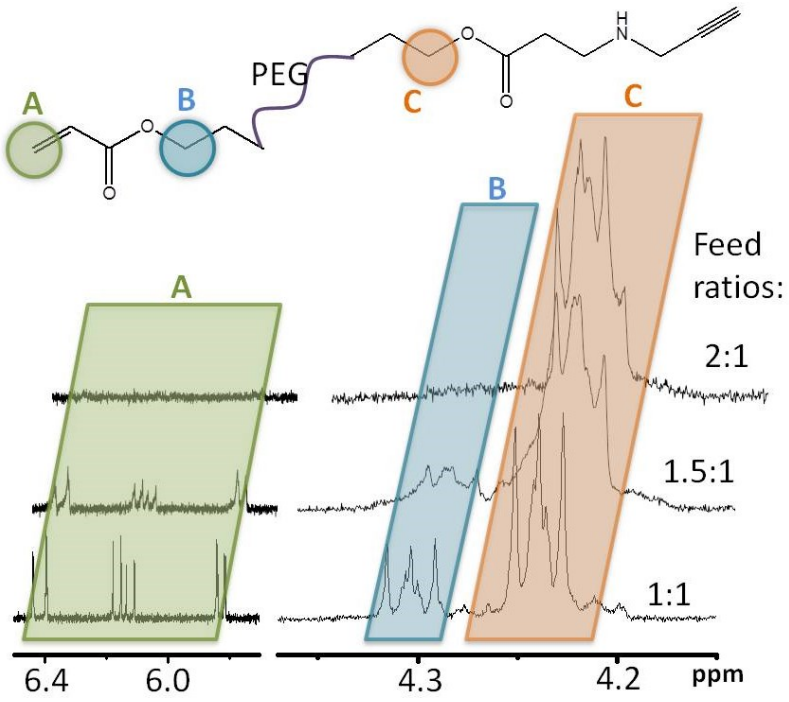

Figure 2. ^{1}H NMR data showing the control of the conversion of acrylate to alkyne by adjusting the feed ratios.

By adjusting the feed ratio of propargylamine, some acrylate groups could selectively be left unreacted, and when the feed ratio of propargylamine and acrylate is 2:1, the acrylate groups were completely consumed as shown by NMR (region A of Fig. 2). The correct choice of solvent was deemed essential for the success of this reaction, with dimethylformamide and chloroform not allowing the reaction to proceed. However, excellent conversion was seen when methanol is used. Interestingly, when the partially converted alkyne was used in UV-catalysed click chemistry reactions (Method C) it was shown the remaining acrylate end-groups do not crosslink with each other (data not shown). This was most likely due to the large distance between remaining groups and suggested that said groups would be available for further functionalisation or crosslinking reactions with another system e.g. acrylate-functionalised biomolecules.

5.3.2 Hydrogel synthesis

The choice of crosslinking method for the gels determined the rate of network formation as well as the architecture of the eventual network structure. Three different methods of crosslinking for the **8PEG** gels were evaluated; A) UV-photopolymerization, B) click chemistry using ascorbate, and C) click chemistry using UV-light, and the swelling behavior of three gels are shown in Table 1. Each of these methods gave gels with different properties. Using Method A to crosslink **8PEG-Acr** (5) in the presence of 40% water using a non-toxic photoinitiator (Irgacure 2959) resulted in the formation of a polymer network which, unlike gels made using click chemistry, did not have an ideal network structure, as more than one crosslink point could be formed at any one junction. The network structure of the radically crosslinked gels consisted of dense clusters consisting of multiple acrylate groups (“polyacrylate chains”) surrounded by a weakly crosslinked matrix, which lead to inhomogeneous gel properties throughout the gel. The gels exhibited rather poor swelling behavior and relatively high stability. Click chemistry (Methods B and C), on the other hand, ensured one-to-one bond formation during crosslinking and resulted

in ideal network structure formation [45]. The integrity of the gel networks made by click chemistry is related to the swelling behavior; gels have ideal network structure and have larger pores or cavities, resulting in greater water adsorption and a more flexible material.

Traditionally, click chemistry relies on the use of a copper (I) catalyst to drive the reaction forward. The click chemistry reactions we investigated were copper-catalysed azide-alkyne 1,3-cycloadditions (CuAAC). The two click methods we looked at have their own distinct catalytic pathway; in Method B copper (II) sulfate was used as the pre-catalyst, which was activated in situ by sodium ascorbate to form the active catalyst, Cu (I). The second click chemistry method (Method C), used UV light and a photoinitiator to transform copper (II) to copper (I).42 The homogeneity of gels formed by Method B was reliant on the even distribution of the sodium ascorbate, which was difficult to obtain as the reaction was so fast and gel formation was complete in a matter of seconds, making it difficult to control the gel formation both on a spatial and temporal level. As a further consequence, these gels were very inconvenient to pattern by the soft lithography methods used in our group. The use of ascorbate was also found to be the reason for uncontrolled degradability within the system as a result of the increased pH value due to the presence of the base.

Table 1 The properties of three different kinds of hydrogels prepared by different methods. UV: Ultra Violet (365nm), Cu: copper ion, +: yes, -: no.

Code	Precursor	Concentration	Swelling degree	UV	Cu	Controlled gelation
Method A	8PEG-Acr	**60 wt%**	**3.18±0.03**	+	-	+
Method B	8PEG-Az, 8PEG-Alk	**60 wt%**	**7.7±0.26**	-	+	-
Method C	8PEG-Az, 8PEG-Alk	**60 wt%**	**4.9±0.14**	+	+	+

On the other hand, Method C did not only eliminate the need for sodium

ascorbate but also gave access to a highly homogeneous gel, the formation of which was easily controlled both spatially and temporally. The photoinitiator, used to transform copper (II) to copper (I), was evenly distributed throughout the precursor mix and activated after and for a designated time. As the gel was formed under UV light, selective crosslinking could also be carried out if photomasks are used [42]. One key point regarding the use of Method C is that the precursor solution was moldable, meaning it allowed these click gels to be used in our soft lithographic patterning techniques. Therefore, in this study the recently developed method of click chemistry using UV-light is the preferred method to yield moldable hydrogels.

5.3.3 Series of degradable gels

Click chemistry was used to crosslink the precursor in order to form a hydrogel with controllable degradability. The strategy to control the rate of degradation of the polymer network relied on inserting specific quantities of degradable linkages into the structure. This was managed with great precision by creating two different types of alkyne-terminated **8PEG** with which the **8PEG-Az** (3) or **hPG-Az** could react; **8PEG-Alk** (4) and **8PEG-E-Alk** (6). The **8PEG-E-Alk** contained a hydrolysable ester linkage, which was eventually incorporated into the hydrogel structure. The amount of ester present in the gel was altered resulting in varying levels of degradability e.g. by reacting one equivalent of **8PEG-Az** (3) or **hPG-Az** with both **8PEG-Alk** (5) and **8PEG-E-Alk** (6) in specific ratios (Fig. 3). The most rapidly degradable gels contained 100% **8PEG-E-Alk** (6) whereas the non-degradable gels contained 100% **8PEG-Alk** (6). Irrespective of the ester content, the hydrogels that were crosslinked using Method C gave the most homogenous gels with an ideal network structure.

The gels that were formed (0% Ester - 100% Ester) all had different physicochemical properties due to the change in the chemical composition of the structure. Changes in elasticity, swelling degree and degradation were investigated as a factor of the percentage of ester present in the gel.

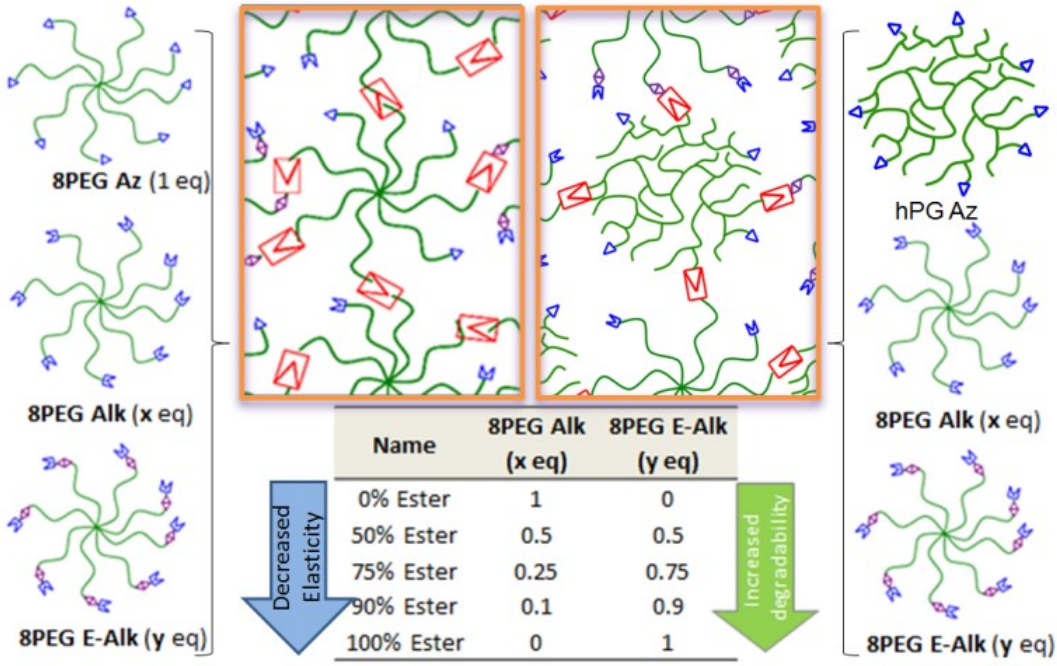

Figure 3. The blending method which leads to the formation of gels with specific percentages of degradable ester linkages

5.3.4 Swelling behavior

8PEG and **hPG-8PEG** hydrogels degraded through hydrolysis of the ester bonds contained by the **8PEG-E-Alk** building blocks. To study the rate of degradation of these hydrogels, at regular time intervals, the swelling degree (Qm) was calculated by rationing the swollen hydrogel weight after exposure to buffer with the initial hydrogel weight after preparation. Fig. 4 shows the swelling profiles of **8PEG** hydrogels with different ester compositions over 24 hours at a pH of 8.3 and 37^{o}C.

With only **8PEG-E-Alk** present as the crosslinking partner for the **8PEG-Az**, it was observed that the 100% Ester gels swell and degrade rapidly over the course of an hour while the 90% Ester gels stay intact for 5 hours before total degradation has taken place. Total degradation is detected by the lack of a sample that can be taken out from the solution and weighed. As the number of ester functionalities in the gels decreased (<75%) (Fig. 4), a large increase in swelling ratio was seen, caused by the hydrolytic cleavage of the ester bonds. At a certain point, the swelling ratios were observed to decrease due to disintegration of the hydrogel network, resulting in

partial dissolution of the hydrogels. Only after all of ester bonds have been cleaved (after around 10 hours), the gels reached an equilibrium swelling degree at which they remain. in contrast, for hydrogels without ester (0%), the swelling ratio remains constant throughout the test (Fig. 4).

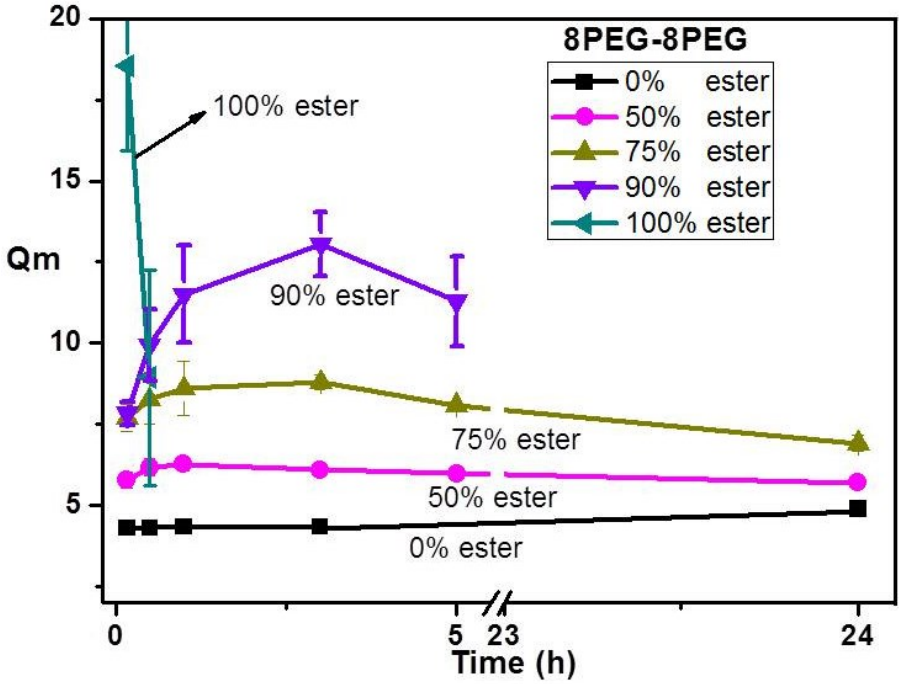

Figure 4. Swelling degree of the different compositions of **8PEG-8PEG** hydrogels at pH=8.3 and 37°C. Data are shown as average (n=3).

In a comparative experiment, the swelling properties of **hPG-8PEG** with different ester compositions have been tested over 24 hours at pH 8.3 and 37^{o}C, and the swelling profiles are shown in Fig. 5. The tendency of swelling of **hPG-8PEG** hydrogels was similar to those of **8PEG-8PEG** hydrogels, due to the similar network structure, but the degradation rate of **hPG-8PEG** hydrogel was slower because **hPG** contains more functional groups than those of **8PEG**, which could be crosslinked to form more linkages for hydrolysis. Therefore, for samples which contained 100% ester groups, **hPG-8PEG** gels needed one hour more than **8PEG-8PEG** gels for full degradation. In addition, temperature has shown to have a great effect on the swelling behavior of the gels; in particular, the ester linkages have shown to be temperature sensitive, with gels with high levels of ester present being degraded much slower at room

temperature than at 37°C e.g. 100% ester samples remained intact and swollen over 32 hours in deionised water at room temperature.

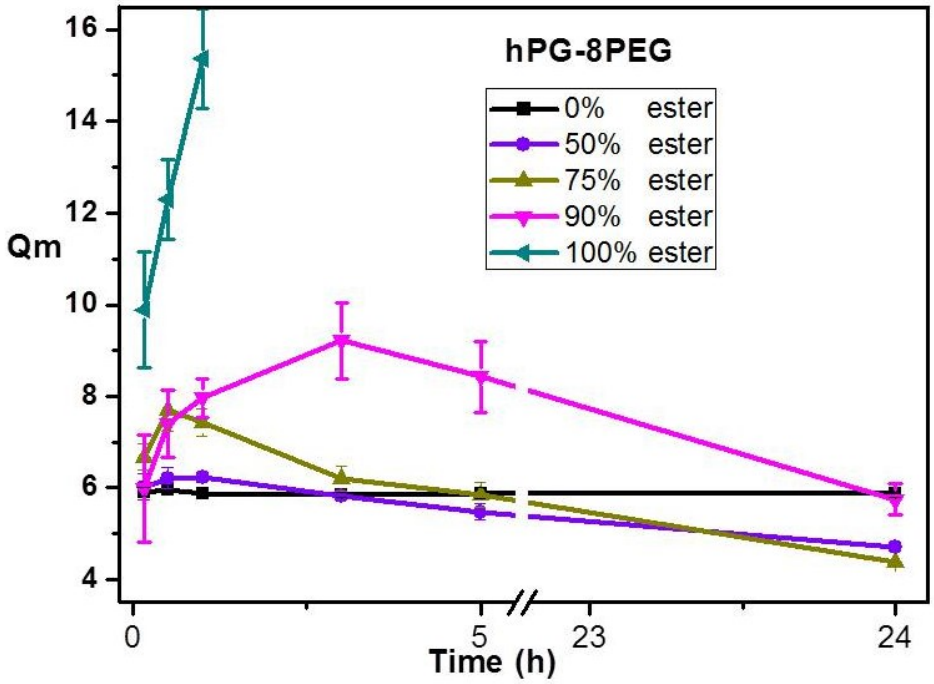

Figure 5. Swelling degree of the different compositions of **hPG-8PEG** hydrogels at pH 8.3 and 37°C. Data are shown as average (n=3).

5.3.5 Degradation under different pH conditions

The ester moiety present in the gels also resulted in a variable rate of degradation of the network structure under different pH conditions. In Method B, the use of sodium ascorbate in the gel formation led to the decreased pH of the deionised water in which the gels were placed during the swelling tests. It was during these swelling tests that the rapid break-down of the gels was observed. In order to study the stability of our gels in different pH conditions, gels made without ascorbate present, e.g. by Method C, into 1) a basic solution (pH 8.3, $NaHCO_3$ solution) and 2) a neutral solution (pH 7.4, PBS buffer solution) were submersed. It can be seen in Fig. 6a that gels with 100% ester present, for both **8PEG-8PEG** and **hPG-8PEG** samples, hydrogels degraded fully after 30 minutes under basic conditions, but continued to swell up to 24 hours, without completed degradation, under neutral conditions. In

addition, at the same pH, **hPG-8PEG** hydrogels swelled much more slowly and absorbed less water than **8PEG-8PEG** hydrogels. This is probably because **hPG** contained more azide groups than **8PEG**, which, when reacted with alkyne groups, led to more crosslinking points being created. Due to this higher crosslinking density it took more time for both hydrolysis and swelling to occur.

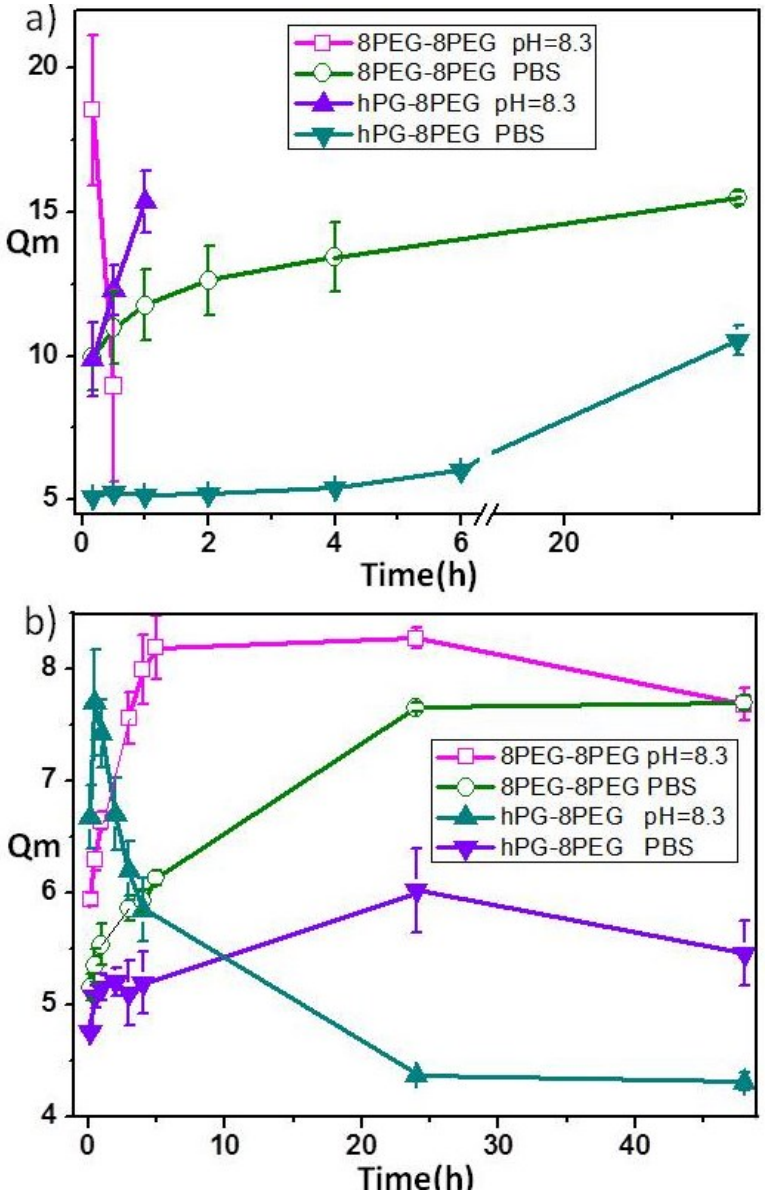

Figure 6. Swelling behavior of a) **8PEG-8PEG** and **hPG-8PEG** hydrogels containing 100% ester groups and b) **8PEG-8PEG** and **hPG-8PEG** hydrogels containing 75% ester groups tested under basic conditions (pH 8.3) or under neutral conditions (PBS) at 37 ºC, respectively. Data are shown as average (n=3).

Moreover, the stability of hydrogels with 75% ester present, for both **8PEG-8PEG**

and **hPG-8PEG**, has been tested (Fig. 6b). For both gels, the swelling was much faster and larger under basic conditions than under neutral conditions due to faster ester bond cleavage in basic solution. Again, due to the tighter crosslinking, **hPG-8PEG** hydrogels were observed to swell much more slowly and absorb less water than **8PEG-8PEG** hydrogels. In contrast to the hydrogels with 100% ester that fully degraded in the course of the swelling experiment, for all of the gels with 75% ester, after swelling to the maximum, the swelling degree was observed to decrease again until an equilibrium was reached. These equilibrium swollen hydrogels owed their stability to the 25% of linkages that have no ester groups. The fact that the pH of the solution had such a significant impact on the degradation rates of these hydrolytically-labile hydrogels allowed us to tune the time window in which the hydrogels remain intact, and available for the application, e.g. as scaffold for tissue regeneration of for drug delivery.

5.3.6 Elasticity

The relationship between network composition and hydrogel properties (i.e., degradation and viscoelasticity) has been examined by rheological measurements. Elasticity measurements can tell a lot about the structure of materials and is related to both the “tightness” of the gel network and to cross-link density. (Degradation of the hydrogel leads to a lower crosslinking density, resulting in a lower stiffness). The elastic modulus of the gels was obtained by first measuring the storage modulus (G’) and then converting these values into values for the elasticity E (Young’s modulus) using the Young’s equation (E = 3 G’). The measurements were performed at pH 8.3 and room temperature using **8PEG-8PEG** hydrogels. In the experiment, we varied the ratios of the ester (100%-50%) incorporation into the gel network, while keeping all other parameters constant (Fig. 7). Non-degradable hydrogels made without ester were used as control samples. The initial elasticity for all hydrogels was in the range of 0.3 – 1 MPa, while for the hydrogels with higher ester content lower values for E were measured. The modulus decreased over the 5 day test period for all hydrogels

synthesized with the degradable ester groups. As expected, the elasticity remained constant for the hydrogels without degradable ester group. The gels containing hydrolysable ester groups rapidly lost some of their mechanical integrity due to degradation. Figure 7 shows the clear and expected trend that the higher the ester content, the faster and greater the decrease in stiffness. Apparently, the decrease in modulus follows the same trend as the degradation of the gels, which was indirectly observed during the swelling tests.

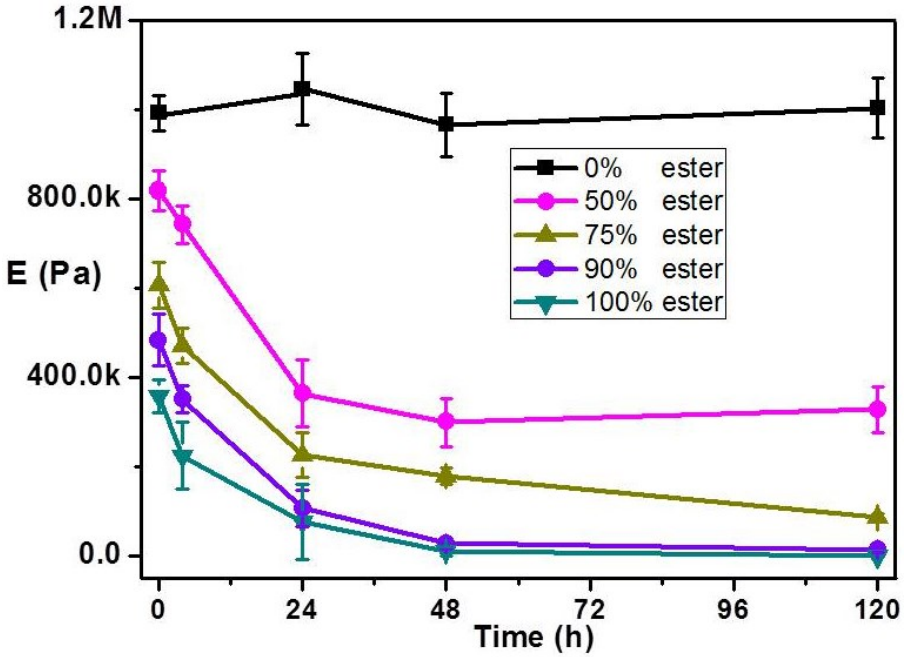

Figure 7. Bulk elasticity values for **8PEG-8PEG** gels of different compositions in dry and swollen state at 25°C Data are shown as average (n=3)

It is interesting to note that, while the **8PEG** hydrogels with 100% ester and 90% ester were fully degraded after 6 days and 10 days, respectively, the hydrogels made with smaller ester percentages retained a certain degree of mechanical integrity; the elasticity remained constant after the initial decrease, which was due to partial degradation of the gels.

5.3.7 Copper concentration

Varying the amount of copper catalyst enabled us to minimize the amount of

copper to prepare non-cytotoxic materials. It was discovered that using even 0.04 wt% copper (compared to the precursor weight) was enough for gel formation to take place; this is far less than the amount usually used in traditional click chemistry reactions (usually 5 wt%) and this is obviously of great benefit to the system if it is to be used in biomedical applications. In particular, the use of cytocompatible irradiation conditions and initiators shows promise in the production of non-toxic materials. Gels with lower copper concentration (0.02 wt%) have shown much softer and faster swelling than those with more, which is likely due to the smaller crosslinking density of in the gel network.

5.3.8 Cytocompatiblity

The cytotoxicity experiments with degradable and non-degradable hydrogels characterized by live-dead assay show that after 24 h of cell culture there was no apparent in vitro cytotoxicity (Fig. 8). Most of cells (> 93%) remained viable on **hPG**-**8PEG** and **8PEG**-**8PEG** hydrogels (Table 2) for a cultivation period of one day. This shows that although the copper ion in the Cu(I)-catalyzed click chemistry is a rather toxic ion [46,47], due to the minimal amount of copper involved in the gel formation of our hydrogels, cells still remained viable after 24 hours. Visual inspection of the cultures indicated that the hydrogels were in various stages of degradation during the cytotoxicity experiments. For example, both the **8PEG-8PEG** and **hPG-8PEG** hydrogels with 100% ester (Fig. 8b, 8d) were completely degraded by the end of the culture period, whereas **8PEG-8PEG** and **hPG-8PEG** hydrogels with 0% ester (Fig. 8a, 8c) remained intact.

The quantitative analysis of the cytotoxicity (Table 2) shows that even in the case of full degradation of the hydrogels, the degradation products apparently had no influence on cell viability. Moreover, after complete degradation, cells could adhere on the cell culture plate and start to spread, as can be seen in Fig. 8b. In the case of non-degradable hydrogels, however, cells were observed to maintain their round shape, which is indicative of poor adhesion and little interaction with the substrate.

This cell-repellent property is very well-known for PEG and **hPG** materials, and makes these polymers highly useful as inert background material onto which we can introduce cues for specific biointeraction.

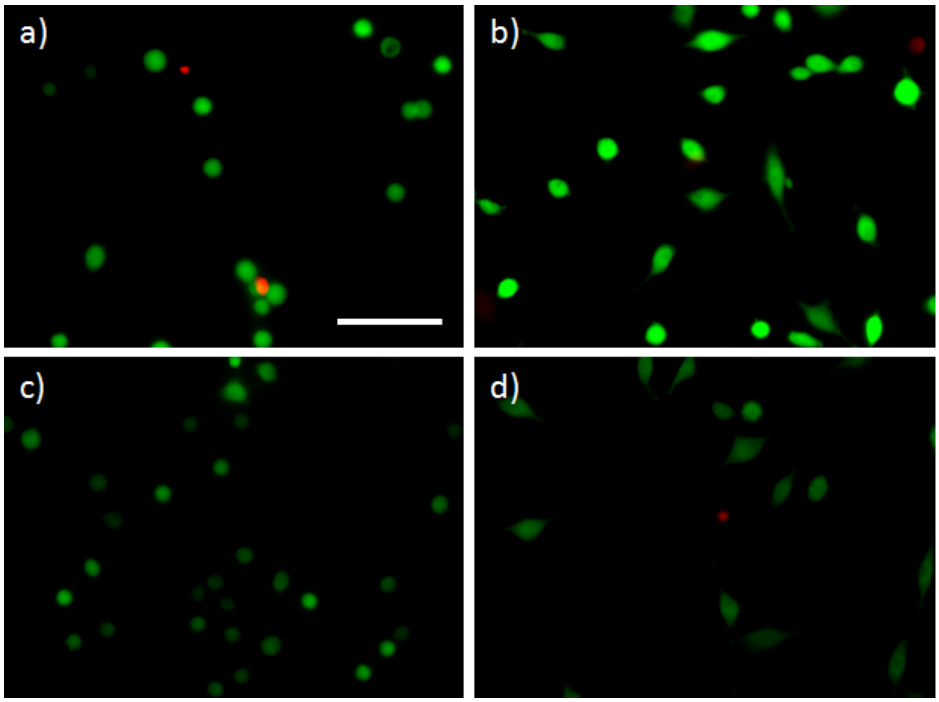

Figure 8. Live-dead assay indicating viable (green) and dead (red) L-929 cells after 24h on a) **8PEG**-**8PEG** hydrogel without ester b) **8PEG**-**8PEG** hydrogel with 100% ester, c) **hPG**-**8PEG** hydrogel without ester, d) **hPG**-**8PEG** hydrogel with 100% ester. Scale bar represents 100 µm

Table 2 Characterization and cellular behavior on degradable and non-degradable hydrogels after 24 h of cell culture. +: yes, -: no.

Samples	Degradability	Cell repellency	Cell Viability
8PEG-8PEG 0%	-	+	93.2±1.1
8PEG-8PEG 100 %	+		95.0±1.2
hPG-8PEG 0%	-	+	98.5±0.7
hPG-8PEG 100%	+		99.3±1.0

5.4 Conclusions

In this study, hydrogel networks from polyethylene glycol (PEG) and hyperbranched polyglycerol (**hPG**) have been obtained using three crosslinking

methods; A) photopolymerisation of acrylate groups, B) alkyne-azide click chemistry C) “UV-click”. In particular, the latter “UV-click” method, the recently developed copper-catalyzed alkyne−azide cycloaddition (CuAAC) reaction via photochemical reduction of Cu(II) to Cu(I), was investigated in detail. This approach does not only eliminate the need for sodium ascorbate but also gives access to a highly homogeneous gel with ideal network structure. We have shown to be able to minimize the amount of the copper catalyst, which can be cytotoxic, and have synthesized non-cytotoxic hydrogels from PEG and **hPG**. Two kinds of hydrogels, **8PEG-8PEG** and **hPG-8PEG**, have been prepared by this novel “UV-click” method and were characterized.

Moreover, by mixing aqueous solutions of precursors with azide end-group and alkyne end-group containing hydrolytically labile ester linkages, the resulting hydrogels are degradable. We have shown to be able to control their degradation properties first and foremost by the ratios of ester in the gel matrix, and further tune their integrity by changing the pH or temperature.

The elasticity was tuned by altering the ester composition in the **8PEG-8PEG** hydrogels matrix and it was demonstrated that the loss of mechanical stability due to partial degradation could be accurately followed by rheology. Finally, through live-dead assays, it was demonstrated that there was no cytotoxicity observed for any of the hydrogels.

These results indicate that PEG and **hPG** hydrogels made by the novel “UV-click” (CuAAC) reaction could be employed as a promising alternative of PEG-based hydrogels made by traditional UV-curing with minimal design changes to provide a gel-based device with similar properties and cell-material interactions and added tunable degradability.

References

[1] Soppimath, K. S.; Aminabhavi, T. M.; Kulkarni, A. R.; Rudzinski, W. E. Biodegradable polymeric nanoparticles as drug delivery devices. *Journal of Controlled Release* **2001**, *70*, 1-20.

[2] Discher, D. E.; Mooney, D. J.; Zandstra, P. W. Growth Factors, Matrices, and Forces Combine

and Control Stem Cells. *Science* **2009**, *324*, 1673-1677.
[3] Buxboim, A.; Rajagopal, K.; Brown, A. E. X.; Discher, D. E. How deeply cells feel: methods for thin gels. *Journal of Physics-Condensed Matter* **2010,** *22*, 194116.
[4] Allen, T. M.; Cullis, P. R. Drug Delivery Systems: Entering the Mainstream. *Science* **2004**, *303*, 1818-1822.
[5] Adams, M. L.; Lavasanifar, A.; Kwon, G. S. Amphiphilic block copolymers for drug delivery. *Journal of Pharmaceutical Sciences* **2003**, *92*, 1343-1355.
[6] Peppas, N.; Langer, R. New challenges in biomaterials. *Science* **1994**, *263*, 1715-1720.
[7] Langer, R.; Vacanti, J. Tissue engineering. *Science* **1993**, *260*, 920-926.
[8] Gilding, D. K.; Reed, A. M. Biodegradable polymers for use in surgery—polyglycolic/poly(actic acid) homo- and copolymers: 1. *Polymer* **1979**, *20*, 1459-1464.
[9] Langer, R. New methods of drug delivery. *Science* **1990**, *249*, 1527-1533.
[10] Middleton, J. C.; Tipton, A. J. Synthetic biodegradable polymers as orthopedic devices. *Biomaterials* **2000**, *21*, 2335-2346.
[11] Bryant, S. J.; Anseth, K. S. J. Hydrogel properties influence ECM production by chondrocytes photoencapsulated in poly(ethylene glycol) hydrogels. *Biomed. Mater. Res.* **2002,** 59, 63–72.
[12] Peppas, N. A.; Hilt, J. Z.; Khademhosseini, A.; Langer, R. Hydrogels in Biology and Medicine: From Molecular Principles to Bionanotechnology. *Advanced Materials* **2006**, *18*, 1345-1360.
[13] Peppas, N. A.; Bures, P.; Leobandung, W.; Ichikawa, H. Hydrogels in pharmaceutical formulations. *European Journal of Pharmaceutics and Biopharmaceutics* **2000,** 50, 27-46.
[14] Hennink, W. E.; van Nostrum, C. F. Novel crosslinking methods to design hydrogels. *Advanced Drug Delivery Reviews* **2002**, *54*, 13-36.
[15] Zalipsky, S.; Harris, J. M. Introduction to chemistry and biological applications of poly(ethylene glycol). *Poly(Ethylene Glycol)* **1997**, *680*, 1-13.
[16] Iza, M.; Stoianovici, G.; Viora, L.; Grossiord, J. L.; Couarraze, G. Hydrogels of poly(ethylene glycol): mechanical characterization and release of a model drug.. *Journal of Controlled Release* **1998**, *52*, 41-51.
[17] Suh, K. Y.; Seong, J.; Khademhosseini, A.; Laibinis, P. E.; Langer, R. A simple soft lithographic route to fabrication of poly(ethylene glycol) microstructures for protein and cell patterning. *Biomaterials* **2004**, *25*, 557-563.
[18] Kim, P.; Kim, D. H.; Kim, B.; Choi, S. K.; Lee, S. H.; Khademhosseini, A.; Langer, R.; Suh, K. Y. Fabrication of nanostructures of polyethylene glycol for applications to protein adsorption and cell adhesion. *Nanotechnology* **2005**, *16*, 2420-2426.
[19] Schulte, V. A.; Diez, M.; Hu, Y.; Moeller, M.; Lensen, M. C. The combined influence of substrate stiffness and surface topography on the anti-adhesive properties of Acr-sP(EO-stat-PO) hydrogels. *Biomacromolecules* **2010,** *11*, 3375-3383.
[20] Diez, M.; Schulte, V. A.; Stefanoni, F.; Natale, C. F.; Mollica, F.; Cesa, C. M.; Chen, J.; Moeller, M.; Netti, P. A.; Ventre, M.; Lensen, M. C. Molding Micropatterns of Elasticity on PEG-based Hydrogels to Control Cell Adhesion and Migration. *Advanced Engineering Materials* **2011**, *13*, B395-B404.
[21] Schulte, V. A.; Diez, M.; Moeller, M.; Lensen, M. C. Topography induced cell adhesion to Acr-sP(EO-stat-PO) hydrogels: the role of protein adsorption. *Macromolecular Bioscience* **2011,** *11*, 1378-1386.
[22] Kelleher, S.; Jongerius, A.; Loebus, A.; Strehmel, C.; Zhang, Z.; Lensen, M. C. AFM

Characterization of Elastically Micropatterned Surfaces Fabricated by Fill-Molding In Capillaries (FIMIC) and Investigation of the Topographical Influence on Cell Adhesion to the Patterns. *Advanced Engineering Materials* **2012,** 14, B56-B66.
[23] Sisson, A. L.; Haag R. Polyglycerol nanogels: highly functional scaffolds for biomedical application. *Soft Matter* **2010,** 6,4968-4975.
[24] Kainthan, R.K.; Janzen J.; Levin, E.; Devine, D.V.; Brooks, D.E. Biocompatibility Testing of Branched and Linear Polyglycidol. *Biomacromolecules* **2006,** 7, 703-709.
[25] Khandare, J.; Mohr, A.; Calderon, M.; Qelker, P.; Licha, K.; Haag, R. Structure-biocompatibility relationship of dendritic polyglycerol derivatives. *Biomaterials* ***2***0**10,** 31, 4268-4277.
[26] Marion, H. M.; Oudshoorn, R. R.; Bouwstra, J. A.; Hennink, W. E. Synthesis and characterization of hyperbranched polyglycerol hydrogels. *Biomaterials* **2006,** 27, 2471-2479.
[27] Ekinci, Duygu.; Sisson, A. L.; Lendlein, A. Polyglycerol-based polymernetwork films for potential biomedical applications. *Journal of Materials Chemistry* **2012,** 22, 21100-21109.
[28] Lutolf, M. P.; Hubbell, J. A. Synthesis and Physicochemical Characterization of End-Linked Poly(ethylene glycol)-co-peptide Hydrogels Formed by Michael-Type Addition. *Biomacromolecules* **2003**, *4*, 713-722.
[29] Lutolf, M. P.; Tirelli, N.; Cerritelli, S.; Cavalli, L.; Hubbell, J. A. Systematic Modulation of Michael-Type Reactivity of Thiols through the Use of Charged Amino Acids. *Bioconjugate Chemistry* **2001**, *12*, 1051-1056.
[30] Matsunaga, T.; Sakai, T.; Akagi, Y.; Chung, U.-i.; Shibayama, M. Structure Characterization of Tetra-PEG Gel by Small-Angle Neutron Scattering. *Macromolecules* **2009**, *42*, 1344-1351.
[31] Sakai, T.; Matsunaga, T.; Yamamoto, Y.; Ito, C.; Yoshida, R.; Suzuki, S.; Sasaki, N.; Shibayama, M.; Chung, U.-i. Design and Fabrication of a High-Strength Hydrogel with Ideally Homogeneous Network Structure from Tetrahedron-like Macromonomers. *Macromolecules* **2008**, *41*, 5379-5384.
[32] Li, X.; Tsutsui, Y.; Matsunaga, T.; Shibayama, M.; Chung, U.-i.; Sakai, T. Precise Control and Prediction of Hydrogel Degradation Behavior. *Macromolecules*, **2011,** *44*, 3567-3571.
[33] Peppas, N. A.; Keys, K. B.; Torres-Lugo, M.; Lowman, A. M.; Poly(ethylene glycol)-containing hydrogels in drug delivery. *Journal of Controlled Release* **1999,** 62 81–87.
[34] Zheng, Y.; Andreopoulos, F. M.; Micic, M.; Huo, Q.; Pham, S. M.; Leblanc, R. M. A Novel Photoscissile Poly(ethylene glycol)-Based Hydrogel. *Advanced Functional Materials* **2001**, *11*, 37-40.
[35] van de Manakker, F.; van der Pot, M.; Vermonden, T.; van Nostrum, C. F.; Hennink, W. E. Self-Assembling Hydrogels Based on β-Cyclodextrin/Cholesterol Inclusion Complexes. *Macromolecules* **2008**, *41*, 1766-1773.
[36] Rossow, T.; Heyman, J. A.; Ehrlicher, A. J.; Langhoff, A.; Weitz, D. A.; Haag, R.; Seiffert, S. Controlled Synthesis of Cell-Laden Microgels by Radical-Free Gelation in Droplet Microfluidics, *J. Am. Chem. Soc.* **2012,** 134, 4983−4989
[37] Steinhilber, D.; Seiffert, S.; Heyman, J. A.; Paulus, F.; Weitz, D. A.; Haag, R. Hyperbranched polyglycerols on the nanometer and micrometer scale. *Biomaterials* **2011,** 32, 1311−1316.
[38] Hawker, C. J.; Wooley, K. L. The Convergence of Synthetic Organic and Polymer Chemistries. *Science* **2005**, *309*, 1200-1205.
[39] Kolb, H. C.; Sharpless, K. B. The growing impact of click chemistry on drug discovery. *Drug Discovery Today* **2003**, *8*, 1128-1137.

[40] Kolb, H. C.; Finn, M. G.; Sharpless, K. B. Click chemistry: diverse chemical function from a few good reactions. *Angew. Chem. Int. Ed.* **2001**, *40*, 2004-2012.
[41] Bock, V. D.; Hiemstra, H.; van Maarseveen, J. H. CuI-Catalyzed Alkyne–Azide "Click" Cycloadditions from a Mechanistic and Synthetic Perspective. *European Journal of Organic Chemistry* **2006**, 51-68.
[42] Adzima, B. J.; Tao, Y.; Kloxin, C.J.; DeForest, C. A.; Anseth, K.S.; Bowman, C. N. Spatial and temporal control of the alkyne-azide cycloaddition by photoinitiated Cu(II) reduction, *nature chemistry,* **2011,** 3, 256-259.
[43] Sisson, A. L.; Steinhilber, Dirk.; Rossow, T.; Welker, P.; Licha, K.; Haag, R. Biocompatible Functionalized Polyglycerol Microgels with Cell Penetrating Properties. *Angew. Chem. Int. Ed.* **2009,** 48, 7540 –7545.
[44] Cai, L.; Wang, S. Elucidating Colorization in the Functionalization of Hydroxyl-Containing Polymers Using Unsaturated Anhydrides/Acyl Chlorides in the Presence of Triethylamine. *Biomacromolecules* **2010,** 11, 304–307.
[45] Kloxin, A. M.; Kloxin, C J.; Bowman, C. N.; Anseth K. S. Mechanical Properties of Cellularly Responsive Hydrogels and Their Experimental Determination. *Adv. Mater.* **2010,** 22, 3484-3494.
[46] Lodge, T. P. A Virtual Issue of Macromolecules: "Click Chemistry in Macromolecular Science". *Macromolecules,* **2009,** 42, 3827–3829.
[47] Letelier, M. E.; Sa´nchez-Jofre´, S.; Peredo-Silva, L.; Corte´s-Troncoso, J.; Aracena-Parks, P. Mechanisms underlying iron and copper ions toxicity in biological systems: Pro-oxidant activity and protein-binding effects. *Chem. Biol. Interact.* **2010,** 188, 220-227.

Summary

Hydrogels are three dimensional crosslinked matrices, which are often physically and mechanically similar to the extra-cellular matrix of cells, making them suitable as biomaterials. Particularly, PEG based hydrogels are currently the most widely employed material in the biomedical field, due to its nontoxicity, non-immunogenicity, non-antigenicity, and high hydrophilicity. In this thesis, the main goal of investigation is the development of novel PEG based hydrogels with cytocompatibility, controlled degradable properties and multi functionality for potential biomedical applications. In order to reach the goal, three synthetic strategies have been explored for the formation of the gels; i) our newly discovered amine Michael type addition chemistry (Chapter 2), ii) *in situ* incorporation of hydroxyapatite (Chapter 4), and iii) click chemistry with degradable moieties (Chapter 5).

Chapter 1 describes the general features of hydrogels, with respect to the different type of hydrogels and their cross-linking methods. The characteristics of natural and synthetic polymers, with special focus on poly(ethylene glycol) (PEG) are also briefly overviewed. Star-shaped PEG molecules, having 8 arms with acrylate end groups; 8PEG, are the main components of the hydrogel studied in this thesis. The various types of hydrogels characterized based on their derivation and composition as natural, synthetic, hybrid, or composite hydrogels, are introduced. Both chemically as well as physically cross-linked networks for gel formations are discussed, with particular emphasis on networks formed by Michael addition and click chemistry, since these are methods investigated in this thesis. Meanwhile, Michael addition and click reaction to prepare PEG-based hydrogels proceed via a step growth mechanism, which is different from the chain growth mechanism of photopolymerization, and the resulting network structures are also highlighted. In addition, the use of hydrogels for tissue engineering and protein delivery is shortly discussed.

Chapter 2 reports on the design of a novel hydrogel system fabricated from 8PEG

and ammonium hydroxide solution via a Michael-type addition between the acrylate and amine groups. Due to the low reactivity of amine towards acrylate groups, after gel formation more than 50% acrylate groups are still available for further functionalization. The simultaneous gelation is investigated by rheological analysis, demonstrating that the networks are progressively stabilized as the Michael addition reaction proceeds. The networks degraded under hydrated conditions by hydrolysis of the ester bonds in the crosslinking moieties. Simply by adjusting the amount of ammonia added to the reaction, the mechanical properties and degradation kinetics can be tuned as shown in rheological analysis and swelling tests, respectively. Higher amounts of NH_3 in the reaction lead to a faster crosslinking process and higher crosslinking density, resulting in higher bulk and surface elasticity and longer stability in the hydrated state. Furthermore, it is demonstrated that the incomplete amine-Michael type addition chemistry leads to gel formation, as verified by LC-MS analysis and Raman spectra. Taking advantage of post-network formation reactivity due to plenty of unreacted, pendant acrylate groups present in the gel, a second Michael-type addition between thiol and acrylate groups has enabled facile modification of the gel. At last, a live-dead assay via direct contact of cells (fibroblast cell line L-929) with gels has been performed to verify the cytocompatibility of our new hydrogels.

In a subsequent study, reported in **chapter 3**, we explore how the network structures of hydrogel influence the crystalline structure within the gel matrix. In order to clarify the relationship between the network structure and the crystalline structure of the gel, three kinds of networks are created via chain-growth polymerization (**8PEG-UV**), step-growth polymerization (**8PEG-NH_3**), and mixed-mode chain and step growth polymerization (**8PEG-NH_3-UV**), respectively, for comparison and investigation. Although WAXD results reveal almost no difference of the crystalline phases among the corresponding hydrogels, POM, SEM and AFM studies confirm that the **8PEG-NH_3** and **8PEG-NH_3-UV** have a framework of crystalline domains sized in 30 μm-500 μm, in contrast to only nanoscaled crystalline

domains in **8PEG-UV**. DSC results show 8PEG-UV exhibited the lowest melting point, due to the less crystallinity and flexibility of network chain. Because of the nearly perfect network structure and flexible polymer chain, the long-range ordered crystalline structures has been found from **8PEG-NH_3** hydrogels, revealing that the regular molecule's orientation in nano-scale scope can lead to the ordering structure formation in micro-scale scope.

Chapter 4 reports on *in situ* nucleation process of the desired phase of calcium phosphate (CP) that is formed, i.e. nano-crystalline hydroxyapatite (nHAp), in an **8PEG** hydrogel matrix and the concurring, spontaneous gelation of the bioactive nanocomposite material. The spontaneous gelation is achieved by the addition of mixtures of calcium and phosphorous salt-solutions with ammonium hydroxide to the **8PEG**-precursor solution. The perfect homogeneity of nHAp is proved by scanning electron microscopy (SEM) elemental mapping, and In-situ TEM-XRD analysis reveals crystalline regions in the generally amorphous system. The effect of nHAp concentration on thermogravimetric analysis (TGA) measurement was evaluated, suggesting that a concentration of 20wt% nHAp within the gel matrix reveals the strongest interaction between the organic and inorganic phase. Mouse connective tissue fibroblasts (L-929) and MC3T3-E1 osteoblasts are utilized for cell adhesion tests, verifying the specific bio-interaction between osteoblasts and (**8PEG**-nHAp based) composite hydrogels. The unique property combinations of the hydrogels and HAp reported in this research offer new approaches for complex composite biomaterials engineering.

Another interesting crosslinking method, click chemistry, has been employed in gel formation, explored in **Chapter 5**. The building blocks were functionalized with alkyne- and azide-groups to allow for hydrogel synthesis. The copper-catalyzed alkyne−azide cycloaddition (CuAAC) reaction via photochemical reduction of Cu(II) to Cu(I) utilized for gel formation, require the presence of a minimal amount of copper catalyst to prepare non-cytotoxic materials. Using these methods, hydrogel formation is rapid and efficient with ideal network structure, and we can control

their degradation properties by tuning the ratios of ester in the gel matrix. The elasticity also can be tuned by altering the ester composition in the hydrogels matrix and it was demonstrated that the loss of mechanical stability due to partial degradation could be accurately followed by rheology. Finally, live-dead assays shown that there was no cytotoxicity observed for any of the hydrogels thus having great potential as tissue engineering and drug delivery matrices.

In conclusion, this thesis describes novel PEG based hydrogels, exhibiting biodegradability, cytocompatibility, functionality and high degree of tailorability, with respect to mechanical properties and degradation behavior. The ability of these hydrogels can serve several biomedical functions, from controlled protein release to tissue engineering. The results reported in this thesis bring this hydrogel technology one step forward towards biomedical application.

Abstract

The successful engineering of hydrogels with functionality, tunable mechanical properties, and degradation rates has led to significant advances in the field of tissue engineering. Depending on the chemical composition and the method of crosslinking, hydrogels vary in their morphology, network structure, mechanical properties, degradation behavior and biological activities. The major themes pursued in this thesis are the development of technology to facilitate the fabrication of hydrogels with controlled properties and functionality, the role of inorganic phase in the composite hydrogel system, and the study of the cellular response and cytocompatibility to our developed hydrogels.

The present work has been organized into three parts. In the first part (Chapter2-3), the hydrogels are prepared by amine-Michael type addition chemistry, and subsequently stabilized by means of additional photopolymerization to prolong the degradation time for cell test. The mechanical and degradation behavior of the gels have been adjusted in a controlled and tailorable fashion, and the functionality of gels is introduced, which allows biological motifs or soluble factors to be incorporated into the hydrogel matrices. Meanwhile, this step-growth polymerization method leads to long-ranged crystalline structure.

The second part (Chapter 4) describes the in-situ formation of PEG-CP composite hydrogels, and the influence of inorganic CP phase on the gel properties. Cell adhesion test has confirmed the strong affinity between osteoblast and composite hydrogels containing CP phase, which is potentially used for the regeneration of bone tissue engineering.

In the third part (Chapter 5), the hydrogel matrices with defined mechanical properties as well as tunable degradability have been created by click chemistry. Degradation time and the monitored mechanical properties of the hydrogels changed predictably as degradation proceeded until the gels reached complete degradation. These unique properties indicate that this degradable hydrogels are well suited for the applications in protein/cell delivery to repair soft tissue.

Zusammenfassung

Die erfolgreich Synthese von Hydrogelen mit funktionalen Eigenschaften wie einstellbare mechanische Eigenschaften, chemischer Funktionalität und veränderbaren Degradationsverhalten hat zu großem Fortschritt im Feld des Gewebe-Engineering geführt. Abhängig von der chemischen Zusammensetzung und der chemischen Vernetzungsprozedur können Hydrogele ihre mechanischen Eigenschaften, Morphologie, Degradationsverhalten, Netzwerkstruktur und biologischen Aktivität ändern. In diesem Rahmen sind die Hauptthemen dieser Arbeit die Entwicklung einer neuen Herstellungsmethode für Hydrogele, die Synthese von Hydrogelen mit kontrolierbaren funktionalen Eigenschaften, die Untersuchung der Rolle von der inorganischer Phase in Komposit Hydrogelen und die Untersuchung des Zellverhaltens und der Zytokompatibilität auf den neu entwickelten Hydrogelen.

Die vorgestellte Arbeit ist in drei verschiedene Hauptpunkte unterteilt. Im ersten Punkt (Kapitel 2 und 3) werden die Hydrogele mittels Amine-type-Michael-addition-chemistry hergestellt um im Anschluss durch photopolymerisation stabilisiert zu werden. Das verlängert die Degradationszeit, notwendig für Zelltests. Die mechanischen Eigenschaften und das Degradationsverhalten der Gele ist dabei kontrolierbar und gezielt veränderbar. Des Weiteren wurde eine chemische Funktionalität eingeführt, welche erlaubt biologische Interaktion zu verändern bzw. lösliche Reagenzen in der Hydrogelmatrix zu transportieren und ggf. abzugeben. Zudem führt eine step-growth Polymerisation zu großén kristallinen Polymerstrukturen.

Der zweite Punkt (Kapitel 4) befasst sich mit der in-situ Formation von Polyethylenglykol (PEG) – Kalziumphosphat (CaP) Komposit Hydrogelen und dem Einflussder inorganischen CaP Phase auf die Hydrogeleigenschaften. Zelladhäsionsuntersuchungen ergaben starke Affinität von Osteoblasten auf die untersuchten Komposit Hydrogele, welche folglich große Eignung für Gewebe-Engineering aufweisen.

Der Dritte Punkt der Arbeit (Kapitel 5) beschäftigt sich ebenfalls mit Hydrogelen mit kontrollierbaren mechanischen Eigenschaften und Degradationsverhalten. Diese wurden aber mittels Click-Chemistry erstellt. Die Degradationszeit und mechanischen Eigenschaften können bis zur vollständigen Auflösung der jeweiligen Gele vorhergesagt werden. Diese einzigartigen Eigenschaften zeigen, dass diese degradierbaren Hydrogele geeignet zu sein scheinen um Zell/Proteintransport im Rahmen von weich-Gewebe-Reparatur Prozeduren erfolgreich zu gestalten.

List of publications:

From this thesis the following manuscripts have resulted, which have already been published as journal articles, which are ready to be submitted or in preparation; + indicates equal contribution

Chapter 2

Zhenfang Zhang+, Axel Loebus+, Gonzalo de Vicente, Fang Ren, Manar Arafeh, Zhaofei Ouyang and Marga C. Lensen. Synthesis of Poly(ethyleneglycol)-based hydrogels via amine-Michael type addition with tunable stiffness and post-gelation chemical functionality. *Chemistry of materials* **2014**, 26, 3624−3630.

Chapter 3

Qian Li+, **Zhenfang Zhang**+**,** Xiaoyuan Zhang, Axel loebus, Jinhui Wang, Zhaofei Ouyang, Zhiqiang Su, Marga C. Lensen. Chemically cross-linked PEG-based hydrogel with crystalline domains in long-range ordering. Ready to be submitted to *ACS Macro Letters.*

Chapter 4

Zhenfang Zhang+**,** Axel loebus+, Qian Li, Christine Strehmel, Jinhui Wang, Zhiqiang Su, Marga C. Lensen. Calciumphosphate Incorporation into Chemically Crosslinked Poly(ethylene glycol) based composite Hydrogels for bone tissue engineering. Ready for submission to *Biomacromolecules*.

Chapter 5

Zhenfang Zhang, Susan Kelleher, Christine Strehmel, Axel Löbus, Gonzalo de Vicente, Cathleen Schlesener, Dirk Steinhilber, Rainer Haag and Marga C. Lensen Fabrication of hydrogels from star-shaped and hyperbranched polyether macromonomers with tuneable degradation properties via click chemistry. Ready to be submitted to *Polymer chemistry*.

Other Publications

Christine Strehmel, **Zhenfang Zhang,** Nadine Strehmel and Marga C. Lensen, Cell phenotypic changes of mouse connective tissue fibroblasts (L-929) to poly(ethylene glycol)-based gels. *Biomaterials Science,* **2013**, 1(8),850-859

Susan Kelleher, **Zhenfang Zhang,** Axel Löbus, Christine Strehmel and Marga C. Lensen

"Blending PEG-based polymers to obtain a library of new biomaterials and their use in surface micro-patterning by the FIMIC method" *Biomaterials Science*, **2014**, 2 (3), 410 – 418.

Susan Kelleher, Aniek Jongerius, Axel Loebus, Christine Strehmel, **Zhenfang Zhang,** Marga C. Lensen. AFM Characterization of Elastically Micropatterned Surfaces Fabricated by Fill-Molding In Capillaries (FIMIC) and Investigation of the Topographical Influence on Cell Adhesion to the Patterns. *Advanced Engineering Materials,* **2011**, 14, B56-B66.

Christine Strehmel, Heidi Perez-Hernandez, **Zhenfang Zhang,** Axel Löbus, Andrés F. Lasagni, and Marga C. Lensen. Geometric Control of Cell Alignment and Spreading within the Confinement of Anti-Adhesive Poly(Ethylene Glycol) Microstructures on Laser-Patterned Surfaces. In review at *ACS Biomaterials Science and Engineering.*

Axel Loebus+, **Zhenfang Zhang**+, Christine Strehmel, Gonzalo de Vicente Lucas, Marga C. Lensen. Soft lithographic surface patterning of *in-situ* PEG Nanocomposite Hydrogels for selective interface interaction. Ready to be submitted to *Advanced Functional Materials*.

Axel loebus+,**Zhenfang Zhang+,** Qian Li, Christine Strehmel, Wolfgang Wisniewski, Zhiqiang Su, Christian Rüssel, Marga C. Lensen. 3D-structured scaffolds from in situ mineralized PEG-based nanocomposite hydrogels In preparation.

Poster presentations

Synthesis of new poly(ethylene glycol) (PEG)-based hydrogels using photo-initiated cross-linking and click chemistry. **Zhenfang Zhang,** Susan Kelleher, and Marga C. Lensen EuroBiomat in Jena (2011) Poster

Novel hydrogels based on bioactive PEG/hydroxyapatite composites for bone tissue engineering **Zhenfang Zhang**, Axel loebus Christine Strehmel, and Marga C. Lensen. Bio-inspired Materials in Potsdam (2012) Poster

In situ PEG-based hydrogels formation via Michael-Type addition reaction between the acrylate and amines groups. **Zhenfang Zhang,** Axel Loebus and Marga C. Lensen Tag der Chemie in Berlin (2012) poster

In situ Synthesis of Nanocomposites from Poly(Ethylene Glycol)-Based Hydrogels and Calcium Phosphates with Improved Mechanical and Biological properties **Zhenfang Zhang,** Axel Loebus, Christine Strehmel and Marga C. Lensen. Junior Euro Mat in Lausanne (2014) Poster

Acknowledgement

First and foremost, I would like to show my deepest gratitude to my supervisor, Prof. Dr. Marga C. Lensen, a respectable, responsible and resourceful scholar, who has provided me with valuable guidance in every stage of the writing of this thesis. Without her enlightening instruction, impressive kindness and patience, I could not have completed my thesis. Her keen and vigorous academic observation enlightens me not only in this thesis but also in my future life.

This thesis grew out of a number of collaborations with other research groups, and I would like to gratefully acknowledge their valuable contribution to this work. I am indebted to Prof. Rainer Haag from Freie Universität Berlin, and Prof. Zhiqiang Su and Dr. Qian Li from Beijing University of Chemical Technology.

All the best wishes to my colleagues, Christine Strehmel, Jingyu Chen, Fang Ren, Tina Sabel, Susan Kelleher, Gonzalo de Vicente, Manar Arafeh, Zhaofei Ouyang, Rahima Rahman, Cigdem Yesildag, Anne Bannuscher and Arina Tyushina, for all their kindness and help. Especially thank Axel Loebus for his warm heart, productive teamwork and invaluable suggestions throughout the course of this research.

Also, I'd like to thank all my friends, especially my three kind roommates, for their encouragement and support.

Finally, I would like to dedicate this research work to my family. To my parents and girlfriend, for their endless support and encouraging me to pursue my goals, always succeed, and never admit defeat.